Antimicrobial, anticancer and catalytic activities of green synthesized Avocado seed extract-gold nanoparticles

UNIVERSITY *of the*
WESTERN CAPE

by

Yonela Ngungeni

(BSc (Hons) Biotechnology)

A thesis submitted in partial fulfilment of the requirements for the degree Master of Science in Nanoscience, in the Department of Biotechnology University of the Western Cape

Supervisor: Prof. Abram Madiehe

Co-supervisor: Prof. Admire Dube

ABSTRACT

Nature through billions of years of trial and error has produced an immeasurable amount of natural systems like plants, birds and animals. The intelligence of nature is hidden in these natural systems and researchers are turning towards "Nature's intelligence" to find inspiration and advance novelty in the development of nanomaterials. Gold nanoparticles (AuNPs) have unique optical, electronic and physicochemical features which has gained them popularity and widespread exploitation in various applications. The conventional methods used for AuNPs synthesis employs toxic chemicals which makes these NPs unsafe for biomedical applications. Hence, there is a search for new, 'green' and more cost effective methods for AuNPs synthesis. Plant extracts are regarded as a highly desirable system for nanoparticle synthesis due to their tremendous capability to produce a wide range of phytochemicals that can act as reducing agents. The main goal of this study was to synthesize AuNPs in a cost effective manner without the use of toxic chemicals in the synthesis process. Avocado seeds which are an agricultural waste by-product were used for the biosynthesis of AuNPs. The study reports on the synthesis optimization, characterization and activities of the biogenic AuNPs.

The avocado seed extract mediated - AuNPs (AvoSE-AuNPs) were optimized by varying reaction parameters and characterized by UV-visible, Dynamic Light Scattering (DLS) and High Resolution Transmission Electron Microscopy (HRTEM), Zetasizer and Fourier Transform Infrared Spectroscopy (FTIR). The formation of AvoSE-AuNPs had an absorption maximum at 534 nm. HRTEM and DLS confirmed that the NPs were polydispersed and present in different shapes. The presence of phytochemical constituents on the AvoSE-AuNPs were confirmed by FTIR. Their potential antibacterial activity was tested on bacterial strains known to exhibit resistance to a number of current antibiotics. The catalytic activity of AvoSE-AuNPs was also assessed as a means to contribute to the development of new methods aimed at alleviating organic pollutants such as nitrophenols in the environment. The AvoSE-AuNPs demonstrated excellent catalytic activity in the reduction of 4-NP by $NaBH_4$ as shown by the rapid decrease in the nitrophenolate absorption band at 400 nm and the appearance of new absorption band at 298 nm, revealing the formation of the 4-aminophenol. Furthermore, the rate constants calculated demonstrated that the reaction occurs faster in the presence AvoSE-AuNPs. The AvoSE-AuNPs showed low significant cytotoxicity. Cell cycle analysis was conducted to further investigate the apparent exhibited toxicity of the AvoSE-AuNPs. The results showed that in both cell lines treated with AvoSE-AuNPs and AvoSE there was a

disruption in the regulation of cell cycle. Cell cycle analysis helped improve understanding of the low cytotoxicity observed by the MTT assay results.

The results presented in this study clearly demonstrate the feasibility of using AvoSE for the synthesis of AuNPs. This study demonstrated that AvoSE mediated AuNPs synthesis is a greener alternative as it abides by the green chemistry principles. Furthermore, the study outcomes contributed to minimizing environmental pollution by finding use for agricultural waste and thus ultimately adding value to the field.

KEYWORDS

Nanotechnology

Green synthesis

Persea americana

Avocado seeds

Agro-processing waste

Gold nanoparticles

Anticancer

Antimicrobial

Catalytic activity

DECLARATION

I, **Yonela Ngungeni**, declare that this study titled "Antimicrobial, anticancer and catalytic activities of green synthesized Avocado seed extract-gold nanoparticles" is my own work and has not been submitted before for any degree or examination at this university or any other tertiary institute. All the sources I have used or quoted have been indicated and acknowledged by complete references.

Signature: …… Y. Ngungeni

Date: ……06 December 2019…….

ACKNOWLEDGEMENTS

- First and foremost I would like to extend a huge thank you to the Nanobiotechnology lab for the support, encouragement and lessons. I am especially grateful to Prof Madiehe for the knowledge, backing and patience he has shown throughout my time under his supervision. I am thankful for the opportunity you provided for me and will forever cherish your teachings and the work ethic you instil in all your students.
- My sincere gratitude also goes out to my co-supervisor Prof Dube and the nanomedicine lab for all the help and guidance.
- I would also like to thank all my colleagues from the NIC and the rest of the department of Biotechnology (third floor) who have helped me along the way. A huge thank you to Ms Jamalie for the helpfulness and advice which always came with a friendly face. My greatest appreciation goes out to the National Nanoscience Post Graduate Teaching and Training Platform for the opportunity, I truly would not have made it here without the assistance.
- To my beloved family and everyone I have been friends with from undergraduate to this point. I am who I am today because of those moments and life lessons we shared together. A special thank you to my Mother, Irvs, Nande, Nicole, Kuhle and my sister Yolanda for being my pillars of strength and allowing me to vent and cry about life and its hardships.
- Thank you to my Dr Leitch. I am grateful for your patience even when the little township girl in me doubted your science. It is an ongoing battle but I am grateful to have you see me through.
- Even in the greatest turmoil, Jeremiah 29:11 “For I know the plans I have for you, plans to prosper you and not to harm you, plans to give you hope and a future”. This has been the most difficult year of my entire existence but through Christ our saviour I made it through.
- I truly cannot believe I am writing acknowledgements for my Masters degree. I started this journey as a 17 year old who came to UWC with hopes of just being the first graduate in my immediate family, I am beyond proud of myself for having reached this point.

LIST OF ABBREVIATIONS

β	Beta
λ_{max}	Maximum wavelength
µl	Microliter
%	Percentage
~	Approximately
°C	Degree Celsius or degree centigrade
A_0	Initial absorbance
Ag	Silver
Ag^+	Silver ion
AgNPs	Silver nanoparticles
Al	Aluminium
A_{max}	Maximum absorbance
AMR	Antimicrobial resistance
AP	Aminophenol
A_t	Absorbance at time point
ATR-FTIR	Attenuated total reflection -Fourier Transform Infrared spectroscopy
Au	Gold
AuNPs	Gold nanoparticles
AvoSE	Avocado seed extract
Br	Bromide
C	Carbon
Ca	Calcium
Caco-2	Human epithelial colorectal adenocarcinoma cell line
CASE	*Coffea arabica* seed extract
Cd	Cadmium
CDK's	cyclin-dependent kinases
Co	Cobalt
Cu	Copper
ddH_2O	Distilled deionized water
DLS	Dynamic light scattering
DMEM	Dulbecco's Modified Eagle's Medium

DMSO	Dimethyl sulphoxide
ξ	zeta
E.coli	*Escherichia coli*
FBS	Foetal Bovine Serum
Fe	Iron
FRET	Fluorescent resonance energy transfer
FTIR	Fourier Transform Infrared spectroscopy
H	Hydrogen
$HAuCl_4$	Hydrogen tetrachloroaurate (III)
HepG2	Human liver hepatocellular carcinoma cell line
HR-TEM	High Resolution-Transmission Electron Microscopy
IC_{50}	Half maximal inhibitory concentration
ISO	International Organization for Standardization
K. pneumoniae	*Klebsiella pneumoniae*
LDL-C	Lipoprotein-cholesterol
M	Molar
M phase	Mitosis phase
mg	Milligram
MIC	Minimum inhibitory concentration
min	Minutes
min^{-1}	per minute
ml	Millilitre
mM	millimolar
mm	Millimeter
MRSA	Methicillin-resistant *Staphylococcus aureus*
MTT	3-[4,5-dimethylthiazol-2-yl]-2,5-diphenyltetrazolium bromide
N	Nitrogen
$NaBH_4$	Sodium Borohydride
NADH	Nicotinamide adenine dinucleotide
NIH	National Institutes of Health
NPs	Nanoparticles
Pb	Lead
PBS	Phosphate buffered saline
PET	Photo induced electron transfer

p-NP	p-nitrophenol
ROS	Reactive oxygen species
S phase	DNA Synthesis phase
S. aureus	*Staphylococcus aureus*
S. epidermidis	*Staphylococcus epidermidis*
S. pyogenes	*Streptococcus pyogenes*
SDS	Sodium dodecyl sulphate
SPR	Surface Plasmon Resonance
UV-Vis	UV-Vis Ultraviolet visible
WHO	World Health Organisation
Zn	Zinc

LIST OF FIGURES

LIST OF TABLES

TABLE OF CONTENTS

CHAPTER 1

INTRODUCTION

1.1 Background

The term 'nano' is a prefix that describes 'one billionth' or 10^{-9} of a particular something. The concept of nanotechnology was first introduced by Richard Feynman in his famous lecture entitled "There's plenty room at the bottom" in 1959 (Feynman, 1960). The International Organization for Standardization (ISO) defines nanotechnology as the "application of scientific knowledge to manipulate and control matter at the nanoscale in order to make use of size- and structure-dependant properties and phenomena, as distinct from those associated with individual atoms or molecules or extrapolation from larger sizes of the same material" (ISO, 2015). Nanotechnology has been characterised as a general-purpose technology (Shea, Grinde, & Elmslie, 2011). It is universal and has the inclination to enable novel applications across many technological sectors. Nanotechnology is fast becoming an integral part of many modern-day products either in the manufacturing process or product itself (Saidi & Douglas, 2017). Nanomaterials exhibit novel and unpredictable characteristics such as extraordinary strength, chemical reactivity, electrical conductivity, superparamagnetic behaviour and other characteristics (Benelmekki, 2015). Their respective bulk material does not possess these characteristics at micro or macroscale. For example, 20 nm gold, platinum, silver and palladium NPs have characteristic wine red colour, yellow grey, black and dark black colours respectively (Dreaden *et al*., 2012). Figure 1 is an illustration of this example, the nanoparticles (NPs) show characteristic colours and properties with the variation of size and shape.

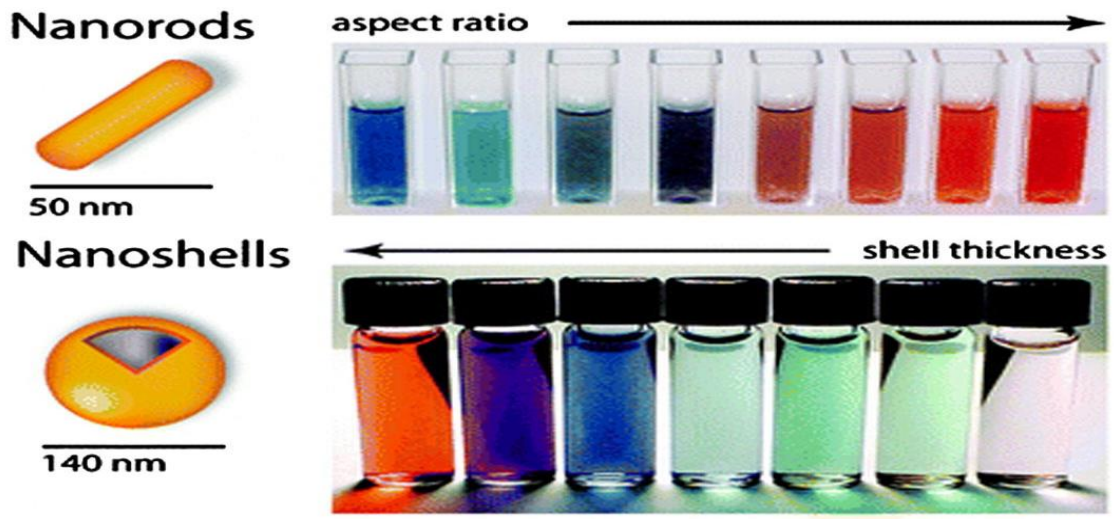

Figure 1: Size and shape dependant colour variation of gold nanoparticles (AuNPs). Image adapted from Dreaden *et al*. (2012).

These unique characteristics allow for a wide range production of materials which ultimately lead to novel applications (Adams & Barbante, 2013). This has been the driving force behind nanoparticle synthesis and the rapid development of nanomaterial production (Pal *et al.*, 2013). An assortment of nanomaterial are currently being produced at an industrial scale and there is a lot effort being put for research and development of NPs (Benelmekki, 2015).

Gold NPs (AuNPs) are one of the widely studied NPs as a result of their exceptional features (Montazer & Harifi, 2018). AuNPs are used in a broad range of applications in various areas such as catalysis, bio-labelling, optical devices and drug delivery (Daniel & Astruc, 2004; Pal *et al*., 2013). The beautiful colour and unique physical and chemical properties of AuNPs has attracted a tremendous amount of attention in their synthesis (Dreaden *et al*., 2012). The chemical reduction method is the most common and widely used method for AuNPs preparation. Their conventional synthesis methods involve toxic chemical use and physical processes which are expensive, require high-energy consumption and frequent use of harmful material which later on become accountable for various risks such as environmental toxicity, cytotoxicity and excessive energy consumption (Jiménez *et al*., 2010; Noruzi *et al*., 2011). Furthermore, the hazardous reagents used has prevented their use in clinical and biomedical applications, despite the nanoparticle considerable potential (Noruzi *et al*., 2011). For these above mentioned reasons, the use of biological material for gold nanoparticle synthesis has emerged as an ideal substitute to conventional methods.

On the other hand, agricultural waste and post-harvest losses possess a huge challenge in its disposal and management (Domínguez *et al*., 2014). Agro-processing produces many by-products which are discarded as they are regarded as waste. These by-products have an organic charge and when discarded as waste they have a significant environmental impact (Gómez *et al*., 2014). Additionally these by-products require handling, transportation and storage which results in added costs. Therefore, there is a need for more alternative uses of these by-products aside from use as animal feed and fertilizers (Gómez *et al*., 2014). For example, *Persea americana* (Avocado) is one of the largest fruit crops in the world with an estimated global production of over 5,92 tonnes (Shahbandeh, 2019). Majority of the avocado produced in the world is commercialized by the retailer and food industry for human consumption, as fresh fruit or after processing in the form of avocado derivatives (guacamole, avocado oil, flavouring agents, *etc*) (Caballero, Finglas, & Toldra, 2015). These products are derived from the flesh of the avocado, while the rest of the fruit (peels and seeds) has no commercial use and is managed as waste (Domínguez *et al*., 2014). The avocado seed contains many phytochemicals which are

beneficial and have been proven to have antimicrobial, anti-oxidant, anti-inflammatory and anticancer activities (Alkhalf *et al*., 2018; Nurliza & Savitri, 2017; Villarreal-Lara *et al*., 2019; Widiyastuti *et al*., 2018). These phytochemicals have also been employed for nanoparticle production (Chandrappa, Vinay & Chandrashekar, 2017; Sneharani, Prabhudev, & Sachin, 2019).

1.2 Problem statements

- There is a need for the development of more green synthetic methods for gold nanoparticle production, which presents cleaner, reliable, biologically compatible and environmentally friendly NPs.
- Due to the large amounts of seeds produced as waste for disposal in centralized avocado transformation plants, there is a need to find alternative uses for these by-products. Furthermore, utilising these by-products may generate an additional source of revenue for this industry and may reduce the environmental burden associated with agricultural waste disposal.

Green synthesis is an emerging area in the field of bionanotechnology that provides economic and environmental benefits as an alternative to chemical and physical methods used for nanoparticle synthesis. It is aimed at minimizing generated waste and implementing sustainable processes (Zhu, Pathakoti, & Hwang, 2019). This synthesis includes the use microorganisms and plants or plant extracts for the production of NPs (Menon, Shanmugam, & Kumar, 2017). Green synthesis using plants is a green chemistry approach that interconnects nanotechnology and plant biotechnology (Parveen, Banse, & Ledwani, 2016). Plants/plant material can be used for the bioreduction of metal ions to form NPs. It has been demonstrated that plant metabolites like sugars, terpenoids, polyphenols, alkaloids, phenolic acids and proteins play an important role in the bio-reduction of metal ions to produce NPs and in supporting their subsequent stability (Nath & Banerjee, 2013). Green synthetic methods present a cleaner, reliable, biologically compatible, environmentally friendly option for gold nanoparticle synthesis (Jain *et al*., 2011; Kulkarni & Muddapur, 2014). In light of the above mentioned:

1.3 Aim:

- This study aims to synthesize biogenic gold NPs from aqueous avocado seed extract (AvoSE) and study the effects of parameters which affect synthesis to optimize production
- To evaluate the AuNPs produced for their potential antibacterial, anti-cancer and catalytic activity

1.4 Objectives

- To prepare an aqueous extract from avocado seed
- Synthesize AuNPs from the AvoSE using a green synthesis method and to characterize the produced AuNPs
- To evaluate the antibacterial effects of AvoSE-AuNPs against known antibiotic-resistant bacterial strains.
- Investigate the catalytic activity of the AuNPs in the reduction of 4-NP by NaBH4.
- Evaluate the anti-cancer effects of the AvoSE-AuNPs on cancer cells.

1.5 Thesis Outline

Chapter 1: Presents a brief background on the study, including conventional methods used for AuNPs synthesis, issues which the use of conventional methods presents, issues of agricultural waste, avocado seeds as a waste product, green synthesis, its importance and as a solution. The problem statements, study aims and objectives towards solving the problems.

Chapter 2: Review of literature on nanotechnology, AuNPs, conventional nanoparticle synthesis methods, drawbacks of conventional methods, green synthesis, biosynthesis using plants, background on avocado, and applications of AuNPs.

Chapter 3: Materials and methods used for the synthesis, characterization and testing of biological activities of AvoSE-AuNPs

Chapter 4: This chapter reports and discusses the green synthesis of AvoSE-AuNPs. It also details the characterization of the produced NPs using various techniques such as UV-vis spectroscopy, HRTEM, FTIR and DLS analysis

Chapter 5: This chapter reports on the tested antimicrobial, catalytic and anticancer activities of the produced AvoSE-AuNPs

Chapter 6: Summary, conclusions and recommendations for future work.

CHAPTER 2

LITERATURE REVIEW

2.1 Nanotechnology

The introduction of the concept of "nanoscience" is generally attributed to a visionary talk "There's plenty of room at the bottom" which was given by Nobel Prize Laurette Richard Feynman in 1959 (Feynman, 1960). It was only in 1974 that the word "nanotechnology" was first defined by Norio Taniguchi in a scientific conference (Nunes *et al*., 2019). The prefix "nano" refers to one billionth of a unit ($x10^{-9}$) and it stems from the Greek word "nanos" which means "dwarf". The nanoscale is used to describe very small diameters. Hence, "nano"-technology is defined as the fabrication, manipulation, production and application of structures, devices and systems with size diameters below 100 nm. Nanotechnology is a multidisciplinary science encompassing a variety of fields including engineering, medicine, biotechnology, physics and chemistry (Iravani, 2011). The exponential growth of interest in this science is due to the potential and realised benefits. Nanotechnology is deemed to potentially bring beneficial advancements in areas such as the development of therapeutics, decontamination of water and material sciences by enabling the production of lighter and stronger material (Benelmekki, 2015). The key feature of nanotechnology and its potential in different industries revolves around unique properties which are the outcome of 'the miniaturization of bulk materials". The reduction in size results in physical and chemical property changes (Wadhwani *et al*., 2014). If the bulk materials are reduced to have their four dimensions lower than a few hundred nanometers, they are referred to as nanoparticles (NPs) (Tiwari, Tiwari, & Kim, 2012). The manufacturing of NPs, both in nature and by humans, dates back to pre-Christian times with the beginning of glass –making in Egypt and Mesopotamia. Since then its been established that some ordinary material when reduced to the nanoscale demonstrate a novel change in characteristics such as reactivity, conductivity, extraordinary strength and superparamagnetic behaviour which is dissimilar to its characteristics at macroscale (Schaming & Remita, 2015). This change is beneficial because it allows a wide range of design and production of materials with novel applications which translates in economic benefits. In the year 2010, more than 1000 products containing nanoparticles were produced and became commercially available (Robertson *et al*., 2010). Furthermore, an assortment of nanomaterials is currently produced at an industrial scale, while others are being produced at a smaller scale because they are still under research and development (Benelmekki, 2015).

NPs are manufactured according to required applications and can be made up of different elements such as metals (gold, silver), metal oxides (titanium dioxide), semiconductors (silicon) or carbon (Schaming & Remita, 2015). The classification of NPs is generally broadly divided into organic, inorganic or carbon based groups (Ealias & Saravanakumar, 2017).

- Carbon-based NPs: Fullerenes and carbon nanotubes represent the two major classes of this group (I. Khan, Saeed, & Khan, 2019). Fullerenes are made of globular hollow cage made from arranged pentagonal and hexagonal carbon units (Figure 2.1). These NPs created noteworthy commercial interest due to their electrical conductivity, high strength, structure, electron affinity and versatility (Astefanei, Núñez, & Galceran, 2015). Carbon nanotubes structurally resemble graphite sheets rolling upon itself (Figure 2.1). They are elongated and tubular structures 1-2 nm in diameter. Due to their unique physical, chemical and mechanical characteristics, these materials are not only used in original form but also in nanocomposites for many commercial applications such as fillers, gas adsorbents for environmental remediation and as support mediums for different inorganic and organic catalysts (I. Khan *et al*., 2019; Saeed & Khan, 2016).
- Organic NPs: These NPs are commonly described as solid particles composed of organic compounds mainly lipids or polymeric. They include dendrimers, micelles, liposomes and ferritin *etc* (Figure 2.1). These NPs are biodegradable, non-toxic and some have hollow cores , also known as nanocapsules and are sensitive to thermal and electromagnetic radiation such as heat and light (Tiwari, Behari, & Sen, 2008). These particles are generally an ideal choice for drug delivery and are mostly used in the biomedical field.
- Inorganic NPs: Include metal and metal oxide based NPs (Figure 2.1). Metal NPs are synthesized from metals such as aluminium (Al), cadmium (Cd), cobalt (Co), copper (Cu), zinc (Zn), iron (Fe), lead (Pb), silver (Ag) and gold (Au) etc. (I. Khan *et al*., 2019). Metal NPs have distinctive size and surface characteristics like high surface area to volume ratio, pore size, surface charge and density, crystalline and amorphous structures, colour reactivity and sensitivity to environmental factors such as air, heat and sunlight (Ealias & Saravanakumar, 2017). Due to the optical properties metal NPs find applications in many research areas (I. Khan *et al*., 2019). The metal oxide NPs are made to modify the properties of their respective metal NPs for example iron NPs oxidise to iron oxide in the presence of oxygen at room temperature and that increases its reactivity compared to FeNPs (Ealias & Saravanakumar, 2017). Metal oxide NPs are mainly synthesized due to their increased

reactivity and efficiency. These NPs possess exceptional properties which have drawn much attention in research fields (Prasanna *et al*., 2019).

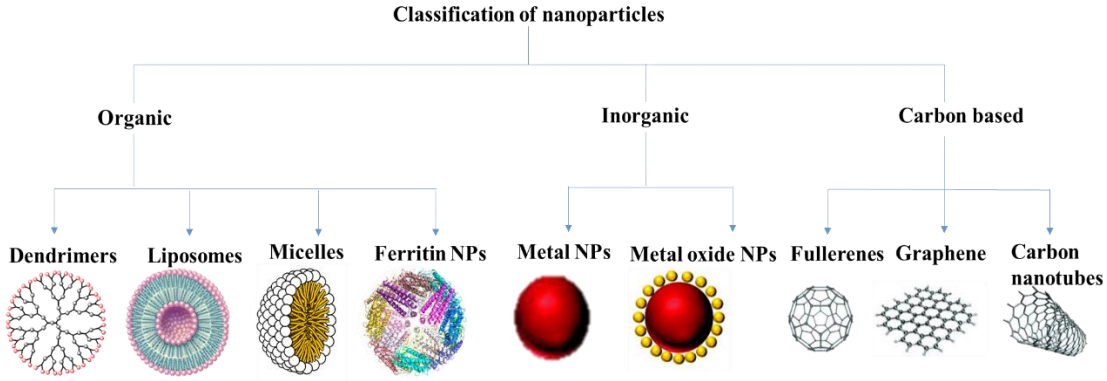

Figure 2.1: Classification of NPs based on their nature.

2.2 Gold nanoparticles

Gold colloids also known as AuNPs are amongst the most widely studied NPs (Majdalawieh *et al.*, 2014). AuNPs are nanometer sized particles of gold in suspension. The history of AuNPs dates back to Roman times when they were used in glass staining for decorative purposes. The modern scientific studies of AuNPs was driven by Michael Faraday's work in the 1850s. Faraday was fascinated by the ruby colour of AuNPs (Faraday, 1997). He discovered that the optical properties of AuNPs differ from the corresponding bulk metal. In large amounts, Au is yellow due to the reduced reflectivity of blue light in light conditions. The colour progressively changes towards orange/red as the particle size decreases and this an effect of changes occurring in its surface plasmon resonance (Yeh *et al.*, 2012).

AuNPs possess unique properties such as size and shape dependent optoelectronic properties, large surface to volume ratio, excellent biocompatibility and low toxicity which makes useful tools in nanotechnology (Khlebtsov & Dykman, 2011; Sau *et al*., 2010). The important physical properties of AuNPs include surface plasmon resonance (SPR) and the ability to quench fluorescence.

In aqueous solution these particles exhibit a range of colours attributed to a change in core size and they generally exhibit a size-relative absorption peak between wavelengths 500 – 550 nm (Jain *et al*., 2006). The absorption band arises as a result of the collective oscillation of electrons which are excited by incident photons and this is referred to as the SPR band (Harish *et al*., 2018). This phenomena is influenced by size, shape, solvent, surface ligand, core charge and temperature (Toderas, Baia, Maniu, & Astilean, 2008). Hence, it is absent in bulk material. The aggregation of the AuNPs can be monitored by a significant red-shift in the SPR frequency,

broadening of the band and colour change in solution from red towards blue due to the interparticle plasmon coupling (Alizadeh & Nazari, 2019).

AuNPs can quench flourophores that are nearby (Swierczewska, Lee, & Chen, 2011). The quenching ability of AuNPs to flourophores results from an overlap of the SPR band of the AuNPs and the emission spectrum of the excited flourophores and this phenomena is known as fluorescent resonance energy transfer (FRET) (Kochuveedu & Kim, 2014). AuNPs can also act as electron acceptors to quench fluorophores and this is known as the photo induced electron transfer (PET) process (Barazzouk, Kamat, & Hotchandani, 2005). The PET process is modified by charging or discharging the Au core and can be utilised in the fabrication of sensors. The quenching ability of AuNPs is dependent on size and shape, with the smallest AuNPs possessing the strongest quenching effects (Swierczewska *et al*., 2011).

2.3 Nanoparticle synthesis (chemical, physical and bio-mediated)

Faraday reported on the effects of quantum size and the first synthesis of AuNPs in solution in the year 1857 (Faraday, 1997; J. Khan *et al*., 2011). Since then there have been numerous methods employed for the synthesis of AuNPs. Generally synthesis of NPs involves 2 approaches: Top down and bottom up (Figure 2.2). The top down method involves size reduction of starting bulk material to smaller sized particles (Adams & Barbante, 2013). The bottom up process involves a build up of smaller units, for example assembling from atoms, molecules and smaller particles. The initial step involves the formation of nanostructured building blocks which are subsequently used for the NP synthesis process. The final NP structure is an assembly of these building blocks. The methods require physical, biological and chemical means for the synthesis processes. Plasma arcing, ball milling, thermal evaporate, spray pyrolysis, ultrathin films, pulsed laser desorption, lithographic techniques, sputter deposition, layer by layer growth, molecular beam epistasis and diffusion flame are some examples of physical methods used for synthesis of NPs (Adams & Barbante, 2013).

Chemical methods include electrodeposition, sol-gel process, chemical solution deposition, chemical vapour deposition, soft chemical methods, hydrolysis co-precipitation method and wet chemical methods (Adams & Barbante, 2013).

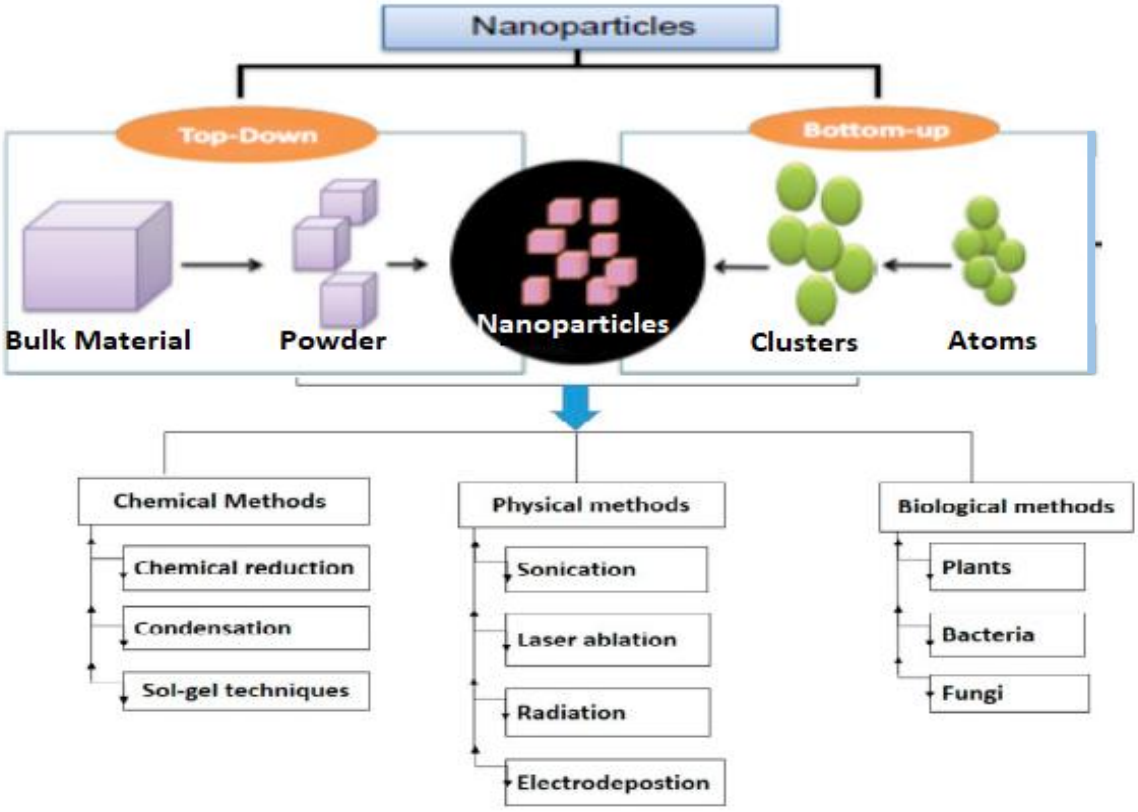

Figure 2.2: Schematic representation of nanoparticle synthesis methods

2.4 Conventional approaches for AuNPs synthesis

2.4.1 Chemical synthesis

AuNPs are produced chemically through reactions which involve the reduction of Au ions by reducing agents or by externally sourced energy. The chemical reduction method involves two main steps, i.e. (i) reduction using agents such as borohydrides, formaldehyde, sugars, citric and oxalic acids and (ii) stabilization using agents such as trisodium citrate dehydrate, nitrogen-based ligands, dendrimers and surfactants to avoid aggregation (Sengani *et al.*, 2017). The Turkevich method was first developed in 1951 and has since been highly utilised due to its simplicity, ease of synthesis, controllable size and stability of the colloidal nanoparticles produced (Polte *et al*., 2010). This technique involves the use of citrate for the reduction of hydrogen tetrachloroaurate (III) ($HAuCl_4$) in water. The $HAuCl_4$ solution is boiled, followed by the addition of trisodium citrate dehydrate under vigorous stirring (Brust *et al.*, 1994). The solution changes from a yellow colour to wine red after a few minutes and results in approximately 20 nm sized AuNPs. The citrate acts as both a reducing and stabilizing agent. Since 1951 the method has been modified by controlling the ratio of reducing agent to gold in order to produce AuNPs with diameters ranging from 15-150 nm (Kimling *et al.*, 2006). A study by Kimling *et al.* (2006), reported that a high citrate concentration leads to AuNPs with

a smaller size and that a lower concentration leads to the aggregation of smaller sized AuNPs which result in larger particles. The major contribution following Turkevich's methods was made in 1994 when Brust-Schiffrin reported a method which utilized the potent thiol-gold interaction to protect and stabilize AuNPs with thiol ligands (Brust *et al.*, 1994). In the two phase (water-toluene) reaction, $AuCl_4^-$ is reduced by sodium borohydride in the presence of alkanethiols to produce nanoparticles in the 1-3 nm diameter range (Wadhwani *et al.*, 2014). The Brust-Schiffrin method allows an easy approach to synthesizing thermally stable and air-stable AuNPs of controlled size and low poly-dispersity (Herizchi *et al.*, 2016).

The main advantage of chemical mediated synthesis approach is that it allows production of particles with defined size, dimension, composition and structure that allows for ease of use in many research areas such as catalysis, data storage, drug delivery, imaging and sensing. Furthermore, the mechanisms of chemical NP synthesis can be easily predicted (Deepak *et al.*, 2019). Chemical methods for NP synthesis have helped with the development nanotechnology. However, it has also increased pollution, including water and air pollution (Shinde, Keskar, & Argade, 2012). The toxic chemicals used as reducing and stabilising agents for NP synthesis are reported to be hazardous and the association may hinder the use of these NPs in biomedical applications due to possible adverse effects (Noruzi *et al*., 2011). The reagents used are often used in excess because they are not in stoichiometric quantities therefore resulting in high costs for synthesis and wastage (Kulkarni & Muddapur, 2014).

2.4.2 UV-assisted synthesis of AuNPs

Photochemical reduction methods have been explored to produce metal nanoparticles. The approach includes the use of photosensitizer, dendrimers (as stabilisers), surfactants or the placement of metal salts in polymer films (Zhou *et al.*, 1999). These agents act as soft templates during AuNPs fabrication and prevent aggregation by providing a steric hindrance effect (Sengani *et al.*, 2017). UV radiation at different wavelengths encourages the chemical reactions with Au^- ions and the presence of surfactant/polymers has an effect on the particle dimensions by ensuring that with an increasing polymerization degree, the particle size is reduced (Sau *et al.*, 2001). This method results in the formation of single crystallite-based AuNPs (Majdalawieh *et al.*, 2014).

Eustis *et al.* (2005) reported an improved photochemical synthesis technique for the production of AuNPs. The synthesis utilised continuous wave UV irradiation (250 - 400nm), PVP (capping agent), ethylene glycol (reducing agent) to form the AuNPs. The study reported

that the formation of the NPs was dependent upon the concentration of glycol and the viscosity of the solvent mixture. The process was further enhanced by the addition silver ions (Ag^{+}) to the solution, resulting in an increase in AuNP production (Callegari, 2003).

Radiation mediated synthesis methods allow for proper control of the nucleation process depending on the dose and rate of dose (de Freitas *et al*., 2018). This method does not require reducing agents and the possibility of combining NPs synthesis with simultaneous sterilization. On the other hand, the drawbacks include that there may be low availability and restricted access to gamma irradiators, electron beam accelerators or X-ray devices in certain parts of the world which are still developing. Additionally, some materials (capping or stabilizing agents) may be sensitive to high energy irradiation and thus may not work effectively (de Freitas *et al*., 2018).

2.4.3 Laser ablation synthesis of AuNPs

Laser ablation is a simple and versatile physical technique used to produce NPs (Pareek *et al*., 2017). In this method laser beam irradiation is used to gradually remove solid target materials (Kim *et al.*, 2017). The process involves high energy concentrated at a specific point of a solid surface, the surface absorbs the laser energy and is heated resulting in evaporation or sublimation of the material (Amendola *et al.,* 2006; Pareek *et al.,* 2017). The laser energy is absorbed at a low laser flux for the evaporation or sublimation to occur, a higher laser flux converts the precursor material to form plasma (Pareek *et al.*, 2017). The optical properties of the precursor material and the wavelength at which the laser energy is applied have an effect on the amount of material removed in the process (M. Kim *et al*., 2017). Fumitaka *et al.* (2001), produced AuNPs with a size range lower than 5 nm using the laser ablation technique. The synthesis required a Au (III) tetrachloroaurate metallic precursor in an aqueous solution of sodium dodecyl sulphate (SDS). Laser energy was irradiated at 532nm considering that the optical absorption of AuNPs is within that vicinity, therefore a further photo-induced effect was expected. The size and abundance of the AuNPs were examined by changing the concentration of SDS and the wavelength of the ablation laser. An increase in surfactant concentration shifted the size distribution of the nanoparticles to a smaller size range (Fumitaka *et al*., 2001).

An advantage of laser ablation synthesis is that metal NP synthesis can be conducted in both aqueous and organic solvents. Additionally there is no requirement for removal of excess reagents (Pareek *et al*., 2017). The production results in high yield, fast processing time and

the size, morphology and composition of NPs produced can be controlled (Pareek *et al*., 2017). Laser ablation is costly because of the high price of the laser systems and the most diffused laser sources are not capable of producing nanomaterials at an industrial scale (Sportelli *et al*., 2018). This method also requires a considerable amount of energy due to high energy consumption (Jendrzej *et al.*, 2017).

2.4.4 Green synthesis of AuNPs

The use of microorganisms and biological systems in the production of NPs has become an important discovery in nanotechnology. Green synthesis of nanoparticles is a method which utilises biological materials such as plant-based compounds/derivatives, fungi and bacteria (Khandel *et al.*, 2018; Thakkar, *et al.*, 2009). Green synthesis mimics nature's mode for nanomaterial synthesis (Dahl, *et al.*, 2007). The biological materials serve as sources for precursor biomolecules such as proteins, polyphenolics, alkaloids, carbohydrates and lipids used as the reducing and stabilizing agents in NP synthesis (Dahl *et al*., 2007). The use of microorganisms and biological systems in NP synthesis has shown to be the critical solution that conventional techniques such as those mentioned previously fell short of (Anastas & Eghbali, 2010; Dahl *et al*., 2007). The practise of a set of principles aimed at reducing or eliminating hazardous substances generated or used in the design, manufacturing and application of chemical products is called green chemistry. Green chemistry constitutes of a set of 12 principles used to navigate and regulate materials exposed to the environment (Dahl *et al*., 2007). Green synthesis is based on green chemistry principles and can thus be deemed as an ecological alternative which also presents benefits such as reduced downstream processing costs of the synthesized nanoparticles and increases the possibility of applications as a result of their biogenic nature. Therefore, this technique can be said to supersede the threats presented by the conventional methods used to synthesize nanoparticles (Anastas & Eghbali, 2010).

2.4.4.1 Green synthesis of AuNPs using microorganisms

The interactions of microbes and metals is well studied (Beveridge *et al.*, 1996) and the science has been employed in biotechnological processes such bioremediation. Studies of these interactions have now extended to synthesis of nanosized materials (Gericke & Pinches, 2006). Microbial cells have highly structured and biosynthetic pathways that have been used for the synthesis of nanosized materials and this has emerged as an alternative eco-friendly approach for the synthesis of metallic NPs (Lal & Nayak, 2012). Microorganisms such as bacteria, fungi, yeast and algae can synthesize nanoparticles by utilizing the inorganic materials which they

produce intra or extracellularly (Khandel & Shahi, 2016). Inorganic materials such as enzymes like ligninases, laccases, reductases and peptides are suggested to be involved in the mechanisms of nanoparticle formation (Kanaras *et al*., 2003). The precise mechanism for nanoparticle formation mediated by microbes has not yet been established because different mircobes react differently with metal ions during the formation process (Hulkoti & Taranath, 2014). However, microbial mediated synthesis of nanoparticles can be grouped and explained in two approaches:

i) Intracellular synthesis of nanoparticles

Intracellular synthesis involves ion transportation through the cell wall of microorganisms driven by electrostatic interactions (Khandel *et al*., 2018). The metal ions are reduced by enzymes present and nanoparticles formed are transmitted through the cell wall (Hulkoti & Taranath, 2014). The processes involved in intracellular approach are trapping, bio-reduction and capping (Mukherjee *et al*., 2001). An example of intracellular synthesis of gold nanoparticles is reported by Mukherjee *et al*. (2001), where they suggest that the bio-reduction of gold metal ions mediated by the fungus *Verticillium sp*. occurs through a mechanism which is initiated by an electrostatic force. The electrostatic force causes the metal ions to bind to the cell surface and the interaction is caused by the opposite charges on the metal ion and fungal cell surface (Kashyap *et al.*, 2013). The absorbed metal ions are reduced by the enzymes present in the cell wall of the fungi. The enzymes contain groups which are positively charged and thus the interaction leads to the aggregation of nano structures and ultimately leading to the formation of gold nanoparticles (Mukherjee *et al*., 2001).

ii) Extracellular synthesis of nanoparticles

The extracellular mechanisms of nanoparticle synthesis involves the secretion of reductases which interact with metal ions forming nanoparticles on the outer area of the microorganism cell (Khandel & Kumar, 2016). In previously reported studies NADH and NADH- dependant enzymes are suggested to be the important factors responsible for the synthesis of metal nanoparticles (Mukherjee *et al.*, 2001; Senapati e*t al*., 2005). He *et al*. (2007), studied extracellular biosynthesis of gold nanoparticles mediated by the NADH cofactor and NADH-dependent enzymes secreting bacteria *Rhodopseudomonas capsulate*. The study suggests that the bio-reduction is initiated by an electron transfer from NADH through NADH-dependant reductase which acts as the electron carrier. The gold ions (Au^{3+}) gain electrons and are reduced to Au^{0} ultimately resulting in the formation of gold nanoparticles.

Microorganisms are used for cost-effective nanoparticle synthesis due to their ease of handling, growth in low cost-medium like cellulosic wastes or wastelands. This method can provide controlled size and morphology through manipulation of parameters such as pH, temperature, concentration of substrate and incubation time (Pareek *et al*., 2017). It is an eco-friendly method which produces products compatible for pharmacological applications (Khandel *et al*., 2018) . However, this approach requires high aseptic conditions, special maintenance of microorganisms resulting in complex and costly large scale production (Singh *et al.*, 2015). Of the various biological materials, plant biomass possesses several advantages over microorganisms in nanoparticle synthesis. Plant extracts for nanoparticle synthesis is fast-becoming the favoured and popular approach.

2.4.4.2 Green synthesis of Au NPs using plant material

Almost all parts of plants have been successfully used in the synthesis of several metallic Nps including Au, platinum, cobalt, copper, zinc and Ag (Sharma, Yngard, & Lin, 2009). Plants produce biomolecules which have been employed for nanoparticle synthesis as reducing and capping agents, and have been found to stabilize and govern morphology of the nanoparticle produced (Qidwai *et al*., 2018). Examples of these biomolecules include and are not limited to phenols, polysaccharides, flavones, terpenoids, alkaloids, proteins, amino acids and enzymes. More than one of these groups may be responsible for the production of metallic NPs (Nath & Banerjee, 2013). Several plants have been reported for the metal accumulation property and reduction of the accumulated metals producing NPs (Vijayaraghavan & Ashokkumar, 2017). For synthesis, the plant biomass which can be in different forms (i.e. powder or extracts), is mixed with a metal salt solution with or without agitation and within a span of time nanoparticles are formed (Vijayaraghavan & Ashokkumar, 2017). Plants may be used in their live or dead forms for biosynthesis of NPs. The first report on the formation of gold nanoparticles using live plants was made by Gardea-Torresdey *et al*. (2002), where Au^{3+} ions were reduced in solid media to Au^0 by the Alfalfa plant, the metal atoms were absorbed into the plant where nucleation and growth of the gold nanoparticles proceeded to take place.

The unique properties of AuNPs permit their use in applications such as biomedical, catalysis, drug and gene delivery (Siddiqi & Husen, 2017). For most of these applications these nanoparticles are most desired when synthesized through eco-friendly and chemical free routes (Vijayaraghavan & Ashokkumar, 2017). The reaction below summarizes plant mediated gold nanoparticle synthesis.

$H^+Au^{3+}4Cl^-\cdot 4H_2O$ + Plant molecules (OH, COOH, NH_2 etc.) → Au^0 nanoparticles

The formation of AuNps can be visually observed through the formation of reddish colour. A study by Begum *et al.* (2009), produced gold nanoparticles using leaf extract from black tea. The study identified that the bioreduction of the Au ions was due to the presence of polyphenols from the tea. Some natural compounds isolated from plants like polyphenols show activity against various diseases. Cai *et al*. (2004), identified antioxidant and anticancer properties from phenolic compounds extracted from medicinal plants. Advantages of using plants for NP synthesis include availability of plant material, ease of handling and the broad assortment of metabolites available to serve as precursor biomolecules for synthesis (Geraldes *et al*., 2016). Screening medicinal plants for their biological activity has been a major interst in research since the 1960's (Cai *et al*., 2004).

2.5 Persea americana (Avocado)

Persea americana commonly known as Avocado is a flesh fruit which contains a single seed (Figure 2.3). The skin of the fruit is identified as green, black, purple or reddish depending on the stage of maturity of the fruit (Bertling, Tesfay, & Bower, 2007). *Persea americana* belongs to the flowering plant family Lauraceae. There are eight well-defined geographical types of Avocado (Bertling *et al*., 2007). The commercial avocado crop is defined under 3 horticultural races, namely the Mexican (*Persea americana* variety *drymifolia*), West Indian (*P. americana variety americana*), and Guatemalan (*P. americana variety guatemalensis*). The 3 horticultural races have over 1000 cultivars between them. The current commercial varieties in the world are hybrids of the races. More than eighty percent of the cultivars produced in South African nurseries are the dark skinned Hass and Hass-type cultivars. The rest of the twenty percent is made up by the green skinned cultivars such as 'Fuerte', 'Pinkerton', 'Ryan' and 'Reed' (Augustyn *et al*., 2019). In South Africa majority of Avocado orchards are located in the North Eastern regions of the country like Limpopo and Mpumalanga provinces. The South African Avocado industry consists of approximately 17 500 ha spread over the above mentioned regions and certain areas of KwaZulu-Natal, Eastern Cape and Western Cape (Augustyn *et al*., 2019). The Avocado industry is growing by 1000 ha per annum and has a significant value to the economy as over 50% of total production is exported while the rest is consumed domestically (Augustyn *et al*., 2019).

Figure 2.3: Image of dry Avocado seeds used in this study

2.5.1 Phytochemical profile of Avocado

Avocado has one of highest oil content amongst other fruits (Dabas *et al.*, 2011). Avocado pulp contains 30% oil rich in water based matrix of monounsaturated fatty acid which seem to enhance the bioavailability of nutrients and phytochemicals. A high avocado enriched diet is reported to improve the lipid profile in healthy and especially mild hyperclosterolemic patients. Essentially, the consumption of avocado is believed to have beneficial effects on cardiovascular diseases. Avocado is rich in nutrients such as unsaturated fatty acids, vitamins B and E, fiber, proteins, fats and others (Wang *et al*., 2010; Dabas *et al*., 2011). Various classes of bioactive compounds have been reported to be present in avocado pulp including phytosterols, triterpenes, flavonoid dimers, proanthocynidins and fatty acids, which are the main component of the lipid fraction of the fruit. Avocados are also the richest fruit source of phytosterols. Salgado *et al.* (2008), evaluated the composition of phytosterols which are plant derived analogs of cholesterol and reported that the most abundant sterol present in avocado pulp is β-sitosterol. The β-sitosterol compound has been associated with anti-inflammatory, antioxidant and apoptotic pharmacological activities (Saeidnia, Manayi, Gohari, & Abdollahi, 2014). Wang *et al.* (2010) and Hurtado-Fernández *et al.* (2011), report the presence of protocatechuic, *p*-coumaric, ferulic, sinapic, benzoic, transcinnamic acids and epicatechin from the Hass variety. Lu *et al*. (2009), profiled carotenoids present in avocado flesh as lutein, zeaxanthin, β-cryptoxanthin, α-carotene, β-carotene as the most abundantly occurring carotenoids. The concentrations of the carotenoids were determined by HPLC using external calibrations and xanthophylls predominated over carotenes. Xanthophylls have been previously reported to be the primary carotenoid subclass present in avocados. Xanthophylls are oxygen-containing fat-soluble antioxidants. Xanthophyll carotenoids have been described to have a positive impact

on cardiovascular diseases as they appear to minimize vascular damage caused by oxidized low density lipoprotein-cholesterol (LDL-C). LDL-C is a preliminary biomarker responsible for the initiation and progression of vascular damage and xanthophyll carotenoids act by reducing the circulating oxidized LDL-C (Hozawa *et al*., 2007). Amongst fruits and vegetables Avocados have the highest lipophilic total antioxidant capacity.

Avocado is also a major fatty acid source containing monounsaturated, polyunsaturated and saturated fatty acids (Carvalho *et al.*, 2015). In general, the characteristics of oils present in the fruit are the same throughout however, the proportional distributions often differ between cultivars of different origins. Oleic acid has been reported to be the main fatty acid (about 67-70% of total content) present (Carvalho *et al*., 2015; Q. Lu *et al*., 2009). A study by Donetti & Terry (2014), reported differences in oleic content between Chilean, Spanish and Peruvian cultivars of the fruit. The authors suggested oleic acid as a potential biochemical marker for distinguishing the origin of imported avocado fruits. Linoleic acid is similarly abundant and accumulates differently throughout the ripening of the fruit. Fatty acid content in the fruit can help promote healthy blood lipid profiles, enhance bioavailability of fat soluble vitamins and phytochemicals. Moreover, fatty acid content in avocado can potentially be used as an origin and health quality marker of the fruit (Carvalho *et al.*, 2015).

Studies on the seed specifically have reported high levels of B-type procyanididns and A-type present as minor components. Wang *et al.* (2010) and Hurtado-Fernández *et al.* (2011), report the presence of protocatechuic, *p*-coumaric, ferulic, sinapic,benzoic, transcinnamic acids and epicatechin from the Hass variety. The major polyphenols present in the seed are catechin, epicatechin and leucoanthocyanidins (Melgar *et al*., 2018). The phenolic content and antioxidant capacity of raw blueberry a fruit known for its high antioxidant capacity is several-folds less than that of avocado seeds (Wang *et al*., 2010). Polyphenols are associated with anti-inflammatory and antioxidant properties because they can scavenge free radicals and prevent oxidation. Avocado seed is reported to have higher phenolic content than the pulp and phytochemical studies have also reported health benefits (Bertling *et al*., 2007; Wang *et al*., 2010). A study by Oboh *et al.* (2016) reported higher phenolic content in Avocado leaves compared to the seed and suggested that this may be due to environmental stresses. Stress factors induce an increase in phenolic compound production to prevent the oxidative damage and since the leaves are exposed to the environment than the seed which is more protected, the leaves are expected to contain more phenolic compounds. Each seed phenolic content may vary due to factors such as growth conditions, variety and maturity which influence the content

(Bertling *et al*., 2007). The profiling methods used also influence the content reported. A study by Dabas *et al.* (2011), presented data which showed that Avocado seed extract may also be used as a natural food colourant due to the stable orange colour it forms when crushed in the presence of air.

2.5.2 Avocado seed biological properties

Avocado seeds have high contents of bioactive phytochemicals such as phenolic acids, condensed tanins, flavonoids, hydroxybenzoic and hydroxycinnamic acids as previously discussed in the above section. These bioactive compounds have also been shown to possess biological activities. There have also been studies which report that avocado seed exhibits biological activities such as antioxidant, antibacterial and anticancer properties. A study Dabas *et al*. (2011) assessed the antioxidant and cancer inhibitory activity of AvoSE. Oxygen radical absorbance capacity assays, prevention of lipid oxidation, cell viability, cell cycle analysis and apoptosis analysis were conducted. The AvoSE exhibited dose-dependent radical scavenging activity at maximal effective concentration of 40 µg/ml. The extract also displayed dose-dependent antioxidant activity at tested concentration and reduced the cell viability of four human cancer cell lines in a time dependent manner at maximal effective concentration between 19 - 40 µg/ml. The cell cycle analysis proved that the extract caused G_0/G_1 arrest. The study proved that the extract had considerable antioxidant and anticancer activity *in vitro*. Furthermore, the study suggested that the AvoSE may have a role as a source of novel natural antioxidants and anticancer compounds.

The antibacterial activity of the avocado seed has also been proven in studies. An experiment by Idris, Ndukwe, & Gimba (2010) proved that extracts of avocado seed showed antibacterial activity by well diffusion assays. The extracts displayed inhibition zones at 3.25 g against *Staphylococcus aureus* and *Staphylococcus pyogenes*. Nurliza & Savitri (2017) also proved that an ethanol extract of avocado seed exhibited antibacterial activity. The study reported antibacterial effect *in vitro* against *Porphyromonas gingivalis* with minimal inhibition concentration at 50% of extract concentration and a minimum bactericidal concentration at concentrations of 60%.

2.6 AuNPs in Multidrug resistance

Bacteria have existed on earth for over 3.8 billion years (Cooper, 2000). They exhibit genetic and metabolic diversity and play an essential role in maintaining and sustaining ecosystems (Tshikantwa *et al.*, 2018). For survival, microorganism have developed mechanisms which help them deal with selective pressure exerted by the environment and competition in the

environment (Munita & Arias, 2016). These mechanisms help microorganisms avoid killing by antimicrobial agents and it's a process which has most likely developed over millions of years of evolution. The emergence of antimicrobial resistance (AMR) is a serious global health problem (Golkar, Bagasra & Pace 2014). Since the treatment of the first patient with antibiotics, persistent multidrug-resistant bacteria (MDR) have emerged and spread across the environment, humans and animals (Davies & Davies, 2010). The causes of AMR has been attributed to overuse and misuse of antibiotics, poor sanitation/hygiene in our environments and a lack of new and improved drug development by the pharmaceutical industry due to challenging regulations and reduced economic incentives for drug development (Gould & Bal, 2013; Viswanathan, 2014). Resistance can be natural or acquired. There are genes which naturally confer resistance known as the environmental resistome (Wright, 2010). The genes may be transferred from non-disease causing bacteria to disease causing bacteria which leads to clinically significant antibiotic resistance (Wright, 2010). Natural resistance can also occur when the microorganism does not possess target sites for the drugs (Toma & Deyno, 2015). Therefore, the drug is unable to attach, hence it has no effect on the microorganism or has low permeability to the drug agents which require entry into the microbial cell in order to induce action against. Acquired resistance is the major contributor of AMR (Munita & Arias, 2016). It is the result of specific evolutionary pressure which develops as a counterattack mechanism against antimicrobial molecules (Guidos, 2011). This type of resistance results from changes in the bacterial genome. The mechanisms of acquired resistance are (Figure 2.4):

- The presence of enzymes which act by inactivating the antimicrobial agent
- The presence of alternative enzymes which are activated when an enzyme is inhibited by antimicrobial agents
- A mutation in the binding site of the antimicrobial agent's target, which result on reduced binding
- Post-transcriptional or post-translational modifications of the antimicrobial agent's target which also results in reduced binding between the agent and target
- Reduced uptake of the antimicrobial agent
- An active efflux of the antimicrobial agent
- Overproduction of the target

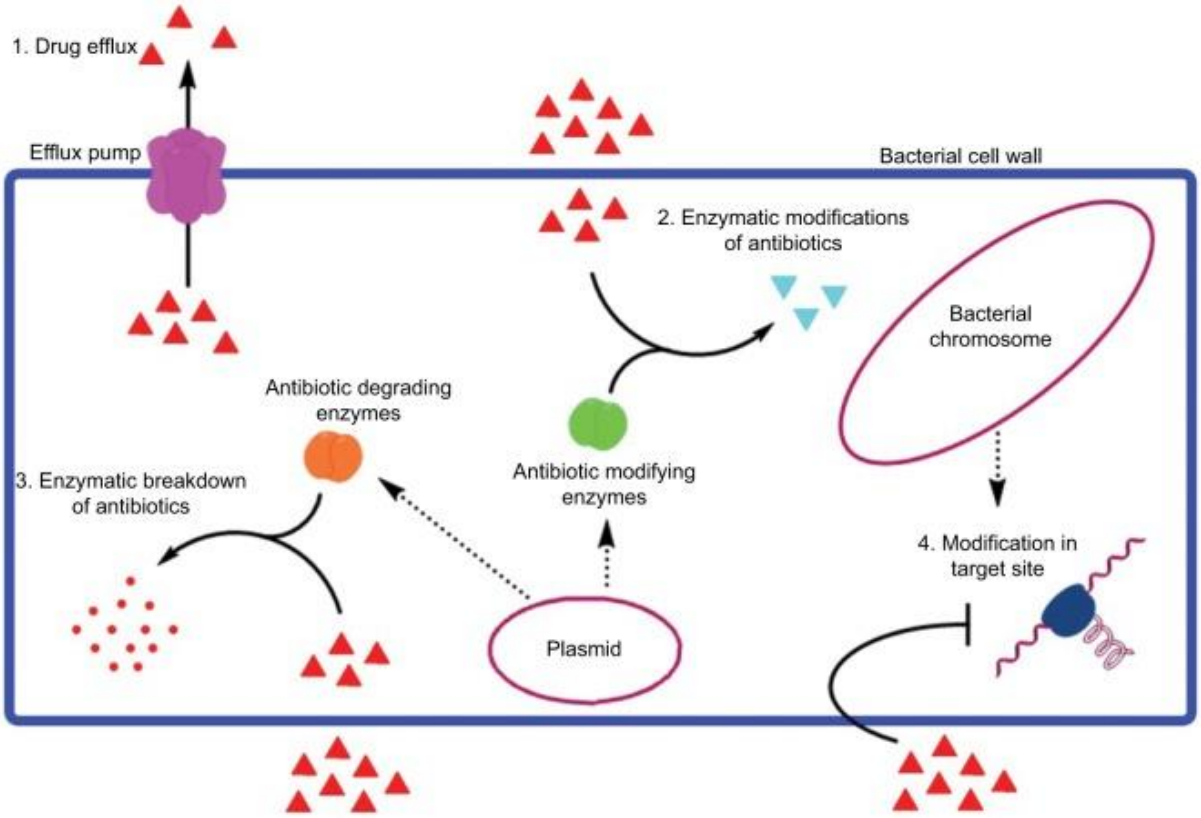

Figure 2.4: Various mechanisms of antibiotic resistance, including drug efflux with the help of efflux pump, enzymatic modifications of the antibiotic, enzymatic breakdown of the antibiotics, and modification in the target sites (Aslam *et al*., 2018).

Nanotechnology has enabled for the discovery and development of new antimicrobial agents (Hemeg, 2017). Their small size of nanoparticles makes them highly fitting for carrying out antimicrobial biological operations as they can easily penetrate the bacterial membrane (Wang, Hu & Shao, 2017). The current major groups of agents used against bacteria generally act by affecting: cell wall synthesis, translational machinery and DNA replication (Magiorakos *et al*., 2012). Nanoparticles require direct contact with the bacterial cell in order to confer their antibacterial function (Niño-Martínez *et al*., 2019). Some of the accepted forms of contact include electrostatic attraction, van der Waals forces, receptor-ligands and hydrophobic interactions (Armentano *et al*., 2014; Gao *et al*., 2014; Li *et al*., 2015). Nanoparticles cross the bacterial membrane through these interactions, gather along the metabolic pathway and influence the shape and function of the cell membrane. Following, the nanoparticles interact with the basic components of the cell (Shrivastava *et al*., 2007; Xu *et al*., 2016). It can be said that the previously described detailed mechanisms of AMR are irrelevant to nanoparticles. Nanoparticle-based materials as antimicrobial agents have received attention because they are seen 1) as less prone to promote resistance in bacteria, 2) they can combat microbes using multiple mechanism simultaneously and 3) they can act as carriers of antibiotics (Huh & Kwon,

2011; L. Wang *et al*., 2017). Different types of nanoparticles present different types of mechanisms for tackling AMR. The general AMR mechanisms of action of nanoparticles is described in terms of three models (Figure 2.5): oxidative stress induction, metal ion release or non-oxidative mechanisms (Singh *et al*., 2018).

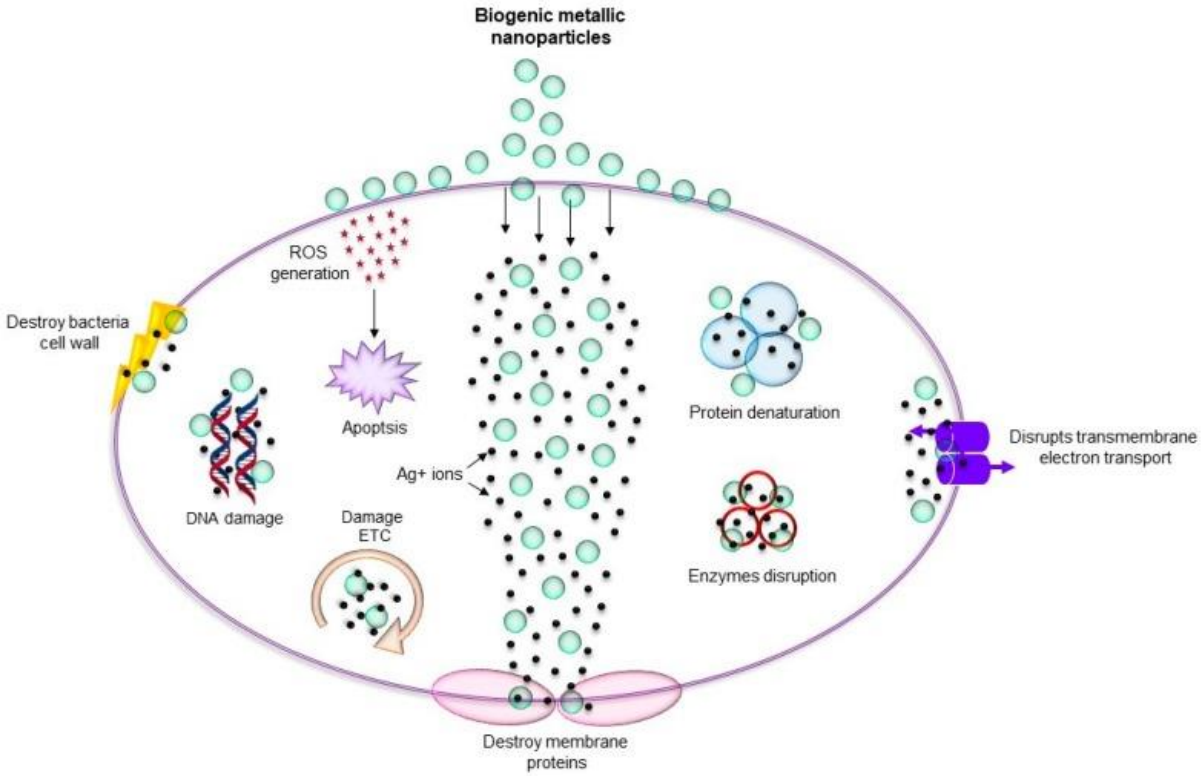

Figure 2.5: An overview of the general mechanisms behind the antimicrobial effect of nanoparticles (Singh *et al*., 2018).

Silver nanoparticles (AgNPs) are widely studied and recognized for antimicrobial effects (Jones *et al.*, 2004). Silver and AgNPs assume a significant role as antimicrobial agents and they are well exploited as it is estimated that nearly 320 tons of AgNPs are manufactured yearly for use in different applications (Jones *et al.*, 2004; Silver & Phung, 1996). The development of drug agents for the treatment of microbial infections is not growing at a fast enough pace as there is still an alarming increase in the number of multi-drug resistant bacterial and viral strains as a result of mutations, pollutions and changing environmental conditions. Thus, it is important to explore all possibilities. Many other metal salts and metal nanoparticles have been reported to have antimicrobial activity (Siddiqi, Husen, & Rao, 2018). However, these other metal nanoparticles are not as well studied as Ag NPs for their bactericidal effects. For example, AuNPs are regarded as biologically inert and they are not generally recognized for their antibacterial activity (Allahverdiyev *et al*., 2011). One of the reasons is that AuNPs have

a high MIC value or small zone of inhibition, especially when compared to AgNPs (Hernández-Sierra *et al*., 2008).

Several studies have shown that AuNPs have antibacterial effects (Zhang *et al.*, 2015). Rai, Prabhune, & Perry, (2010) produced AuNPs from cefaclor as a reducing agent and reported strong antimicrobial activity against *Staphylococcus aureus* as well as *Escherichia coli*. Similarly, another study reports activity in AuNPs coated with fluconazole against *Candida albicans* and *Aspergilus flavus* (Shamaila *et al*., 2016). These results clearly elucidate that different reducing agents give rise to AuNPs with different properties. They can be modified and activated with different molecules to become effective antimicrobial agents (Rai *et al*., 2010). Therefore, it is important to explore the potential of these nanoparticles as they have had limited exposure in research as antimicrobial agents (N. Ahmad *et al*., 2017).

2.7 AuNPs in Cancer

Cancer is the uncontrolled proliferation of cells (Hanan *et al*., 2018). The frantic changes of biochemical and enzymatic parameters that cells undergo during uncontrollable proliferation is a universal characteristic of tumour cells (Kuppusamy *et al.*, 2016) . The presence of free radicals commonly induce cell proliferation and damage in the normal cell function. Studies have shown that the overexpression of cells can be controlled and regulated via systematic cell mechanisms using nanoparticles as controlling agents (Akhtar, Panwar, & Yun, 2013). The nanoparticles relatively control the formation of free radicals and can thus control the overexpression of cell growth (Rosi *et al*., 2006).

Nanotechonology offers specific benefits that enable the future of cancer care. Nanotechnology in cancer concerns the application of both nanomaterials such as NPs for tumour aging or drug delivery and nanotechnology approaches such as NP-based theranostics for the diagnosis and treatment of cancer (Kolhe & Parikh, 2012). The nanomaterials used include NP-drugs and nanodevices. The NP-drugs used in cancer are designed to encapsulate, covalently attach or adsorb therapeutic and diagnostic agents to the NPs (Singh, Rajesh & Lillard, 2009). The structure of the NPs are generally designed to link hydrophobic cancer drugs and tumour targeting ligands to hydrophilic and biodegradable polymer (Dadwal, Baldi, & Narang, 2018). Cancer is a burdensome disease and amongst others, early detection is important to help alleviate the burden (Loud & Murphy, 2017). Tools developed through nanotechnology may be able to help detect the disease present in cells or tissues even in very small amounts. Some of the nanodevices used in cancer include quantum dots, nanopores, dendrimers, cantilever liposomes and gold nanoparticles (Dadwal *et al*., 2018). These nanodevices can easily enter

the cells and organelles due to their relatively small size and once inside interact with DNA and proteins.

AuNPs are an attractive tool for cancer diagnosis and therapy (P. Singh, Pandit, *et al*., 2018). This is partially attributed to the fact that gold is deemed safe for use in treatment of human diseases (Kolhe & Parikh, 2012). AuNPs have been used as a platform for novel experimental cancer therapy. Metallic nanoparticles have proved novel application in the medical field in diagnostics and treatment of various types of cancers (Hanan *et al*., 2018). AuNPs can enter cells, hinder cell proliferation and cause DNA damage (Camberos *et al.*, 2013). Ali et *al.* (2019), tested the cytotoxic effects of AuNPs by investigating the cell viability and morphological changes of MCF-7 for 48 hours. The results showed that the AuNPs had significant inhibition of cell proliferation and suggested that the AuNPs can be considered a valuable source of effective anti-proliferative and cytotoxic substances.

Plant mediated nanoparticles are reported to have an effect against various cancer lines such as HepG2, HCT 116 and Hela. A review by Hanan *et al*. (2018), compared the cytotoxicity of plant-mediated metallic nanoparticles based studies published in the period 2006 to 2017. Most of the studies proved metallic nanoparticles to have cytotoxic effects against various cancer cell lines. Studies have also reported an improved cytotoxic effect of plant mediated nanoparticles due to the presence of secondary metabolites in the nanoparticle (Das *et al*., 2013; Raghunandan *et al*., 2011).

2.8 AuNPs in Catalysis

For a long time Au was believed to be devoid of any catalytic activity (Corma & Garcia, 2008). Recently, there has been an exponential growth in the number of publications reporting catalytic activity of gold nanoparticles. The catalytic activity of gold is directly linked to the size of the nanoparticle in the nanometre scale. Gold catalysis can be observed in nanoparticles and can completely disappear as the particle size increases (Corma & Garcia, 2008). Studies report AuNPs catalysis in i.e i) the reduction of p-nitrophenol (p-NP) by sodium borohydride ($NaBH_4$) (Gangula *et al*., 2011), ii) promoting low temperature carbon monoxide oxidation (Hutchings & Edwards, 2012) iii) isomerization of azobenzene (Hallett-Tapley *et al*., 2013).

The study by Gangula *et al*. (2011), reported AuNPs behaving as catalysts in the reduction p-NP by $NaBH_4$. p-NP is an organic water pollutant that is hazardous and harmful to the environment. The United States Environmental Protection Agency reported p-NP as a priority toxic pollutant due to its high toxicity, stability and solubility in water (Dai *et al.*, 2008). Thus, the removal of this pollutant in the environment is important as it contributes to great

environmental issues. The conventional methods usually used to treat p-NP are biodegradation by aerobic processes using microorganisms, long hydraulic retention time and catalytic liquid-phase oxidation (Gemini *et al*., 2005; Liou, 2012). The aerobic biodegradation has limited application for water treatment and the liquid-phase oxidation requires high temperatures. $NaBH_4$ is cheap and is easily obtained, it is also used as an ideal source of hydrogen for the reduction of p-NP (Gangula *et al*., 2011). This process can be catalysed by AuNPs. The AuNPs catalyse the reaction by reducing the energy barrier in the reaction process and accelerate its kinetics (Kong *et al*., 2017). AuNPs –based catalysts promises applications in energy saving "green' organic synthesis, environmental purification and artificial photosynthesis (Gangula *et al*., 2011).

CHAPTER 3

MATERIALS AND METHODS

3.1 Chemicals, reagents and equipment

Table 3.1: Reagents used and supplier

Reagents	**Supplier**
Sodium tetrachloroaurate (III) dehydrate	**Sigma-Aldrich**
3-[4,5-dimethylthiazol-2-yl]-2,5-diphenyl tetrazolium bromide (MTT)	
Dimethyl sulphoxide (DMSO)	
$NaBH_4$	
4-NP	
Ampicillin	**Biolab, Merck**
Nutrient broth	
Miller Hinton Agar	
Dulbecco's Modified Eagle's Medium	**Lonza**
Phosphate buffered saline	
Bovine serum albumin	**Miles Laboratories (Pittsburgh, PA, USA**
Fetal Bovine Serum (FBS)	**Thermo Scientific (Gibco)**
Trypan blue	
Trypsin-EDTA	

Table 3.2: Equipment used and manufacturer

Equipment	**Manufacturer**
Blender	**Panasonic MX-GX1571WTJ**
Microwave	**LG**
Hot stirrer	**Lasec**
Microcentrifuge	**Eppendorf 5417 R**
Whatmann No. 1	**Sigma-Aldrich**
Lyophilizer	**Labconco**
Thermomixer	**Eppendorf**
Polystyrene 96-well microtitre plates	**Greiner Bio-one**
POLAR star Omega microplate	**BMG Labtech**

Zetasizer	**Nano-ZS90 system, Malvern Inc**
FTIR spectrophotometer (Waltham, MA, USA)	**PerkinElmer spectrum one**
TECNAI F20 HRTEM microscope	**Carl Zeiss**
Nikon TMS-F light microscope	
25 cm^2 cell culture flasks	**SPL Life Sciences**
Countess™ chamber slide	**Invitrogen**
Countess® Automated Cell Counter	
Bench top centrifuge	**Sorvall TC6**
BD FACSCaliburr™	**BD Biosciences, Ontario, Canada**

3.2 Research methodology

3.2.1 Preparation of Persea Americana (Avocado) aqueous seed extract

Fresh avocados were purchased at a local fruit market, the pulp was eaten and the seeds were collected. The collected avocado seeds were left to dry at room temperature for 3 months. The dry avocado seeds were ground into fine powder using a blender. A 10% Avocado seed extract (AvoSE) was prepared by mixing powder with distilled deionized water (ddH_2O). The mixture was heated in a microwave until boiling. The mixture was then left overnight under stirring at 1000 rpm at room temperature. The following day, the extract was microcentrifuged at 9000 rpm at 4˚C for 10 minutes. The pellet was discarded and the remaining supernatant was vacuum filtered through a Whatmann No. 1 filter paper. The filtrate was frozen at -80˚C for lyophilisation.

3.2.2 Synthesis and characterization of AuNPs from aqueous AvoSE

The synthesis and optimization protocol was adapted from Elbagory *et al*. (2016). AuNPs were synthesized by mixing AvoSE and 1mM $HAuCl_4 \cdot 3H_2O$ at a volume ratio of 1:10 and the solution was incubated for 1 hour in a thermomixer at 1000 rpm. After the incubation period, AvoSE-AuNPs formation was observed by visual inspection of the test tubes for a change in colour from light yellow to red/purple. SPR band formation was also monitored by UV-Visible spectrophotometry between wavelength 300 – 1000 nm.

3.2.2.1 UV-Vis Spectroscopy

The formation of AvoSE-AuNPs was confirmed by UV-Vis spectroscopy using a POLAR star Omega microplate reader in the wavelength range of 300 nm to 1000 nm.

i) Effects of temperature and AvoSE concentration on AuNP synthesis

The extract was serially diluted to obtain a concentration range of 1.56 -100 mg/ml. Extracts were mixed with 1 mM $HAuCl_4 \cdot 3H_2O$ and incubated at various temperatures of 25, 37, 50, 80 and 100˚C. The reaction was incubated in a thermomixer for 1 hour at 1000 rpm.

ii) Effects of AvoSE pH on AuNP synthesis

Following the optimized extract concentration and temperature of synthesis, the pH of the optimum extract concentration was adjusted to obtain pH 4 to 10. The effect of pH synthesis was evaluated by mixing AvoSE at different pHs in the reaction mixtures. Synthesis was carried at 80˚C for 1 hour at 1000 rpm.

iii) Effects of $HAuCl_4$ concentration on AvoSE-AuNPs synthesis

The effect of gold salt concentrations (0.75- 5 mM) using $HAuCl_4 \cdot 3H_2O$ as gold (III) source was studied. The optimized seed extract concentration (12.5 mg/ml) was added to the reaction mixture at pH 7 with varying gold salt concentrations and incubated for 1 hour at 80 ˚C shaking at 1000 rpm. The reduction of gold and synthesis of AvoSE-AuNPs were followed by visual observation of the solution turning purple.

iv) Kinetics of AvoSE-AuNPs synthesis

The effects of reaction time on AvoSE-AuNPs synthesis were evaluated. AuNPs were synthesized by mixing 12.5 mg/ml AvoSE at pH 7 to 1 mM $HAuCl_4 \cdot 3H_2O$, incubated for 1 hour at 80 ˚C shaking at 1000 rpm. AvoSE-AuNPs were collected between every minute for 1 hour.

v) Purification of AvoSE-AuNPs

The synthesized AvoSE-AuNPs were purified from unreacted plant extract by micro-centrifugation at 14 000 rpm 25 ºC for 5 minutes. The supernatant was discarded, the pellets were collected and re-suspended in ddH_2O for characterization.

3.2.2.2 Dynamic light scattering analysis (DLS)

The particle hydrodynamic size, particle size distribution, polydispersity index (PDI) and δ-potential were determined using a Zetasizer. An aliquot of 1 ml from each sample was used to determine size, PDI and δ-potential in a cuvette. Measurements were determined in triplicate and averaged to obtain mean size and δ-potential at 25˚C and 90 ˚ angle. Zetasizer software version 7.13 was used to analyse the data.

3.2.2.3 Fourier Transform Infrared spectroscopy (FTIR)

The compounds possibly responsible for the reduction of $HAuCl_4$ in the synthesis of AvoSE-AuNPs were determined using FTIR. The purified AvoSE-AuNPs were analysed on a PerkinElmer spectrum one FTIR spectrophotometer instrument in the diffuse reflectance mode. The spectra were collected in the 4 000 – 400 cm^{-1} at 2 cm^{-1} resolution.

3.2.2.4 High Resolution-Transmission Electron Microscopy (HRTEM)

Studies of size and morphology of the AuNPs were performed by means of HRTEM. Micrographs were obtained on a field emission TECNAI F20 HRTEM microscope. Samples were prepared by drop-coating each test sample solution onto a copper (Cu) grid, supported by a thin film of amorphous carbon. This was then dried under a Xenon lamp for 10 min and samples were analysed under the microscope. HRTEM micrographs were obtained in a bright field mode at an accelerating voltage of 200kV. Finally, the obtained images were processed using ImageJ software (National Institutes of Health (NIH), USA) to determine the core size of the AvoSE-AuNPs.

3.2.3 Antimicrobial Assay

The antimicrobial activity of the synthesized AvoSE-AuNPs was evaluated by using agar well-diffusion assay (Dhand *et al*., 2016). Six bacterial strains were used in this study, namely *Escherichia coli, Staphylococcus aureus, Klebsiella pneumoniae, Staphylococcus epidermidis, Streptococcus pyogenes* and Methicillin-resistant *Staphylococcus aureus*. All six bacterial strains included in this study are biomedically important and exhibit resistance to a number of current antibiotics.

Table 3.3: Bacterial strains used corresponding ATCC number

Bacterial Strain	**ATCC* number**	**Resistant to**
Escherichia coli	35218	Fluoroquinolones
Staphylococcus aureus	25923	Methicillin, vancomycin
Klebsiella pneumoniae	13883	Beta-lactam, fluoroquinolones
Staphylococcus epidermidis	12228	Methicillin
Streptococcus pyogenes	19615	Erythromycin
Methicillin-resistant *Staphylococcus aureus*	33591	Methicillin, penicillin

** American Type Culture Collection*

i) McFarland turbidity standard and Agar-well diffusion

To standardize the microbial tests McFarland standards were used as a reference to adjust turbidity of bacterial suspensions so the amount of bacteria used for the assay fell within a range. Single colonies from pure bacterial culture of the test bacteria were inoculated into 2 ml Müeller-Hinton broth, mixed well and incubated for 2 hours at 37 °C in a shaking incubator at 200 rpm. Following incubation the optical density of the bacterial suspensions was measured at a wavelength of 600 nm and the OD value was adjusted to 0.08 - 0.12, which is equivalent to 0.5 McFarland turbidity standard.

The bacterial suspensions at 0.5 McFarland turbidity standard were uniformly spread on Mueller–Hinton agar plate using a sterile swab. After a 5 minute pre-incubation period, the agar was punched with a 6 mm cork borer. The prepared wells were then filled with 50 µL of AuNPs and ampicillin (10 µg/mL) which was used as a positive control. The plates were incubated at 37 °C for 24 hours. The zone of inhibition (ZOI) was measured in millimetres using a Vernier caliper

3.2.4 Catalytic Activity test

The catalytic activity of the AvoSE-AuNPs was evaluated by using 4-NP (Gangula *et al*., 2011). Experiments were performed in a 96-well plate and absorbance spectra was measured using a Polar Star Omega UV-Vis spectrophotometer. Stock solutions of 0.03 M $NaBH_4$ and 2 mM 4-NP were freshly prepared prior to use. The reactions were completed by mixing $NaBH_4$ with AvoSE-AuNPs and ddH_2O. The reaction progress was monitored between 1 and 90 minutes by obtaining UV-vis spectra in the range of 200 - 700 nm.

3.2.5 Cytotoxicity assay

i) Cell Culture

The cytotoxicity of the synthesised AvoSE-AuNPs was evaluated on cancer cell lines Caco-2 and HepG2 (Table 3.4) following a method adapted from Mmola *et al*. (2016). The cell lines were obtained from the ATCC. Frozen cells samples stored in vials were allowed to thaw at 37˚C. The cells were transferred into tubes containing DMEM supplemented with 1% Pen-Strep (Penicillin-Streptomycin) and 10% FBS (cMedia pre-warmed to 37 °C) and centrifuged at 3000 rpm in a bench top centrifuge for 3 minutes. The supernatant was discarded and the pellet containing cells was re-suspended in cMedia. The cells were cultured in 25 cm^2 cell culture flasks and incubated under standard culture conditions. The cells were cultured until

they reached 70-90% confluency. The procedures were performed in the Biological Safety Cabinet (Laminar Flow) under aseptic conditions.

Table 3.4: Tissue cells used and their growth medium

Tissue	Disease	Abbreviation	Growth media and supplements
Colon (large intestine)	Human epithelial colorectal adenocarcinoma	Caco-2	DMEM (1% penstrep, 10% FBS)
Liver	Human liver hepatocellular carcinoma	HepG2	DMEM (1% penstrep, 10% FBS)

ii) Cell sample preparation

Once the cells had reached 70-90% confluency, the medium was discarded and the cells were washed with PBS. The PBS was discarded and Trypsin-EDTA was added to the flask to aid in detaching the cells. The flask was incubated under standard culture conditions for 3-5 mins. The detachment of the cells was periodically inspected using a Nikon TMS-F light microscope. The detachment was facilitated by gently tapping the flask on a hard surface to dislodge the cells. Trypsin-EDTA was subsequently inactivated by the addition of cMedia. The dislodged cells were transferred to pre-labelled conical tubes and centrifuged at 3000 rpm for 3 min. The supernatant was discarded and the cells were re-suspended in cMedia.

iii) Trypan blue dye exclusion assay

An aliquot of the cell suspension was mixed with an equal volume of 0.4% trypan blue dye, the mixture was loaded onto a Countess™ chamber slide for cell count. The number of viable cells was assessed using the Countess® Automated Cell Counter. The number of live cells was used to standardize the concentration of cells (1×10^5 live cells) to be cultured in a 96 well plate. To each well, 100 µl of cells was added (1×10^5 live cells) and the plate was incubated for 24 hours at 37 ºC and 5% CO_2. The remaining recovered cells were either re-seeded or re-suspended in cMedia containing 10% DMSO. The cell suspensions were aliquoted into 2 ml cryo-vials and stored at -120˚C until further use.

iv) Determination of cell viability in the presence of AuNPs

Following 24 hour incubation, the spent medium was discarded and cells were treated with 100 µl of the samples (AvoSE-AuNPs and AvoSE at 12.5 - 200 µg/ml) in triplicate. Untreated cells and 10% DMSO were used as controls. The cells were incubated for a further 24 hours under standard culture conditions. After 24 hours, media was removed and cells were washed with PBS. An MTT assay was used as a test for cell viability. MTT stock solution (5 mg/ml) was

prepared according to manufacturer's instructions and 100 µL of the solution was then added to each well. The plate was covered in foil and incubated for 4 hours at standard culture conditions. After incubation, MTT was discarded and 100 µl of DMSO (>99.5 %) was added to each well and incubated again for 15 minutes until a purple colour appeared. The plates were read on a multi-plate reader. The optical density was used to calculate percentage viability as below (Mmola *et al*., 2016):

$$\text{Viability (\%)} = \frac{Test\ sample\ (OD)}{Control\ sample\ (OD)} \text{ x } 100$$

3.2.6 Cell cycle analysis by Flow cytometry

Caco-2 and HepG2 cells were seeded in 25 ml flasks with supplemented DMEM at a concentration of 5 x 10^5 lives cells. The cells treated with AvoSE-AuNPs and AvoSE IC_{50} and incubated for 24 hrs. After treatment, the cells were dislodged with trypsin-EDTA, centrifuged, fixed in 70 % ethanol and stored overnight at 4˚C. Prior to analysing the cells were resuspended in PBS with 0.1 µg/ml RNase followed by staining with 40 µg/ml propidium iodide for 30 minutes at 37˚C in the dark. Analysis was performed using BD FACSCaliburr™ Flow Cytometer and BD CELLQuest™ Pro software. The values were expressed as fractions of cells in cell cycle phases.

CHAPTER 4

RESULT AND DISCUSSION: SYNTHESIS AND CHARACTERIZATION OF AVOCADO SEED EXTRACT - GOLD NANOPARTICLES

4.1 Introduction

This chapter reports and discusses results of the synthesis of AuNPs using AvoSE and the physicochemical characterization of the NPs. The aqueous AvoSE was used as a potential reductant and stabiliser in AuNP formation. Although there are several approaches used for the synthesis of AuNPs, the biosynthesis approach is highly advantageous because of its rapid, environmentally friendly and ease of control during synthesis (Ahmad *et al.*, 2017). Synthesis methods can affect the nanoparticles and their resulting properties. Therefore, synthesis approaches can be used to manipulate and modify nanoparticles to achieve desirable size and shape properties (Ealias & Saravanakumar, 2017). Controlling the size, shape and media of metal nanoparticles is important as many of their intrinsic properties are determined by these properties (Ahmad *et al*., 2017). Furthermore, size, shape and morphological characteristics are important factors because they contribute to the nanoparticle efficacy (Sloan & Farnsworth, 2006). In this study we conducted a detailed investigation of the effects of various reaction conditions, presented and discussed their effects on NP formation.

AuNPs have unique physicochemical and optical properties which make them employable for many applications such as biosensing, catalysis, biomedicine, electronics, and surface-enhanced Raman spectroscopy (Dhamecha *et al.*, 2015). The main parameters which are studied in the characterization of NP are size and shape (Menon *et al.*, 2017). This is due to the fact that the unique properties of AuNPs are heavily size and shape dependent (Sosa *et al*., 2003). Furthermore, the applications of the AuNPs branch out depending on the size of the nanoparticle (Ahmad *et al.*, 2017). Several techniques are employed to characterize nanoparticles. It is also crucial to characterize the nanoparticles in several ways focusing not only on the nanoparticle core, but also to evaluate the surface chemistry of the particle. The hydrodynamic size and charge, surface coating molecules, core size and SPR of the AvoSE-AuNPs were determined by DLS, FTIR, TEM and UV-vis spectroscopy respectively.

4.2 Results and discussion

4.2.1 Gold nanoparticles biosynthesis visual observation

AuNPs were prepared by a plant extract-mediated method using AvoSE as described in Chapter 3 (section 3.2.2). Aqueous AvoSE was added to $HAuCl_4$ and the bioreduction reaction was

observed by a visible colour change (Figure 4.1). The AvoSE which exhibited an orange colour was mixed with the pale yellow $HAuCl_4$ aqueous solution (0.5 mM) and a rapid colour change from pale yellow to purple was observed. The colour change indicated the formation of AuNPs as reported in published studies (Elia *et al*., 2014; Mulvaney, 1996). Literature reports that the change in colour is due to the localized surface plasmon resonance (L-SPR) which lies in the visible region of the electromagnetic spectrum (Amendola & Meneghetti, 2009; Zhang *et al*., 2016). This means that the nanoparticles absorb and reflect light at particular wavelengths in the visible region and this determines the colour that they will exhibit. The L-SPR formation can be monitored by UV-vis spectroscopy (Zhang *et al*., 2016). AuNPs with a diameter less than 30 nm exhibit a ruby-red colour because smaller sized nanoparticles absorb in the blue-green range of the spectrum and reflect red light (Link & El-Sayed, 1999). With increasing particle size, red light is absorbed and blue light is reflected, resulting in blue or purple nanoparticle coloured solutions (Link & El-Sayed, 1999).

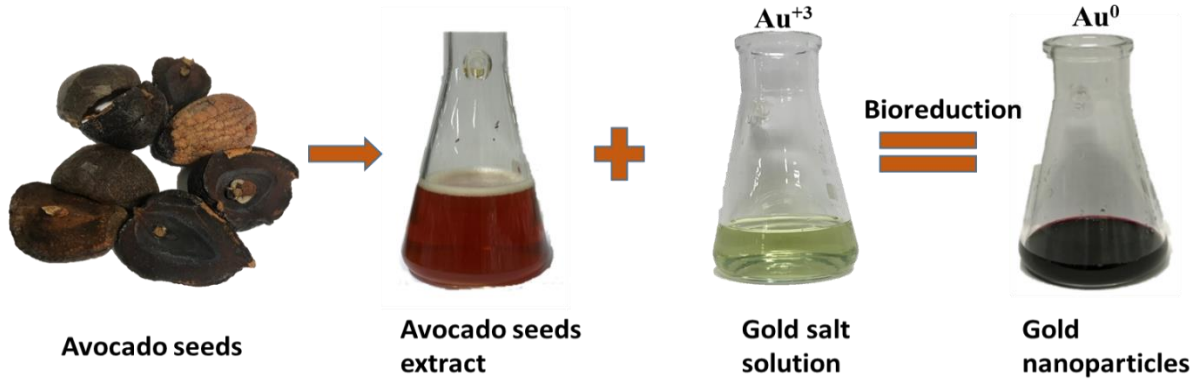

Figure 4.1: Schematic of aqueous Avocado seed extract mediated synthesis of AuNPs

The accepted hypothetical mechanism reported in literature for plant mediated synthesis of AuNPs is by a phytochemical-driven reaction in which the plant extract contains complex reducing molecules such as phenolic moieties, enzymes and antioxidants which reduces the gold cations present into AuNPs (Arun *et al.*, 2014; Sweet *et al.*, 2012). The reaction is a reduction reaction which forms zerovalent gold, which subsequently leads to the agglomeration of gold atoms to form nanosized particles. The nanosized particles are finally stabilized by the phytochemicals to form distinctly shaped AuNPs (Sweet *et al*., 2012). Studies have shown that plant extracts contain many biomolecules including polyphenols, flavonoids, ascorbic acid, sterols, triterpenes, alkaloids, alcoholic compounds, saponins, ß-phenylethylamines, polysaccharides, glucose, fructose and protein/enzyme which may act as reductants in the formation of metallic nanoparticles (Aljabali *et al*., 2018; Y. Lu & Foo, 2002; Rao *et al*., 2016). A study Vimalraj, Ashokkumar, & Saravanan (2018) reports on the biogenic AuNP synthesis

mediated by *Mangifera indica* (MI) aqueous seed extracts. The study suggests that the AuNPs formation and controlled crystal growth is controlled by the MI seed extract which acted as both a reducing and capping agent. Avocado seed also contains various phytochemicals such as alkanols, terpenoids, flavonoids and coumarins and thus it can be said that the AvoSE played a dual role in the synthesis of AvoSE-AuNPs acting as reducing and stabilizing agents.

4.2.2 Characterization of AvoSE- gold nanoparticles

4.2.2.1 UV-visible spectroscopy

The SPR band of the AvoSE–AuNPs was monitored using a UV-vis spectrophotometer. AuNPs formation was evident from the change of colour of the starting solutions previously mentioned. It was further confirmed by the presence of the SPR peak. In general the typical SPR band for AuNPs occurs at λ_{max} in the range 500-580 nm (Haiss *et al.*, 2007). The graphs in Figure 4.2 shows SPR peaks of the synthesized AuNPs at all tested concentrations and temperatures occurred in the range 530-540 nm of the UV-vis spectrum.

Factors such as size, morphology and surface modifications strongly determine the width and position of the SPR band (Amendola & Meneghetti, 2009). These factors can be controlled and improved by altering reaction parameters during synthesis (Wadhwani *et al.*, 2014). A detailed investigation of the effects of various parametes on the formation of AuNPs was conducted. Process parameters; Temperature, plant extract concentration, concentration of aqueous tetrachloroate solution ($HAuCl_4$), pH of extract and reaction time were investigated to optimize AuNPs properties as described in Chapter 3 (section 3.2.2.1).

a) Effect of plant extract concentration and temperature on AuNPs synthesis

Different combinations of extract concentrations and $HAuCl_4$ solution were tested to study the effect of plant extract concentration and temperature in AuNPs formation and its characteristics. Figure 4.2 displays the SPR bands formed:

A- The peaks represent synthesis conducted by reacting 1.56 mg/ml of AvoSE at temperatures ranging between 25-100 ˚C. The peaks were flat and very broad and the maximum absorbance (A_{max}) were below 1 for all temperatures and the highest was 0.9 observed at 80 ˚C. The λ_{max} were right shifted for all temperatures except at 80 ˚C.

B- AuNPs formed at concentration 3.13 mg/ml AvoSE saw an increase in the SPR peaks. The peaks were very low and broad for the lower temperatures 25, 37 and 50 ˚C. More AuNPs were synthesized at 80 and 100 ˚C.

C- The increase in SPR peaks indicate that more AuNPs were formed at 6.25 mg/ml compared to 1.56 and 3.13 mg/ml. The lower and broader peaks were observed at 25 and 37˚C. AuNPs formation at temperature 50, 80 and 100 ˚C were slightly symmetrical with the highest peak observed at 80 ˚C.

D- Synthesis at 12.5 mg/ml AvoSE exhibited the most symmetrical and narrow SPR peaks at all temperatures compared to all AvoSE concentrations tested in this study. The peaks were left shifted and the A_{max} values were above OD reading of 1 indicating successful synthesis of AuNPs at all temperatures.

E- AuNPs synthesized at 25 mg/ml of AvoSE exhibited similar results to synthesis at 12.5 mg/ml however the peaks were slightly broader than those at 12.5 mg/ml. At temperatures 25 and 37 ˚C the A_{max} slightly decreased compared to those at 12.5 mg/ml of the same temperatures.

F- AuNPs formed at 50 mg/ml of AvoSE exhibited SPR peaks which were left shifted and the A_{max} reading were high. However, the peaks were lower and at temperatures 37 and 100 ˚C the peaks were slightly flat

G- At 100 mg/ml the results were similar to synthesis at 50 mg/ml. The SPR peaks were even lower and less narrow than those described in graph F.

AuNPs were formed at all tested concentrations except for 1.56 mg/ml AvoSE tested at 37 ˚C. Graphs A and B (Figure 4.2) exhibited flat and broad SPR peaks and this is likely due to the availability of reducing agents. Since the extract is a source of reducing agents, at the lower AvoSE concentrations there is an insufficient amount of reducing agents available to react with the amount of Au^{3+} present in solution hence less products (AuNPs) are formed. Graphs A and B displayed broad SPR peaks obtained at λ_{max} between 554-568 nm (Figure 4.4). This indicates the formation of larger and anisotropic AuNPs (Shanmugam *et al.*, 2017). Graphs D and E in Figure 4.2 showed the desired properties in SPR peaks. The SPR peaks were narrow, sharp and symmetrical. This is an indication that the ratio amount of available reducing agents to available amount of Au^{3+} metal ions in solution was proportional. The SPR peaks λ_{max} was formed at a narrower range between 532-540 nm and this is an indication of a left shift (Figure 4.4). The SPR band left shift is an indication of the presence of smaller sized NPs and the symmetrical SPR band is due to the formation of more uniformly sized NPs. The SPR peaks displayed in graph F and G in Figure 4.2 indicated the reaction at higher AvoSE concentrations reaction was hasty and this is because there was a much higher amount of reducing agents present to the amount of Au^{3+} present in solution.

The trend in Figure 4.2 shows that absorbance increased with increasing extract concentration and the SPR band peaks were more symmetric with increasing AvoSE. A similar was observed by in a study by Yasmin, Ramesh, & Rajeshkumar (2014), the study optimized the synthesis of AuNPs using herbal plant extract from *Hibiscus rosa-sinensis.* The study showed that with increasing extract concentration, the absorbance intensity steadily increased. Furthermore, the study also showed that at the highest concentration tested the absorbance decreased due to the bioavailability of functional groups in leaf extract to gold ions which led to competition between extract and metal ions during the bioreduction process and this can also be observed graph F and G (Figure 4.2).

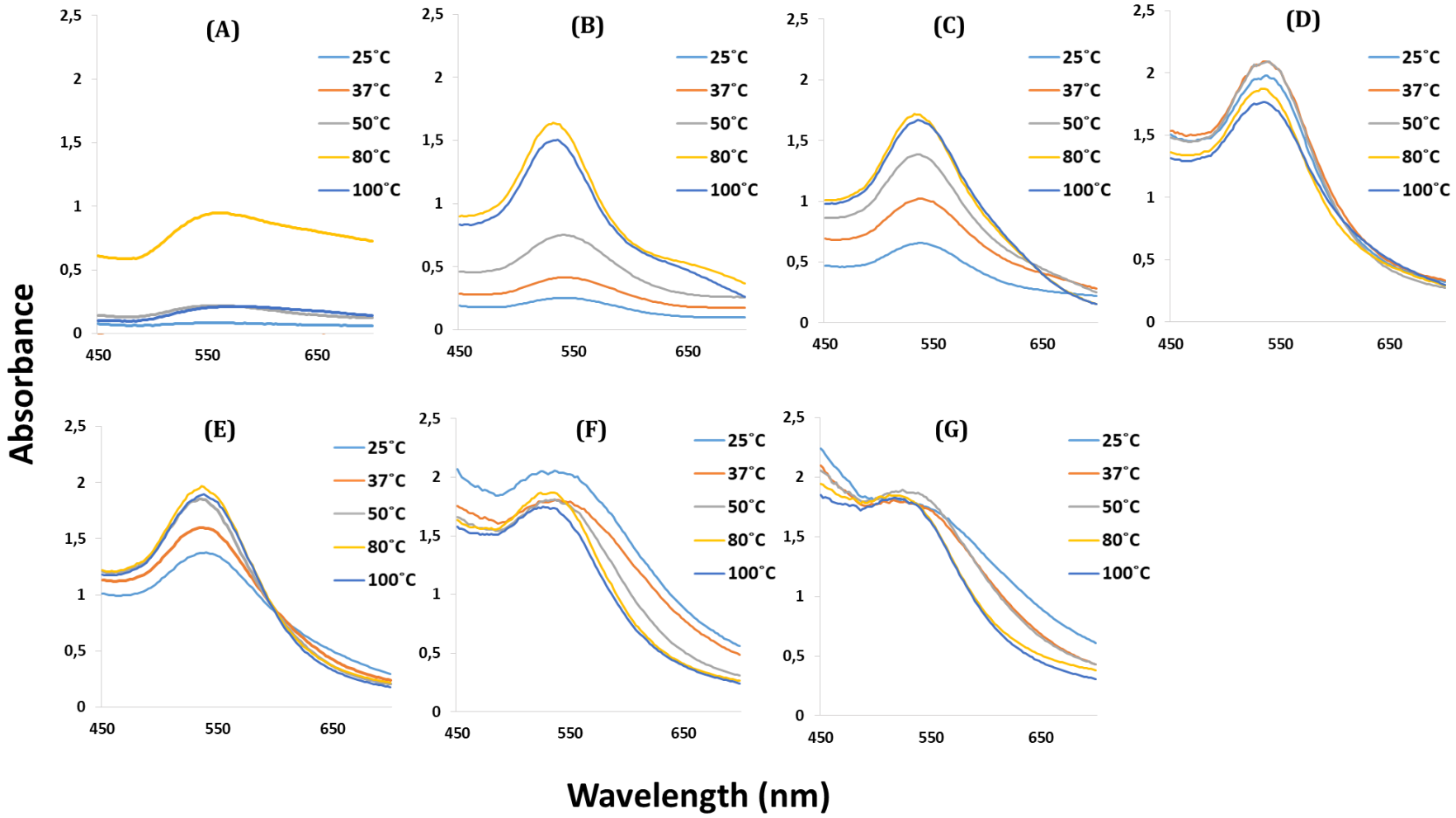

Figure 4.2: Uv-vis spectra of SPR bands recorded for different reactions, indicating AuNPs formation. In each reaction 0.5 mM aqueous $HAuCL_4$ solution was reacted with varying AvoSE concentrations, incubated at temperatures ranging from 25-100˚C for 1 hour. Each graph (A-G) represents AuNPs formation at varying concentrations of extract (A) 1.56 mg/ml (B) 3.13 mg/ml (C) 6.25 mg/ml (D) 12.5 mg/ml (E) 2 mg/ml 5 (F) 50 mg/ml (G) 100 mg/ml.

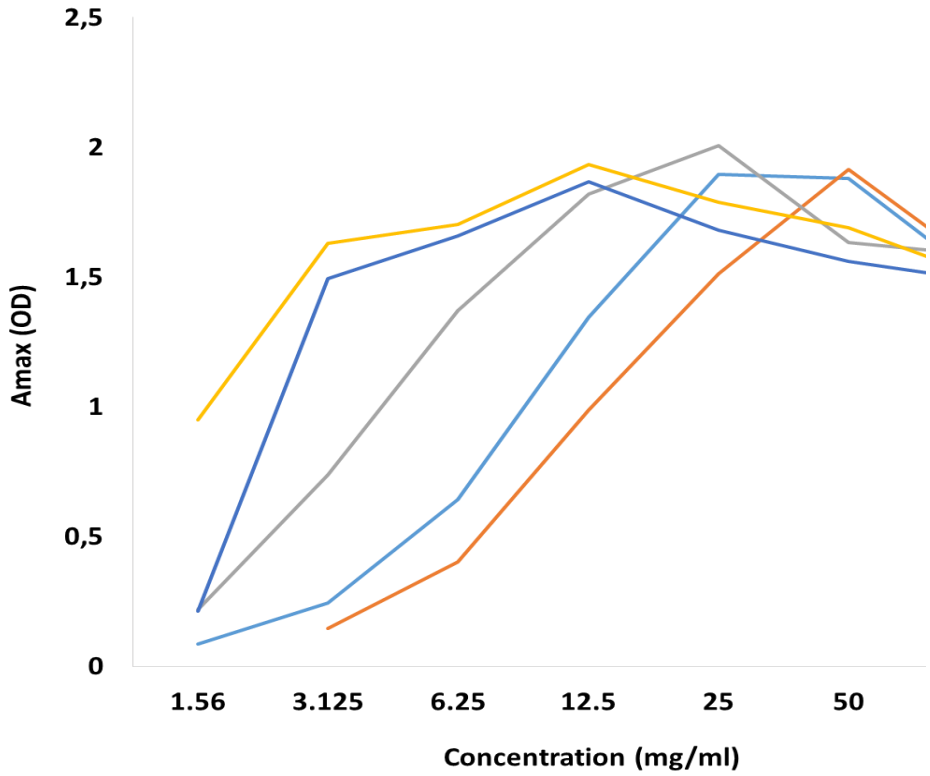

Figure 4.3: Absorbance maxima obtained from reacting 0.5 mM aqueous $HAuCl_4$ solution with varying AvoSE concentrations (1.56, 3.13, 6.25, 12.5, 25, 50 and 100 mg/ml) and incubated at temperatures ranging from 25-100˚C for 1 hour.

	λmax				
	25˚C	37˚C	50˚C	80˚C	100˚C
1,56 mg/ml	552	0	550	528	568
3,13 mg/ml	538	550	536	536	536
6,25 mg/ml	536	538	536	536	536
12,5 mg/ml	540	538	536	536	538
25,0 mg/ml	538	538	540	532	536
50,0 mg/ml	536	538	536	532	526
100,0 mg/ml	534	550	538	562	516

Figure 4.4: Wavelength maxima (λ_{max}) representing the highest point of the SPR peaks obtained from different reactions. In each reaction 0.5 mM aqueous $HAuCl_4$ solution was added to varying AvoSE concentrations ranging from 1.56- 100 mg/ml and incubated at temperatures ranging from 25-100˚C for 1 hour.

Figure 4.5 shows the effects of temperature on AvoSE-AuNPs synthesis. AvoSE and aqueous $HAuCl_4$ solution were mixed and incubated at a range of temperatures between 25 - 100 ˚C. The following describes each graph on Figure 4.5.

A- The peaks represent synthesis conducted at 25 ˚C. There are evident peaks at all concentrations tested indicating successful production of AvoSE-AuNPs. At 1.56 and 3.13 mg/ml the peaks were flat and very broad and the A_{max} values were below 1. The SPR peaks at 50 and 100 mg/ml were also low and broad however the A_{max} values were high. The SPR peaks were right shifted.

B- AvoSE-AuNPs formed at 37 ˚C AvoSE saw an increase in the absorbance of the SPR peaks. It is noticeable that at concentration 1.56 mg/ml the peak was flat indicating that AvoSE-AuNPs were not produced. The highest peaks were observed at 50 and 100 mg/ml indicating that more AvoSE-AuNPs were synthesized at these concentrations. The SPR peaks were broad and also right shifted like in graph A.

C- The increase in SPR peaks indicate that more AuNPs were formed at 50˚C compared to those synthesized at 25 and 37 ˚C. The low and very broad peaks were observed at 1.56 and 3.13 mg/ml. AuNPs formation at 12.5 and 25 mg/ml were more narrow and symmetrical. At 50 and 100 mg/ml the SPR peaks were lower and more right shifted

D- Synthesis at 80˚C exhibited the most symmetrical, sharp and narrow SPR peaks at all temperatures except for the 1.56 mg/ml peak compared to the other temperatures tested in this study. The peaks were left shifted and the absorbance maximum (A_{max}) values were above OD reading of 1 indicating successful synthesis of AuNPs at all temperatures. The most ideal peak was identified at 12.5 mg/ml.

E- AvoSE-AuNPs synthesized at 100 ˚C exhibited similar results to synthesis at 80 ˚C. However, the peaks were slightly broader than those at 100 ˚C. At 50 and 100 ˚C the A_{max} slightly decreased and the SPR peaks were slightly less narrow and more flat.

AuNPs formed at all temperatures including the ambient temperatures 25-37 ˚C as displayed in graph A and B (Figure 4.5). This is significant as the method of synthesis is deemed to follow green chemistry principles (Dahl *et al.*, 2007). Energy efficiency is emphasized as one of the main criteria factors in ‘green’ NP synthesis (Nadagouda *et al.*, 2009).

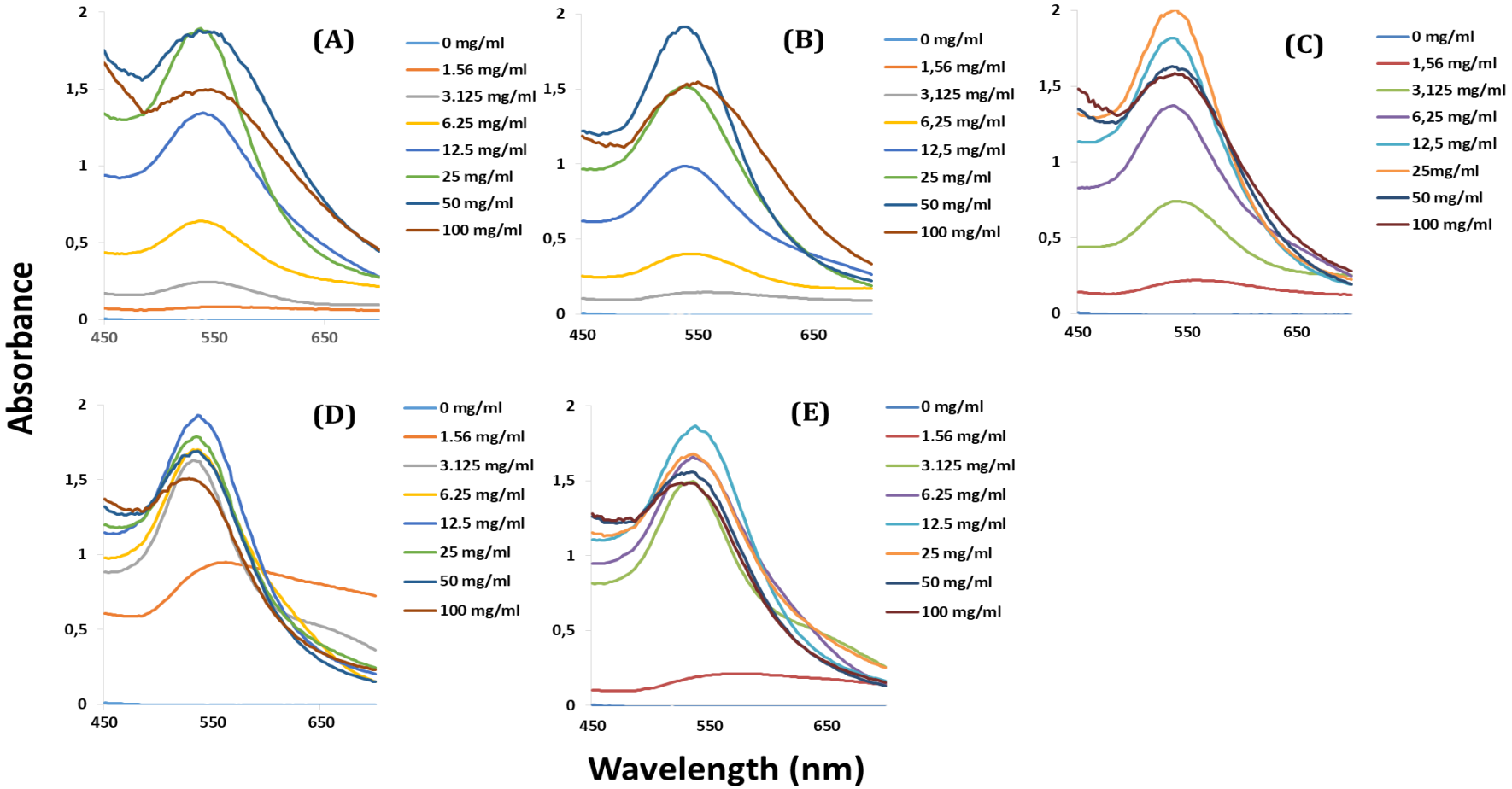

Figure 4.5: SPR peaks recorded via Uv-vis for different reactions, indicating AuNPs formation. In each reaction 0.5 mM aqueous $HAuCL_4$ solution was reacted with varying AvoSE concentrations ranging 1.56-100 mg/ml and incubated at different temperatures for 1 hour. Each graph (A-E) represents AuNPs formation at temperatures (A) 25 ˚C (B) 37 ˚C (C) 50 ˚C (D) 80 ˚C (E) 100 ˚C.

Narrower and sharper SPR band peaks occurred at higher temperatures displayed as graph D and E (Figure 4.5). This result can be explained in terms of the collision theory which states that for reactions to occur reactant molecules are required to collide effectively (Myers, 2003). For an "effective collision" to occur, the reactant molecules must be oriented in space correctly to allow bonds between atoms to break, rearrange and form in order to produce products. A rise in temperature increases the average kinetic energy of reactant molecules (Myers, 2003). Therefore, a greater proportion of molecules will have the minimum energy necessary for an effective collision to occur. The optimum temperature for synthesis occurred at 12.5 mg/ml AvoSE at 80 ˚C as the SPR peaks observed were sharp, narrow and the λ_{max} was positioned at 536 nm indicating the presence of smaller and uniform AvoSE-AuNPs. This result corrobates with studies conducted by Mountrichas *et al.* (2014) and Shanmugam *et al*. (2017), the studies showed that higher temperatures produced more uniform and smaller nanoparticles at a faster rate than lower temperatures. While lower temperatures lead to much slower reaction times and larger hybrid nanoparticles. The study suggests that at elevated temperatures synthesis occurs in 3 steps, while at lower temperatures the pathways are more complex hence the differences in nanoparticles formed. The effect of reaction temperature was found to be significant with respect to the structure and optical properties of the nanoparticles formed (Mountrichas *et al.*, 2014).

b) Effect of pH on AuNPs synthesis

Following studying the effects of temperature and extract concentration, the optimum AvoSE concentration were determined as 12.5 mg/ml and 80˚C. Hence, AvoSE-AuNPs were synthesized as described in Chapter 3 (section 3.2.2.1) and the effect of AvoSE pH was tested to determine the optimum pH for AvoSE-AuNPs formation. Figure 4.6 displays images of the AvoSE at its respective pH values and AvoSE-AuNPs synthesized from corresponding extracts. Interestingly, the intensity and hue of the AvoSE changed from a yellowish colour at lower pH values to darker orange shades as pH of the solutions increased. Visible colour changes indicated the formation of AuNPs at all tested pH values as can be seen in Figure 4.6. The SPR peak formation further proved that AvoSE-AuNPs were synthesized. Figure 4.7 displays the SPR peaks formed at varying pH values ranging from 4-10. Similar results were achieved at pH values tested. Except for pH 4 and pH 10 which had lower SPR peaks with λ_{max} at 536 and 528 nm respectively. A sharp and the highest SPR peak was formed at pH 9.0 and λ_{max} was observed at 532 nm. This is a left shift indicating that the presence of smaller nanoparticles. However, the width was wider than that of pH 7 indicating that AuNPs

synthesized at pH 9 were less uniform than that of pH 7.0 (Figure 4.7). The SPR peak at pH 10.0 was narrower however the SPR peak was much lower than at pH 9.0 indicating that less nanoparticles were present in solution. These results are in agreement with reported studies that state that the addition of hydroxide ions assists in the reduction reaction of metal ions (Feng *et al*., 2007). The absorbance corresponding to SPR peaks at pH values 5, 5.74, 6 and 8 was almost the same and their λ_{max} was at 536 nm for each pH value respectively.

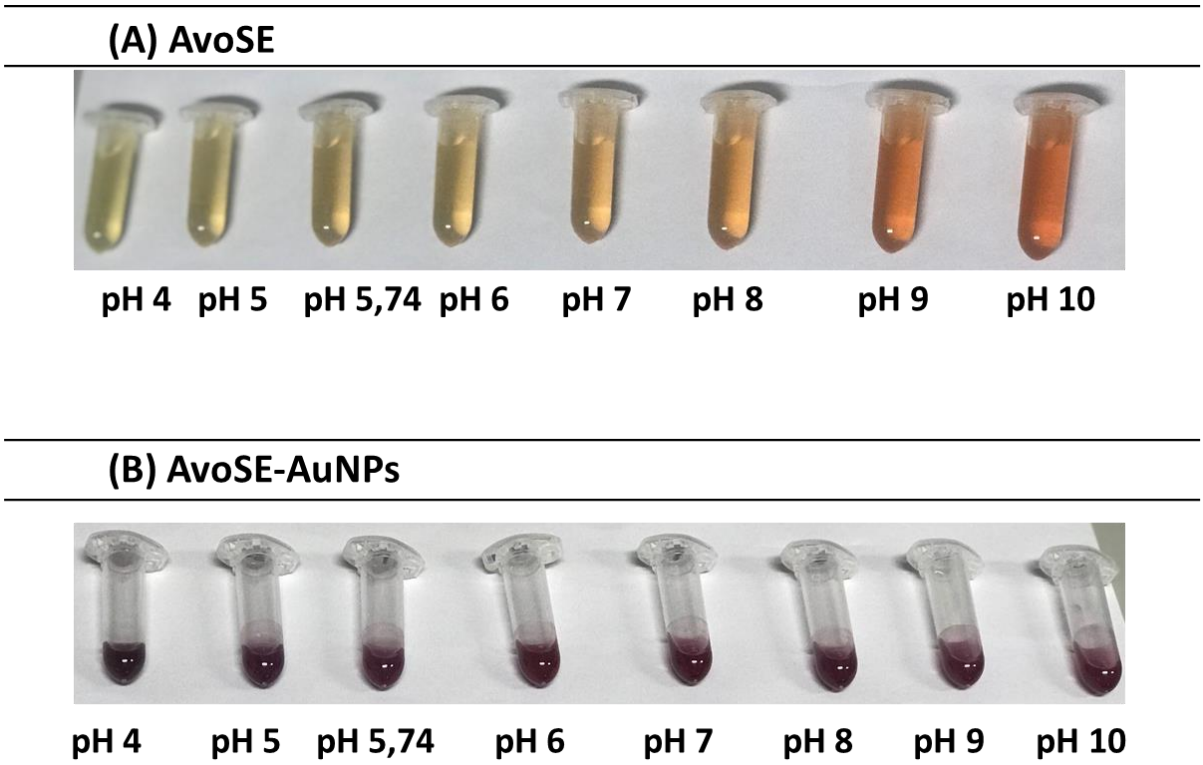

Figure 4.6: (A) Images of the Avocado seed extract showing intensifying colour with increasing pH values. (B) Images of AuNPs synthesized with AvoSE at corresponding pH values (4, 5, 5.74, 6, 7, 8, 9 and 10) mixed with 0.5 mM $HAuCl_4$ aqueous solution incubated at 80˚C for an hour.

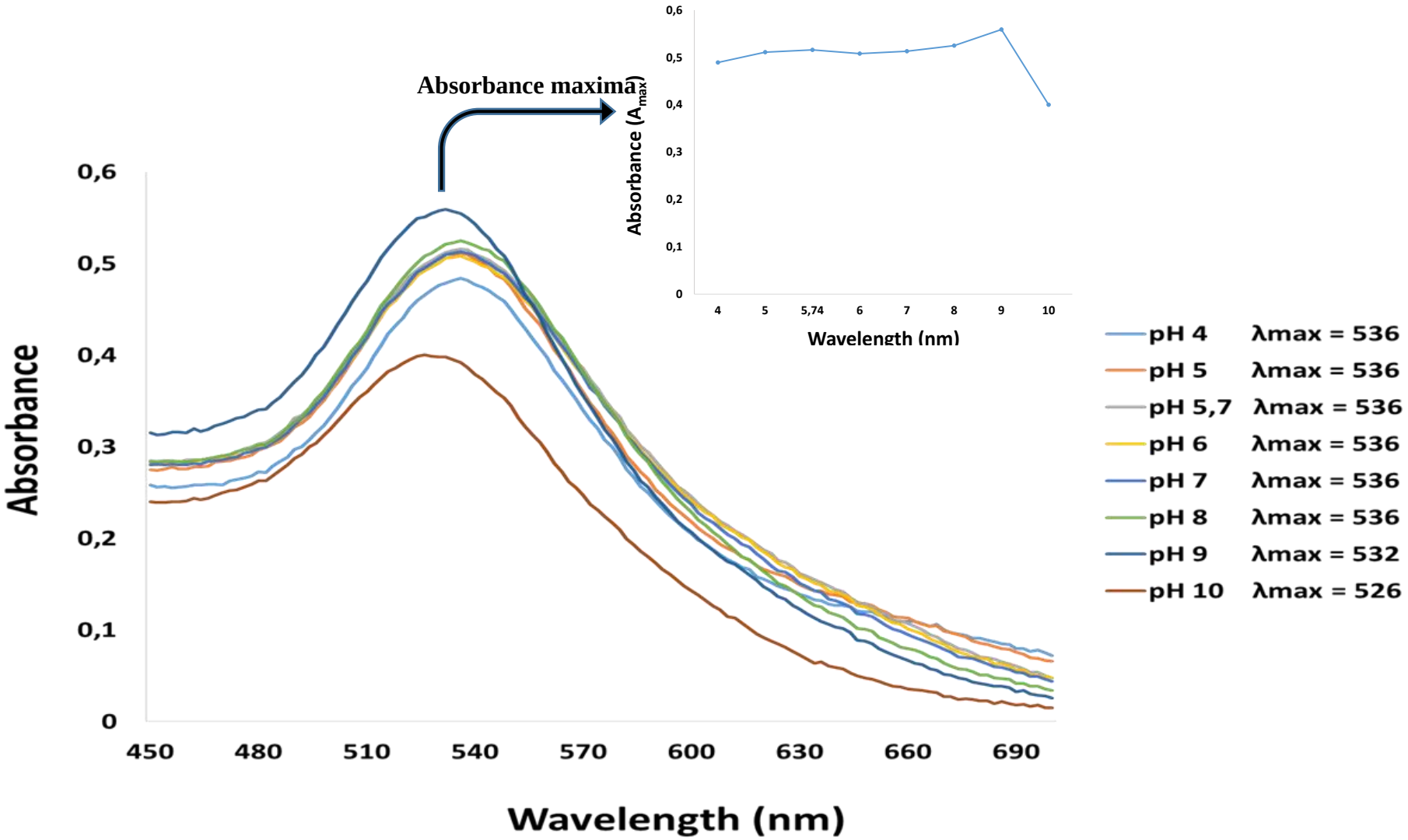

Figure 4.7: UV-vis spectra of SPR bands representing AvoSE-AuNPs formed at pH values 4, 5, 5.74 (pH of the fresh seed extract) 6, 7, 8, 9 and 10 using 0.5 mM $HAuCL_4$ aqueous solution incubated at 80 ˚C for 1 hour. Insert: A_{max} values obtained for each pH studied.
The experiment was repeated (n=3) and the graphs are presented as average results.

The optimum AvoSE-AuNPs formation was selected to be pH 7 due to the SPR peak which was narrow and sharp and the λ_{max} was at 536 nm. Acoording to Esposito *et al.* (2002), pH influences the charge of the extract, which can lead to a repulsion or attraction of metals in solution. It may also affect the conformation of the molecules, which determines whether more or less binding sites will be available for metal binding (Figueira *et al.*, 1999). At the lower pH range there is a high concentration of protons which neutralizes the negatively charged biomolecules from the extract and makes binding groups carry more positive charges. Hence, this may lead to aggregation or distortion of AuNPs formed (Feng *et al*., 2007).

c) Effect of $HAuCl_4$ on AuNPs synthesis by AvoSE

The possibility of controlling the particle size was further investigated by changing the concentration of aqueous $HAuCl_4$ solution to confirm whether it plays a role in AuNPs formation and size reduction. Following the optimization of extract concentration, temperature and pH, in this section synthesis was completed using the previously identified optimum conditions as described in Chapter 3 (section 3.2.2.1). Figure 4.8 shows that synthesis at the lowest concentration (0.25 mM) of aqueous $HAuCl_4$ solution the SPR peak was very broad and flat signifying that AvoSE-AuNPs formation was not favourable. The SPR peak at 0.5 mM was also broad and flat however the absorbance slightly increased indicating that more AvoSE-AuNPs were formed. Narrow, sharp and symmetrical SPR peaks were formed at 0.75 mM and 1 mM and the λ_{max} was 536 nm at both concentrations. At 2 mM and 3 mM the SPR peaks formed well and the absorbance values were high, however the λ_{max} were in the longer wavelength tail of the spectrum at 548 and 562 nm respectively. The right shift suggest significant anisotropy in the AvoSE-AuNPs formed. The results show that increasing the concentration of aqueous $HAuCl_4$ solution increased the absorbance with exception to the higher concentrations (4 mM and 5 mM). The SPR peaks formed at 4 and 5 mM were broad and the absorbance decreased, this was likely due excess gold ions present in proportion to reducing agents which resulted in competition for reducing agents and hindered AuNPs formation. Similar results were obtained by Ahmad *et al*. (2017) who worked with *Mentha piperita* leaf extract. Like this study they tested concentrations from 1 mM to 5 mM and reported that higher concentrations of $HAuCl_4$ solution increased aggregation of the nanoparticles due to competition between the Au^{3+} ions and the functional groups of the leaf extract. The experiment also reported that at 1 mM concentration, the nanoparticle synthesis and size reduction was rapid because of availability of larger number of functional groups. The results in this study are in accordance with literature which states that biosynthesis of

nanoparticles increases with increasing ion salt concentration (Ahmad *et al.*, 2003; Feng *et al.*, 2007). In this study the optimum salt concentration was found to be 1 mM, reflected by a single and narrow peak with a maximum occurring at wavelength 534 nm.

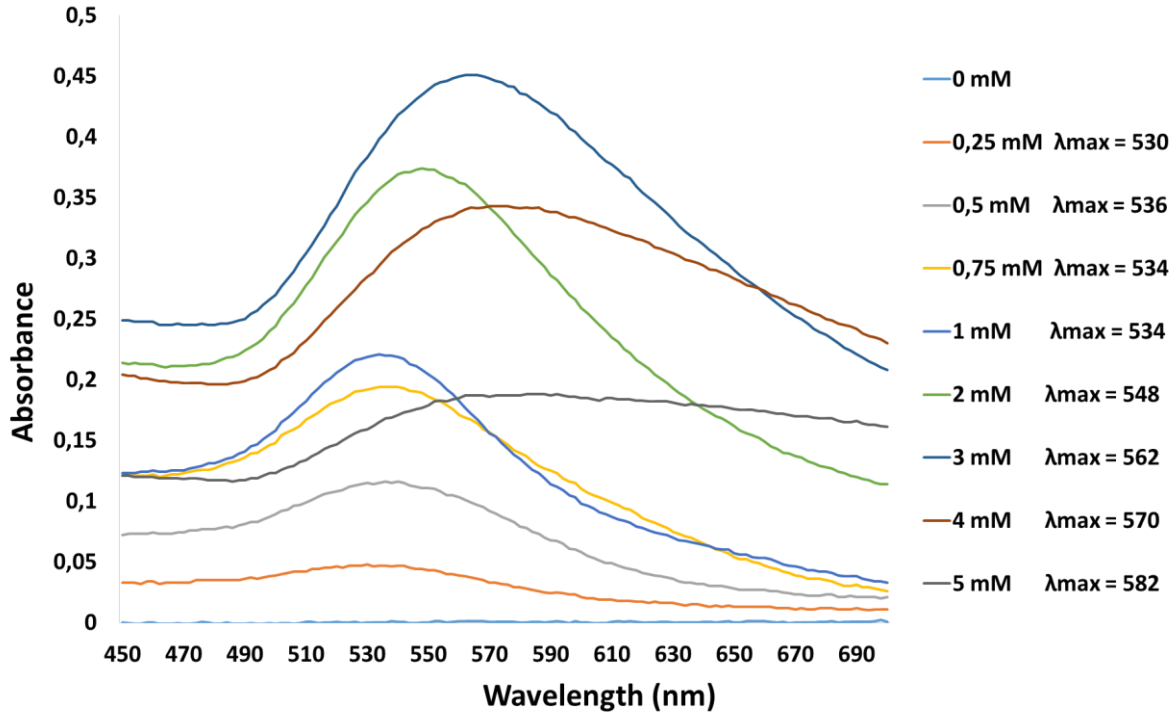

Figure 4.8: Uv-vis spectra of SPR peaks representing AvoSE-AuNPs synthesized using 12.5 mg/ml extract at pH 7 and aqueous $HAuCL_4$ solution at concentrations 0.25, 0.5, 0.75, 1, 2, 3, 4 and 5mM. The reactions were incubated at 80 ˚C for 1 hour. The reaction was repeated (n = 3).

d) Kinetic synthesis of AvoSE-AuNPs

The kinetics of the reaction was studied via UV-vis spectroscopy as described in Chapter 3 (section 3.2.2.1). The AuNPs were synthesized using 3 different extract concentrations (6.25, 12.5. and 25 mg/ml) in order to determine their effects on reaction kinetics. This experiment was conducted to determine the optimum duration needed for the bio-reduction to complete. This is to ensure that the reaction is not terminated prematurely and sees the end of nucleation and capping phases to ensure stable NPs.

We studied the kinetics of the AvoSE-AuNPs formation by examining the changes in the λ_{max} of the UV-vis spectra presented in Figure 4.9. Graph B represents AvoSE-AuNPs formed using a concentration of 12.5 mg/ml AvoSE and 6.25 and 25 mg/ml AvoSE were used and represented in graph A and C respectively. In graph A synthesis was slower and this can be

seen by the low SPR peaks. From minute 1-5 the SPR peaks are under OD value 0.2 which is low compared to graph B and C which are over OD value 0.2 within 1 minute of synthesis. Graph B shows a steady increase in the intensity of the SPR peaks over time. It is suggested that the yield of AuNPs is directly linked to the increase in the number of forming AuNPs (Mishra, Tripathy, & Yun, 2012). Many reports discuss the effect of incubation time and its effect on the SPR peaks. For example, Dwivedi & Gopal (2010) reported that increasing precursors contact time sharpened the SPR peaks of *Chenopodium album* leaf extract-AuNPs. Graph C shows a steady increase in the formation of AvoSE-AuNPs between 0-3 minutes. After 4 minutes there is not significant change in absorbance suggesting that synthesis at 25 mg/ml AvoSE is rapid and this can be confirmed by graphs D, E and F which show changes in λ_{max} over time.

The rate of synthesis was calculated for graph D, E and F as below:

Rate of reaction = $\frac{\Delta OD\ value\ at\ \lambda\text{max}}{\Delta\text{time}}$

	Rate of reaction
Graph D: 6.25 mg/ml	0.1788 min^{-1}
Graph E: 12.5 mg/ml	0.3608 min^{-1}
Graph F: 25 mg/ml	0.3442 min^{-1}

Graph D depicts a less slope and the rate of reaction confirms that the synthesis at 6.25 mg/ml is the slowest. It would be expected that synthesis 25 mg/ml would be the fastest reaction because there are bioavailability of reducing agents at this concentration (graph D). However, synthesis of AvoSE-AuNPs occurs the fastest at 12.5 mg/ml AvoSE. This is an indication that the amount of available reducing agents in solution has an effect on the reaction rate. Furthermore, it gives credence to the optimization done before the determination of the rate of synthesis and confirms that synthesis was completed at the correct determined optimum. The reaction time in this study was found to be lower than several reported studies (Ahmad *et al*., 2016; Dubey, Lahtinen, & Sillanpää, 2010; Dwivedi & Gopal, 2010).

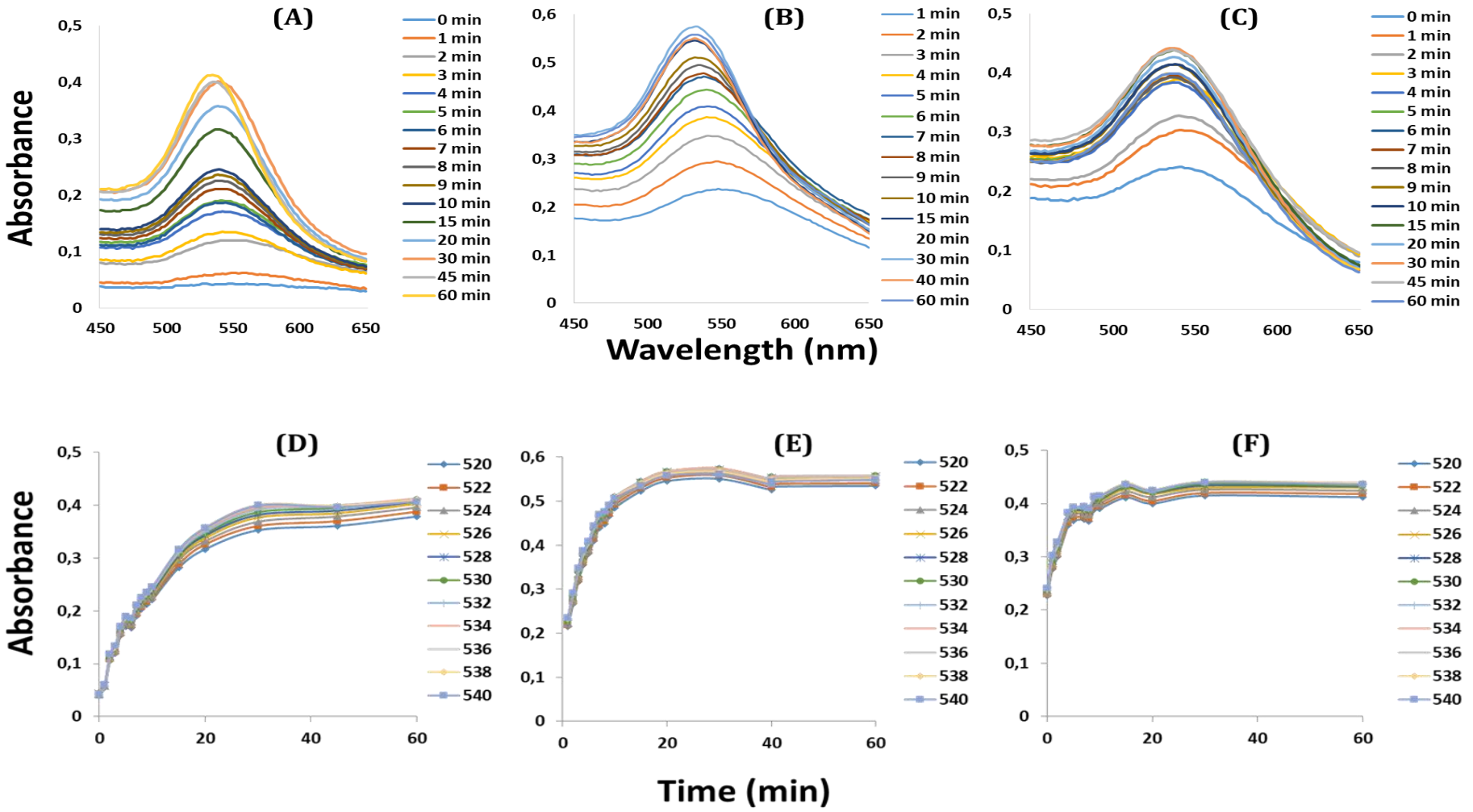

Figure 4.9: Uv-vis spectra recorded as a function of time for the synthesis of AvoSE-AuNPs using (A) 6.25 mg/ml AvoSE (B) 12.5 mg/ml AvoSE (C) 25 mg/ml AvoSE at pH7, 1 mM aqueous $HAuCL_4$ solution. The reaction was incubated at 80 ˚C over 1 hour. Graphs of A,B and C representing change in absorbance over time during synthesis at (D) 6.25 mg/ml AvoSE (E) 12.5 mg/ml AvoSE (F) 25 mg/ml. The reactions were repeated (n = 2).

4.2.2.2 Dynamic light scattering and ζ- potential

DLS spectroscopy was used to study the size distribution of AvoSE-AuNPs. A Zetasizer (Nano-ZS90 system, Malvern Inc.) was used to characterize the particle hydrodynamic size, particle size distribution, i.e. polydispersity index (PDI) and zeta potential as described in Chapter 3 (section 3.2.2.2). Figure 4.10 is a size distribution graph of the AvoSE-AuNPs synthesized at the optimum conditions reported in the above sections. The AvoSE-AuNPs sample was scanned and the mean-average particle size (z-average particle size) was determined to be ~133.3 ± 0.9 nm (Figure 4.10). The formation of relatively bigger NPs in green synthesis is associated with the presence of biomass. The hydrodynamic size provides the whole size of conjugate including core size and ligands on the surface shell surrounding (Aljabali *et al*., 2018). Since PDI predicts the degree of uniformity of the particles size in solution, the PDI values range on a scale between 0 (considered as highly uniform/monodisperse) to 1 (considered highly polydisperse/broad size distribution) (Danaei *et al.*, 2018). In this study the PDI of the AvoSE-AuNPs was 0.5 ± 0.01, PDI values lower than 0.5 are generally considered acceptable and are taken as an indication of a more homogenous distribution. The higher the PDI value, closer to 0.7 and more are considered as a more heterogeneous distribution of sizes of particles. The intensity percentage in Figure 4.10 shows that the particles present in solution were more polydispersed and majority of the particles present were over 100 nm in size. The AvoSE-AuNPs DLS results are similar to several other studies which have produced AuNPs using green synthesis means (Bali & Harris, 2010; Narayanan & Sakthivel, 2008; Philip, 2010). The particle sizes produced in these studies also produced AuNPs in the range of 20 nm to 200 nm. Furthermore, the studies confirm the formation of highly dispersed AuNPs which exist in various geometrical structures such spheres, quasi-spheres, triangle, prisms, and hexagons.

The charge on the surface of the AvoSE-AuNPs was also determined as a reflection of the δ-potential after synthesis using a Malvern Zetasizer Nano ZS. The δ-potential values is generally used as a hallmark indication of the stability of the NPs. It is the net electrical charge on particles' external surface stemming from the attached functional groups. The δ-potential of the AvoSE-AuNPs was -21.5 ± 0.15 mV (Figure 4.11). This suggested that the stability of AvoSE-AuNPs may be of short-term, as the generally accepted stability range lies outside +30 mV and -30mV (Eltarahony *et al.*, 2016).

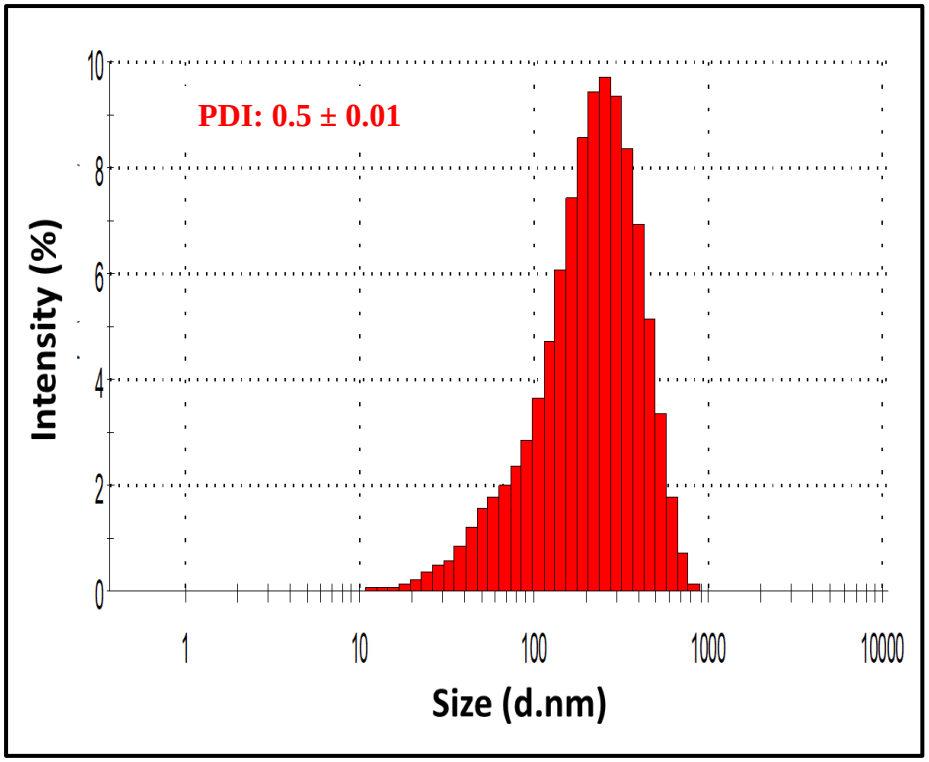

Figure 4.10: Hydrodynamic size distribution of biosynthesized AvoSE-AuNPs

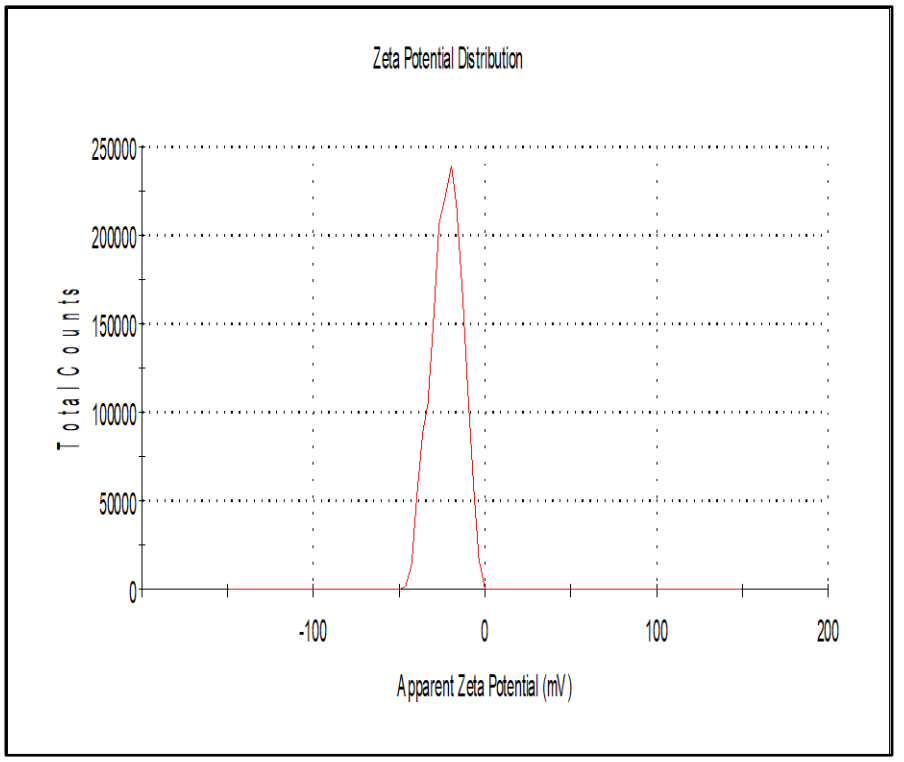

Figure 4.11: Zeta potential distribution curve of biosynthesized AvoSE-AuNPs

4.2.2.3 Fourier-transform infrared spectroscopy (FTIR) of AvoSE-AuNPs

FTIR spectrums of the AvoSE and AvoSE-AuNPs were determined to possibly identify the functional groups which are involved in the biosynthesis of the AvoSE-AuNPs. This information can allow for the identification of the phytochemicals originating from the AvoSE which possibly act as the reducing agents in the bioreduction of gold salt. Several studies suggest that various phytochemicals play a role in the synthesis of AuNPs mediated by plants or plant material (Baker *et al*., 2013; Singh *et al*., 2016). Generally, it is suggested that different classes are involved based on the major constituent of the plant or plant material used (Elbagory *et al*., 2016).

The FTIR spectrum of the biosynthesized AvoSE and AvoSE-AuNPs is shown in Figure 4.12. The overlapping peaks indicate the presence of compounds of the same kind and the sharpness of the peaks suggests the quantity of the corresponding functional groups (Figure 4.12). Some of the peaks appear to be slightly shifted between the AvoSE and AuNPs and this is expected because of the gold metal physically interacts with the phytochemicals (Elia *et al*., 2014). Table 4.1 lists the shifts and identifies the biomolecules which correspond to their IR absorptions from the FTIR spectrum of AvoSE and AvoSE-AuNPs. The peak at 587.32 cm^{-1} is due to the presence of alkyl halides, which is primarily due to a C-Br stretch. A weak peak occured at 1044.86 cm^{-1} due to the presence of aliphatic amines with a C-N stretch. The medium peak occurring at 1637.67 cm^{-1} is possibly due to the stretching of *cis* C-C bonds and primary amines, N-H band. The presence of the very weak peak at 2123.24 cm^{-1} is due to alkynes represented by a stretch arising from C≡C. At 3317.8 cm^{-1} a very strong and broad peak occurs which is considered as the presence of alcohols, phenols and primary/secondary amines.

These results are in accordance with several studies such as by Tiegam *et al.* (2019) which identified bands 3330 cm^{-1}, 3000-2840 cm^{-1}, 2920 cm^{-1}, 1730 cm^{-1}, 1580 cm^{-1} and 1150-1000 cm^{-1} from raw Avocado seeds. The spectra indicates the presence of hydroxyl and carboxylic groups on the AvoSE-AuNPs and this may possibly be a result of the involvement of flavonoids, terpenoids, phenolic compounds and/or carbohydrates in the synthesis process (Tables 4.1). Several studies have reported the role of hydroxyl and carboxylic acids containing compounds in the bioreduction, capping and stabilization of AuNPs (Ajitha, Reddy, & Reddy, 2015; Dorosti & Jamshidi, 2016). Amino acids and proteins are also suggested to act as stabilizers of AuNPs after the reduction process (Balashanmugam *et al*., 2016). The bands listed were identified on the AvoSE-AuNPs and thus we speculate their involvement in the

formation of AvoSE-AuNPs. The vibration bands on this study were assigned using results from literature studies based on the characterization of raw Avocado seed and leaf extract of *Mentha piperita* (Ahmad *et al*., 2017; Tiegam *et al.*, 2019).

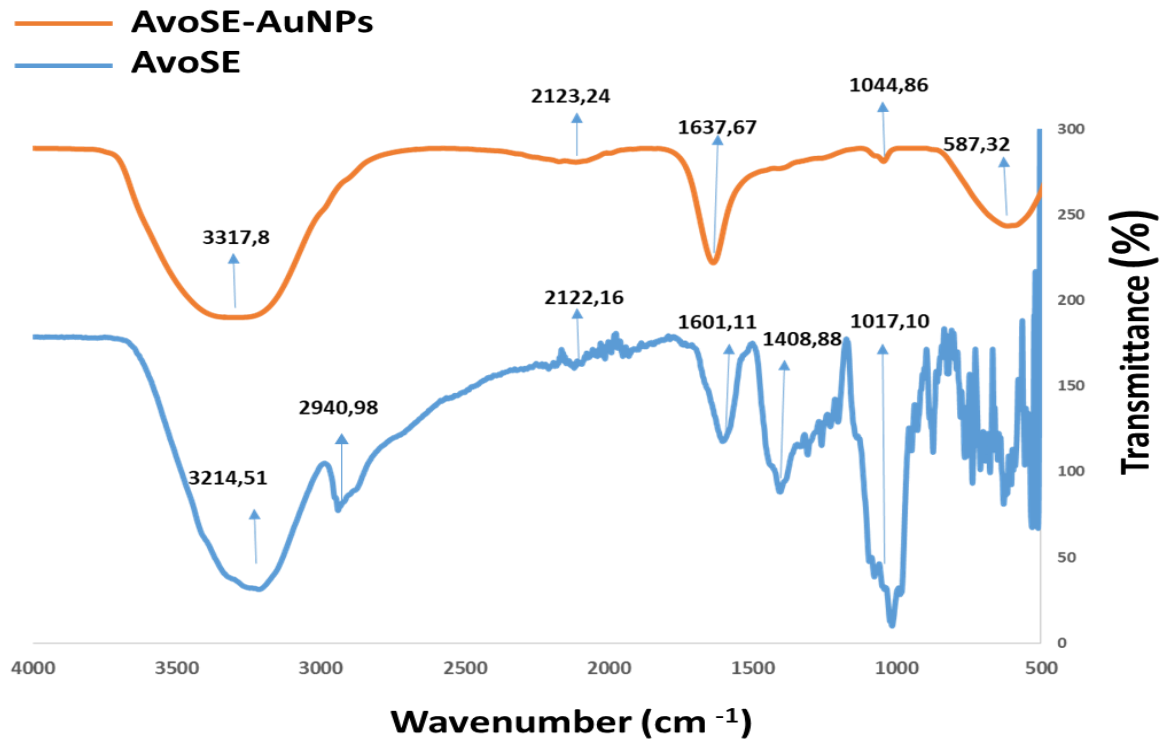

Figure 4.12: A representative ATR-FTIR spectra pattern of AvoSE-AuNPs.

Table 4.1: Characterized IR absorptions from the FTIR spectrum of AvoSE and AvoSE-AuNPs

Peak position In extract (cm $^{-1}$)	**Peak position AuNP (cm $^{-1}$)**	**Shift in position**	**Type of chemical bond**
3214.51	3317.8	103.29	-OH, H-bonded, N-H Alcohols, phenols, carboxylic acids 1˚, 2˚ Amines
2122.16	2123.24	1.08	-C ≡ C alkynes
1601.11	1637.67	36.56	-N-H, cis C-C 1˚ amines, aromatics
1044.06	1044.86	0.80	-C-N Aliphatic amines
629.75	587.32	56.93	-C–Cl Alkyl halides

4.2.2.4 High Resolution Transmission electron microscopy of AvoSE-AuNPs

HRTEM was used analyse the morphology, determine the shape and size distribution of the synthesized AvoSE-AuNPs. It is evident from Figure 4.13 that the AvoSE-AuNPs were anisotropic and predominantly spherical in shape. The other shapes observed were hexagonal, triangular and rod-shaped particles. It is common for NPs synthesized via biological methods to be anisotropic (Shanker *et al*., 2003). In the case of plant/plant material mediated synthesis different phytochemicals in the extracts that are capable of reducing the gold ions. The images in Figure 4.13 do not show signs of aggregation and this can be accounted for by the fact that the biomolecules present in the extract can also act as stabilising agents during the biosynthesis (Geraldes *et al*., 2016).

The particles size range was between 6-24 nm and the average core size estimated using Image J software was ~14 ± 3.7 nm. It is important to note the huge difference between the hydrodynamic particle size as determined by DLS analysis and that of HRTEM (DLS = ~133.3 ± 0.9 nm). The HRTEM size analysis reveals the core size while DLS reveals the hydrodynamic size which includes ligands on the surface coating of NPs. Hence, particle size determined by DLS analysis is usually larger than the particle sized determined by HRTEM (Dorosti & Jamshidi, 2016). This is also true to this study and several other studies in literature support this result (Elbagory *et al*., 2016; Mmola *et al*., 2016). A similar study by Bogireddy *et al*. (2018) produced AuNPs from *Coffea arabica* seed extract (CASE) and reported similar HRTEM analysis results. Comparable to this study, the synthesized CASE-AuNPs were optimized by analysing the effects of pH and the biosynthesis process produced anisotrophic CASE-AuNPs of irregular shapes and spheres. Furthermore, the study confirmed that it is possible to control shape anisotropy and size of AuNPs by controlling the certain parameters like pH of the reaction mixture. Figure 4.14 shows the selected area electron diffraction (SAED) pattern, which confirms the crystalline nature of the AvoSE-AuNPs. The observed rings were found to correspond to the (111), (200), (220), (311) and (222) reflections of face centred cubic gold. The bright observed rings were indexed according to studies which reported similar results to that of biosynthesized AvoSE-AuNPs (Elbagory *et al*., 2016; Yin, Chen, & Wu, 2010).

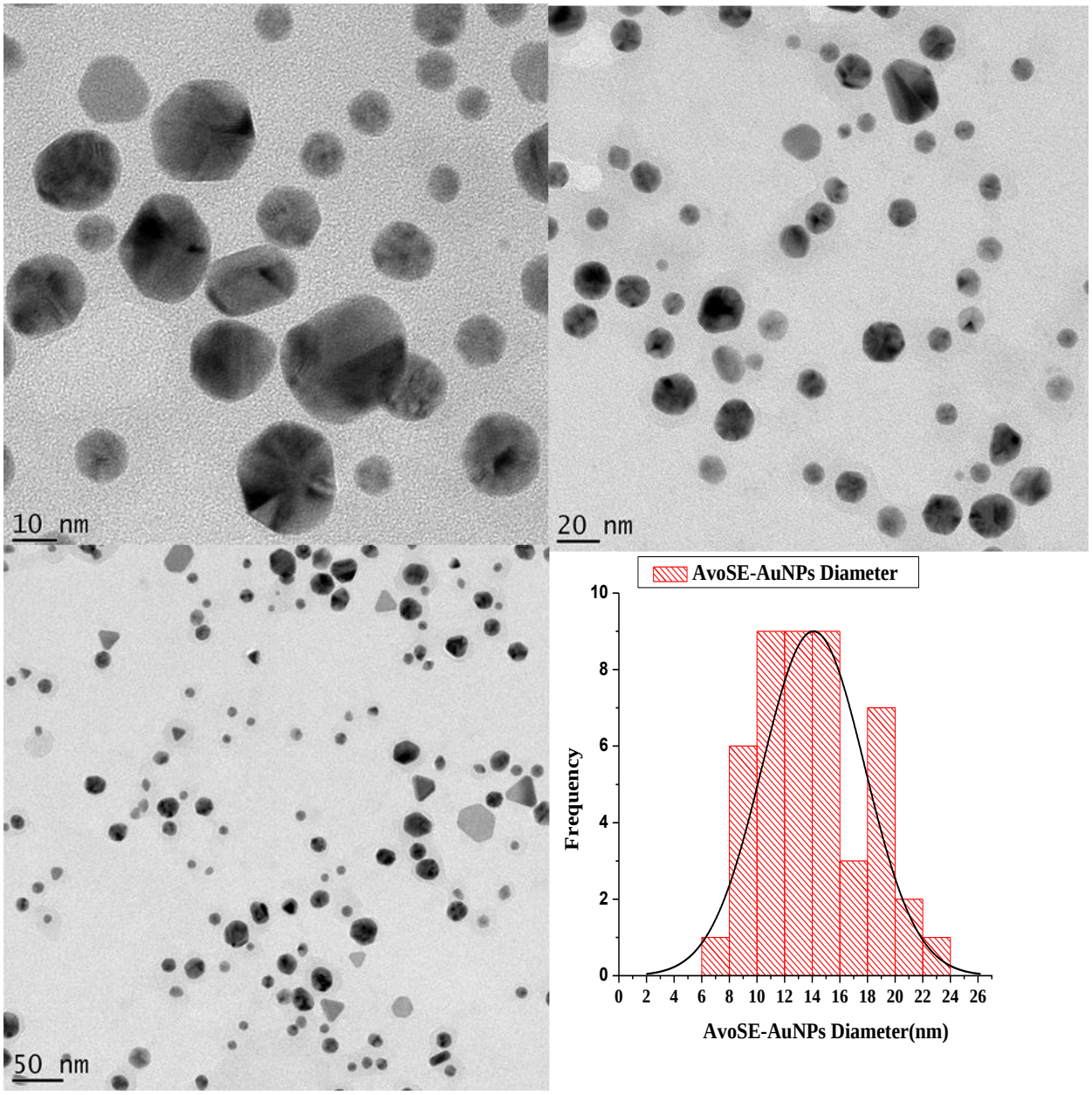

Figure 4.13: TEM images of the biogenic AvoSE-AuNPs and its particle size distribution

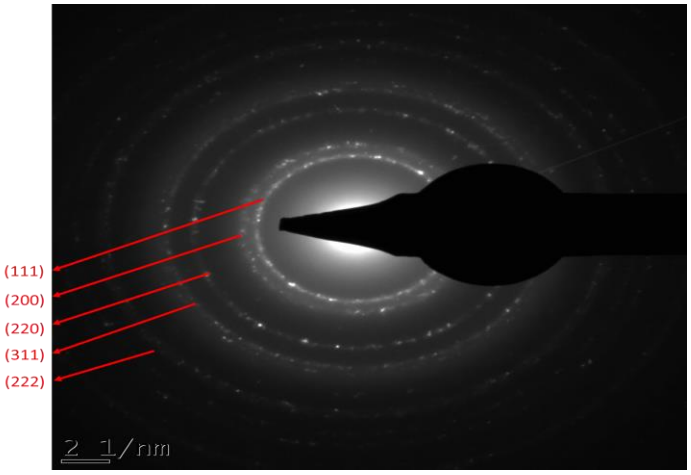

Figure 4.14: Selected area electron diffraction (SAED) pattern of the AvoSE-AuNPs

A green approach for AuNP synthesis was achieved in this study using AvoSE as a source of reducing and stabilising agents. The studied effects of extract concentration, temperature, salt solution concentration and pH proved that these parameters do in fact have an influence in nanoparticle formation. Furthermore, the study proved that the size and shape of the synthesized AvoSE-AuNPs can be modulated by adjusting the extract concentration, temperature, salt solution concentration and pH of AvoSE. DLS analysis revealed the hydrodynamic size factoring the ligands on the surface of the AuNPs and TEM confirmed the core size of the NPs. Furthermore, TEM analysis enabled the determination of various shapes produced during AvoSE-AuNPs. The mechanism of action involved in green synthesis of nanoparticles is in its infancy and has been a challenge to address for many researchers in the field. This is due to the complex systems of the abundant secondary metabolites that plants/plant materials produce. FTIR provided a clue to these mechanisms by enabling the confirmation of biomolecules present on the surface of the AvoSE-AuNPs. This helped support the notion that the phytochemicals from AvoSE were responsible for the reduction of Au ions in AvoSE-AuNP synthesis.

CHAPTER 5

RESULTS AND DISCUSSION: ANTIBACTERIAL, CATALYTIC AND ANTI-CANCER ACTIVITIES

5.1 Antimicrobial Resistance

AuNPs are generally regarded as being biologically inert and not characterized by their antibactericidal properties due to having no or low activity at high concentrations antibacterial (Allahverdiyev *et al*., 2011). AuNPs can appear to kill bacteria possibly due to the antibacterial activity of the co-existing chemicals not completely removed from the particles or that are involved in the synthesis or surface coating agents (Zhang *et al*., 2015). Green synthesized nanoparticles results in NPs with proteins, polysaccharides and bioactive compounds binding as surface coating agents which may further enhance their antimicrobial activity (P. Singh, Garg, *et al.*, 2018). AvoSE is rich in bioactive compounds and studies such as by Fernandez-Castaneda *et al*. (2018) have proved that AvoSE has antimicrobial activity against the bacteria *Salmonella Enteritidis, Citrobacter freundii, Pseudomonas aeruginosa, Enterobacter aerogenes, Bacillus cereus, Staphylococcus aureus, Listeria monocytogenes, and the yeast Zygosaccharomyces bailii.* Hence, in this study the biosynthesized AuNPs using AvoSE as previously discussed in chapter 3 were evaluated for antibacterial activity against *Escherichia coli (E. coli), Staphylococcus aureus (S. aureus), Klebsiella pneumoniae (K. pneumoniae), Staphylococcus epidermidis (S. epidermidis), Streptococcus pyogenes (S. pyogenes)* and Methicillin-resistant *Staphylococcus aureus (MRSA)*. All six microorganism strains included in this study are bio-medically important and exhibit resistance to a number of current antibiotics.

Antibiotic-resistant Staphylococci are a global issue affecting humans, animals, and numerous natural environments. *S. epidermidis* is an opportunistic pathogen frequently isolated from patients and healthy individuals (Schoenfelder *et al*., 2010). *S. aureus* is an important bacteria most common in the clinical setting and is responsible for a number of nosocomial infections (Chambers & Deleo, 2009). This bacterium rapidly acquired resistance to sulfonamides (Saga & Yamaguchi, 2009). Antibiotic-resistant strains of *S. aureus* have reached epidemic proportions globally (Grundmann *et al*., 2006). There is an overall burden of staphylococcal diseases that are particularly caused by MRSA, in healthcare and community settings (Hassoun, Linden, & Friedman, 2017). *K. pneumoniae,* is a gram-negative bacterium, which causes infections such as pneumonia, blood infections, wound or surgical site infections and

meningitis (Paczosa & Mecsas, 2016). This bacterium is commonly found in human intestines where it does not cause any harm (Paczosa & Mecsas, 2016). *K. pneumoniae* has also developed antimicrobial drug resistant strains (Caneiras, Lito, Melo-Cristino, & Duarte, 2019). *S. pyogenes* has remained universally susceptible to β-lactams since the 1940s (Pichichero & Casey, 2007). However, since then a significant number of treatment failures have been reported (Schaar *et al*., 2013). *E. coli* is also one of the main causes of both nosocomial and community acquired infections in humans. The above mentioned bacteria is therefore of clinical importance and finding new antibacterial agents for treatment is crucial. To address this, there is a critical need for new antibiotics we screened the green synthesised AvoSE-AuNPs for activity against these six bacterial strains. The next section discusses the antibacterial activity of the AvoSE-AuNPs.

5.1.1 Results and Discussion: Antibacterial activity of AvoSE-AuNPs

The agar well diffusion method was used to study the antibacterial activity of AvoSE-AuNPs as described in Chapter 3 (section 3.2.3). Bacterial strains including *K. pneumoniae*, *E. coli*, *S. aureus, S. epidermidis, S. pyogenes* and *MRSA* were used in the antimicrobial activity tests. The ZOI in and around each well in different concentrations levels of AvoSE and AuNPs are presented in Table 5.1 and 5.2 respectively. As can be seen in Table 5.1, AvoSE demonstrated antibacterial activity against all the tested strains at concentration 50 mg/ml and 100 mg/ml and had no effect on *K. pneumoniae*. *S. aureus* was the most susceptible to AvoSE due to its inherent ability to generate reactive oxygen species (ROS), hence at all tested extract concentrations it showed inhibition activity (Vimalraj *et al*., 2018).

Idris *et al*. (2010) tested antimicrobial activity of Avocado seed extracts against *E. coli*, *K. pneumoniae*, *B. subtilis*, *S. pyogenes*, *P. aeruginosa*, *S. aureus*, *C. ulcerans*, *S. typhi*, *N. gonorrhoea* and *C. albicans* and reported the potency of the extracts against all of the strains. The tested extracts showed promising activity against the bacterial strains. The study suggested that the antimicrobial activities displayed by the extracts could perhaps be explained by the presence of flavonoids, tannins, saponins and steroids present in the extract. For example, flavonoids are known to be produced by plants in response to microbial attacks and tannins are also reported to possess various biological activities such as anti-irratancy, anti-secretolytic, anti-inflammatory and antimicrobial (Cowan, 1999). Thus, it can be suggested that the extracted phytochemicals in this study are responsible for the identified antibacterial activity. Furthermore, this study corroborate that by Idris *et al*., (2010), and signifies the potential of AvoSE as a source of therapeutic agents which could provide leads in the ongoing search for

antimicrobial agents from plant material. The antibacterial activity of plant extracts is generally well documented. However, the antibacterial activity of biogenic metal nanoparticles produced from those plant extracts remains an area that is largely unexplored.

The AvoSE-AuNPs exhibited no inhibition on all the tested strains despite the inhibition exhibited by the extract at certain concentrations (Table 5.2).

Table 5.1: Antibacterial effect on *E. coli*, *S. aureus*, *K. pneumoniae*, *S. epidermidis*, *S. pyogenes* and *MRSA* tested at different doses of Avocado seed extract (AvoSE) ranging from 6.125 -100 mg/ml.

Concentration (mg/ml)	Zones of inhibition (mm)					
AvoSE-	*Klebsiella pneumoniae*	*Escherichia coli*	Methicillin-resistant *Staphylococcus aureus*	*Staphylococcus aureus*	*Streptococcus pyogenes*	*Staphylococcus epidermis*
6,125	0	0	0	10	0	0
12,5	0	0	0	12	0	0
25	0	0	10	12	0	0
50	0	10	12	12	10	12
100	0	13	13	14	1	14

Table 5.2: Antibacterial effect on *E. coli*, *S. aureus*, *K. pneumoniae*, *S. epidermidis*, *S. pyogenes* and *MRSA* tested at different doses of AvoSE-AuNPs ranging from 0.5 -0.03125 mg/ml

Concentration (mg/ml)	Zones of inhibition (mm)					
AvoSE-AuNPs	*Klebsiella pneumoniae*	*Escherichia coli*	Methicillin-resistant *Staphylococcus aureus*	*Staphylococcus aureus*	*Streptococcus pyogenes*	*Staphylococcus epidermis*
0,03125x	0	0	0	0	0	0
0,0,625x	0	0	0	0	0	0
0,125x	0	0	0	0	0	0
0,25x	0	0	0	0	0	0
0,5x	0	0	0	0	0	0

Mechanisms of bacterial death caused by NPs include impeding electrostatic flux across the bacterial membrane resulting in distortion and enhanced gene expression which help with redox processes that confer a bactericidal effect (Kim *et al*., 2007; Li *et al*., 2010; Nagy *et al*., 2011). The NPs penetrate the bacterial cell wall and the antimicrobial mechanisms are attributed to the small size of the NPs, surface chemistry, polyvalency and photothermic nature (Boisselier & Astruc, 2009; Dykman & Khlebtsov, 2011; Gu *et al*., 2003). The smaller the

nanoparticle the more effective it is at killing bacteria (Slavin, Asnis, Häfeli, & Bach, 2017). The synthesized AvoSE-AuNPs were large (over 100 nm) with a hydrodynamic size of 133.3 ± 0.9 nm. Hence, it can be speculated that the AvoSE-AuNPs could not penetrate the bacterial cell wall to exert antibacterial activity. The AuNPs were also synthesized with 12.5 mg/ml of extract at a 9:1 $HAuCl_4$ solution to AvoSE, respectively. Hence, perhaps the extract concentration is proportional to the amount of active phytochemicals on the NPs and thus may affect antibacterial activity of NPs.

5.2 Catalytic activity of AvoSE-AuNPs

Nitrophenols are common organic pollutants which are broadly present as products of industrial processes and in agricultural waste water (Kong *et al*., 2017). These pollutants are hazardous and harmful to the environment even when present in low concentrations. 4-NP is found in waste water often originating as an end-product in the degradation of pesticides, from industrial plants used for paper manufacturing, pharmaceutics and dye industries (Chiou *et al.*, 2013). It has major adverse effects on the blood, liver and central nervous system and may cause hypoxia (El-Bahy, 2013; Yeh & Chen, 2014). This has inspired the discovery of several actions for the removal of polluting nitrophenols, including adsorption, microbial degradation, photocatalytic degradation, electro-Fenton method, electrocoagulation, electrochemical treatment and others (Cañizares *et al.*, 2004; Dieckmann & Gray, 1996; Marais & Nyokong, 2008; Modirshahla, Behnajady, & Mohammadi-Aghdam, 2008; O'Connor & Young, 1989; Oturan *et al.*, 2000). However, these methods are energy consuming, some are unsafe and require the use of organic solvents (Chiou *et al.*, 2013). The reduction of 4-NP by $NaBH_4$ to 4-AP is a selective hydrogenation reaction in which metallic NPs can be used as catalysts, reported first by Pradhan *et al.* (2002) using silver NPs. The reaction has now since been used to characterize the performance of newly designed catalysts (Kong *et al.*, 2017; Hutchings & Edwards, 2012; Pradhan *et al*., 2002). It is also commonly used as a model to assess the catalytic activity of AuNPs (Seo *et al*., 2017). It has been used in over one thousand published academic articles every year, signifying that it is a general yet important and powerful method (Kong *et al*., 2017b). Furthermore, the amino products are useful and important reactants in many applications. 4-aminophenol could be employed in the synthesis of painkillers, antipyretic drugs and as corrosion inhibitors (Seo *et al*., 2017). It is simple, fast and a clean reaction which can be monitored in real-time following the addition of AuNPs. Hence, this model reaction was used to assess the potential catalytic activity of the AvoSE-AuNPs.

5.2.1 Results and discussion: Catalytic activity of AvoSE-AuNPs

The catalytic reduction of 4-NP by $NaBH_4$ in the present of AvoSE-AuNPs was conducted as stipulated in Chapter 3 (section 3.2.4). Figure 5.1 displays the spectrum of an aqueous solution of 4-NP (2 mM) which showed maximum absorbance at 321 nm. The reduction reaction was initiated with the addition of $NaBH_4$ (0.03 M), upon addition the colour changed from light yellow to a brigh yellowish-green, and there were bubbles which formed due to the release of hydrogen gas (Hashimi *et al.*, 2019). The peak shifted from 321 nm (4-NP) to maximum absorbance of 400 nm, which indicated the formation of 4-nitrophenolate ions as observed in Figure 5.1, indicated by 4-NP + $NaBH_4$ (Li & Chen, 2013; Seo *et al.*, 2017). The peak remained in this position even after 75 minutes of reaction time.

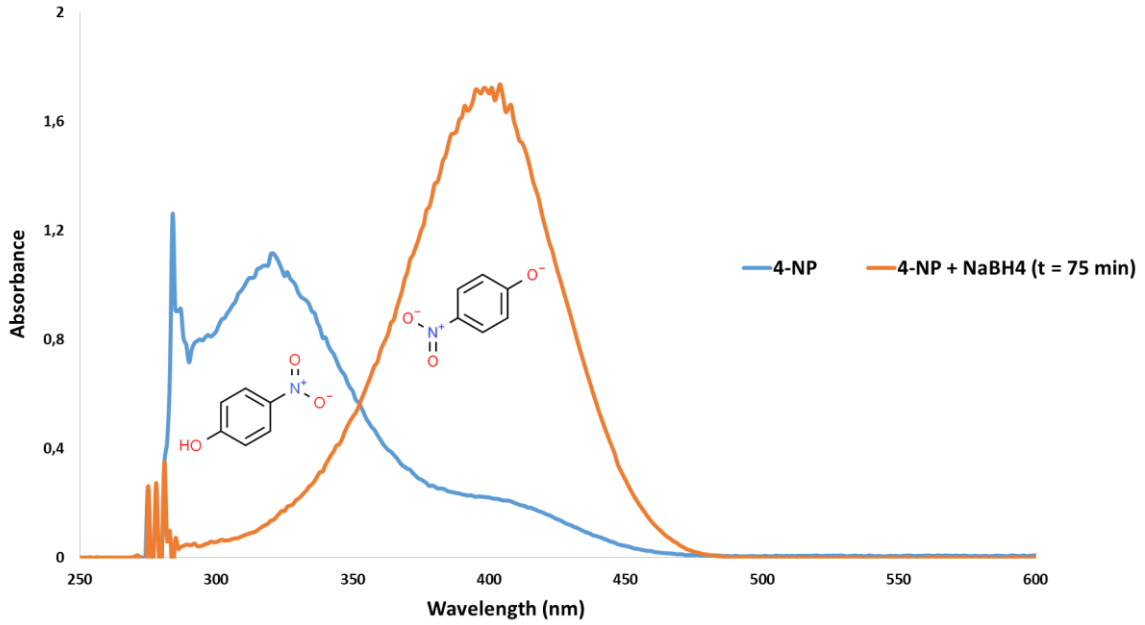

Figure 5.1: UV-vis spectra of an aqueous solution of 4- nitrophenol (4-NP) with A_{max} occurring at 321 nm and of the 4- nitrophenolate ions (4-NP+$NaBH_4$) produced with the addition of $NaBH_4$ with A_{max} occurring at 400 nm.

Figure 5.2 shows the control reactions conducted to illustrate that the reaction without AvoSE-AuNPs added as a catalyst does not proceed to produce 4-AP (graph A). This corroborates with other studies which show that the 4-NP reduction reaction cannot occur without the presence of a catalyst (Kong *et al.*, 2017; Seo *et al.*, 2017). Graph B shows the reaction occurring in the presence of the AvoSE. It can be observed that the peak has not shifted, indicating that the extract on its own was unable to reduce 4-NP to form 4-AP. The additional peak at λ_{max} ~288 nm corresponds to the avocado seed extract (Segovia *et al.*, 2018).

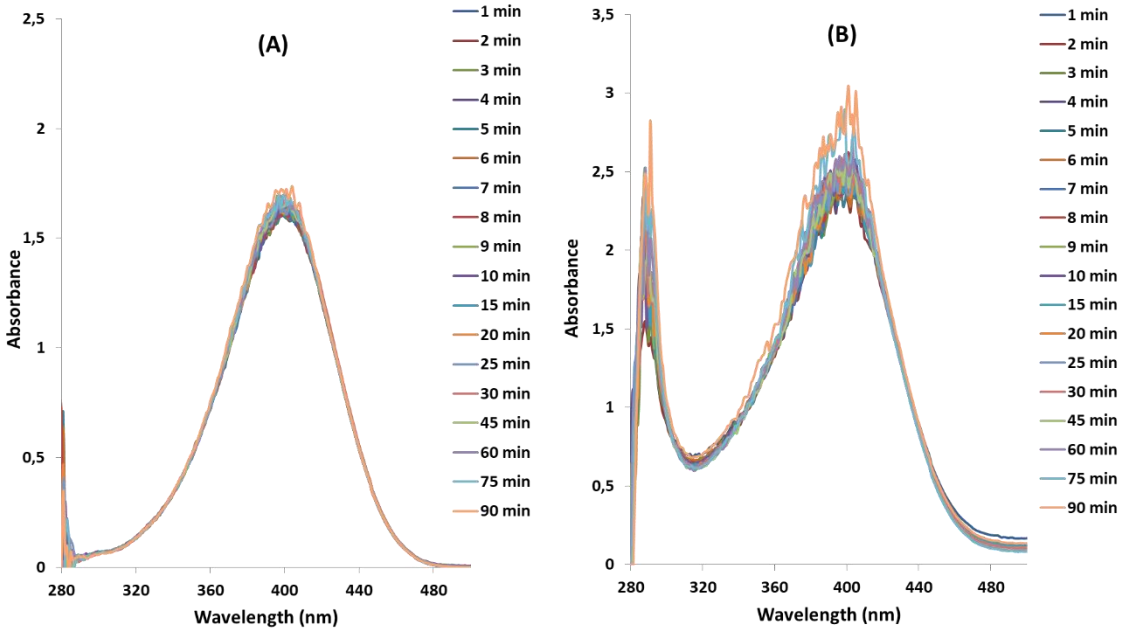

Figure 5.2: UV-vis spectra of the 4- nitrophenolate ions produced with the addition of $NaBH_4$ to 4-NP (A) in the absence of a catalyst Amax occurring ~ at 400 nm and (B) with the addition of AvoSE (λmax = ~288 nm) and absence of a catalyst.

The addition of AvoSE-AuNPs in the reaction resulted in the decrease of the 4-nitrophenolate peak over time; and this was followed by the appearance and gradual increase of a peak at 299 nm (Figure 5.3) indicating the formation of 4-AP (Chiou *et al*., 2013; Li & Chen, 2013; Seo *et al*., 2017). Different concentrations of AvoSE-AuNPs (0.125x and 0.50x) were used with constant concentrations of 4-NP (2 mM) and $NaBH_4$ (0.03 M) as shown by graph A and B in Figure 5.3 to show that 4-nitrophenolate disappears at 400 nm. At the lower concentration of 0.125x AvoSE-AuNPs (Graph A of Figure 5.3), the 4-nitrophenolate peak at 400 nm appears to be greater than at concentration 0.5x of AvoSE-AuNPs (Graph B of Figure 5.3), after 1 minute. This suggested that at the higher concentration the reaction occurs rapidly, and was complete within 10 minutes, whereas this took up to 60 minutes for the reaction to be complete at a lower concentration. At 90 minutes, the 4-nitrophenalate peak is almost at zero using both AvoSE-AuNPs concentrations, suggesting complete reduction of 4-NP. In the presence of 0.5x AvoSE-AuNPs, it is important to note that within 1 minute the 4-nitrophenolate peak is lower than the 4-nitrophenolate peak which formed in the absence AvoSE-AuNPs even after 75 minutes (indicated as 4-NP +$NaBH_4$ (75 min)). This is because in the absence of a catalyst there is a high kinetic barrier which forms as a result of mutually repelling nitrophenolate anions and BH_4 anions (Liang *et al*., 2014). It can be suggested that the AvoSE-AuNPs act by lowering

the kinetic barrier, and thus catalyses the reaction and enables the reaction to occur in a shorter amount of time. It is also important to note the presence of a peak at ~ 530 nm, which shows that the AuNPs are present and still intact. This suggests that the AuNPs can be recovered and reused as catalysts in another reaction. This is important as some of the main concerns regarding the use of metallic NPs as catalysts lies within cost effectiveness, recovery and reusability of the catalyst (Trivedi *et al*., 2019).

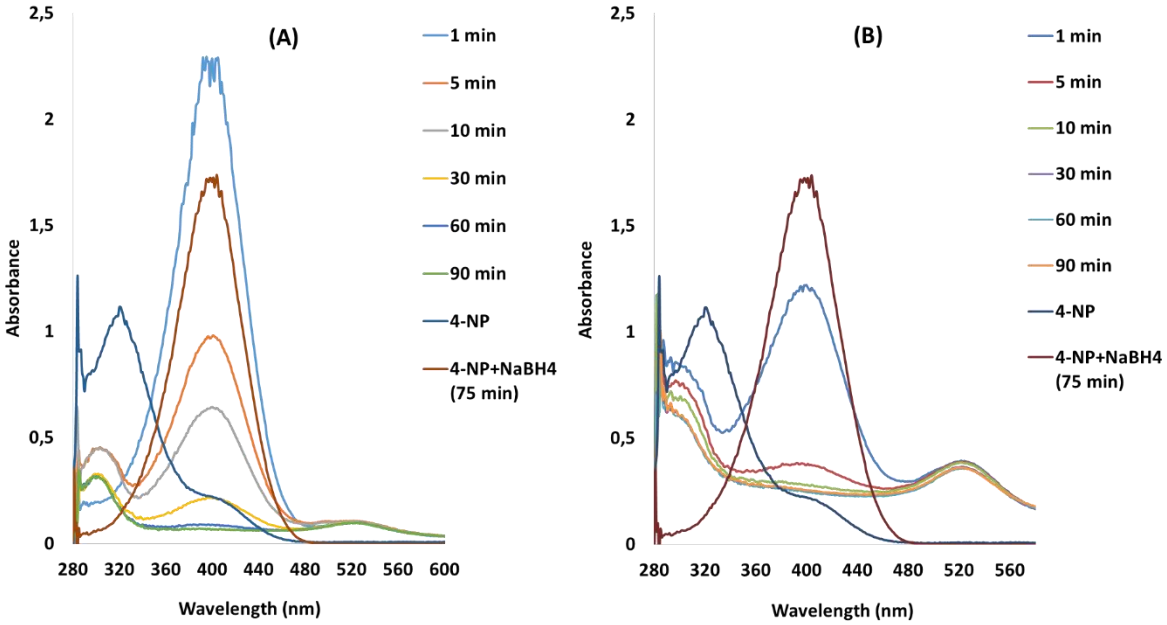

Figure 5.3: Time-dependent UV-vis absorption spectra for the reduction of 4-nitrophenol in the presence of AvoSE-AuNPs and the gradual development of 4-aminophenol over 90 min. (A) [AvoSE-AuNPs] = 0.125x and (B) [AvoSE-AuNPs] = 0.50x

Rate constants for the reduction of 4-NP

The aqueous AvoSE-AuNPs showed acted as catalysts for the reduction of 4-nitrophenol using $NaBH_4$.

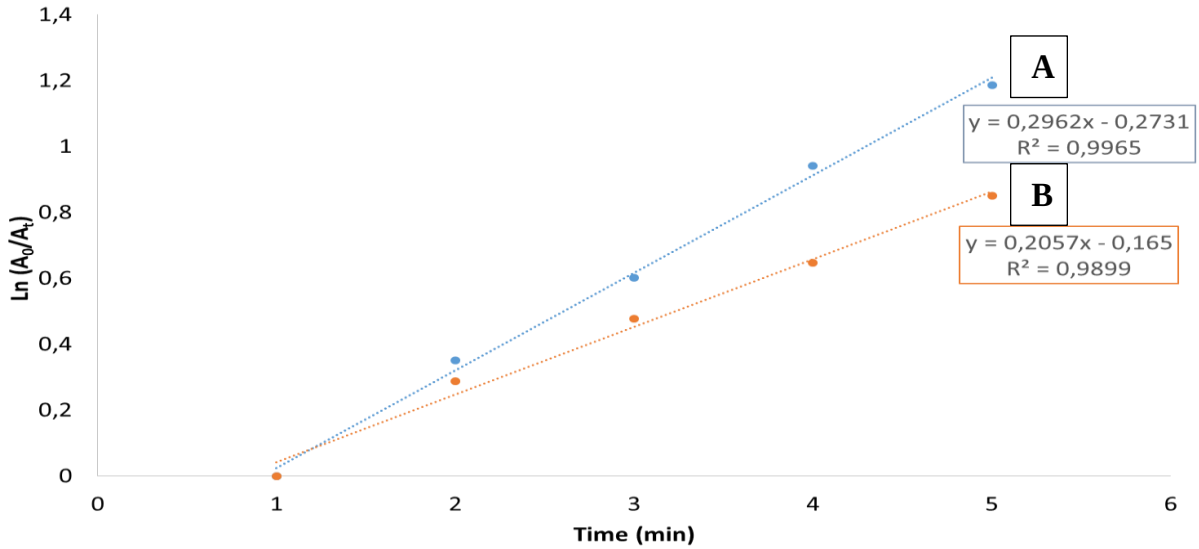

Figure 5.4: Graph depicting Ln (A_0/A_t) versus time plot for the determination of rate constants for the AvoSE-AuNPs at concentrations (A) 0.5x and (B) 0.125x. Reaction rates were 0.2962 min $^{-1}$ and 0.2057 min $^{-1}$ for 0.5 x AuNPs and 0.125 x AuNPs respectively

Figure 5.4 is a plot of ln (A_0/A_t) against reaction time and the apparent rate of reaction for each system were calculated from the slope of the ln(A_0/A_t) vs. time graph. The reaction rates were 0.2962 min $^{-1}$ and 0.2057 min $^{-1}$ for 0.5x and 0.25x AvoSE-AuNPs respectively. This means that at 0.25x AvoSE-AuNPs the reaction occurred within 0.08 seconds and at 0.5x AvoSE-AuNPs the reaction occurred within 0.06 seconds. The reaction was faster at the higher concentration of AvoSE-AuNPs. This study corroborates Zhang *et al*. (2016), they also showed the catalytic reduction of 4-NP by biosynthesized AuNPs and their study also showed a linear increase in the reaction rate constants with increasing AuNPs concentration. Like in the present study Zhang *et al*. (2016) also showed that the reduction reaction only proceeded in the presence of and was catalysed by the AuNPs.

5.3 Anticancer activity of synthesized AvoSE-AuNPs

Studies on toxicity of NPs are needed for intended application in the biomedical field. Human cell models are available for a range of malignancies, enabling for suitable exploration of antiproliferative and cytotoxic effects on NPs (Chang *et al.*, 2015). Data of NPs exposure to cancer cell models is valuable for guiding and designing of *in vivo* testing and potentially developing new anticancer drug agents (Liu *et al.*, 2015). Cell based assays can be used to measure cell morphology, proliferation, viability, toxicity, motility and metabolite production

(Pan, Bartneck, & Jahnen-Dechent, 2012). They are a good starting point for determining anticancer effects of NPs (Pan *et al*., 2012). In this study MTT assay was used to determine the toxicity of the synthesized AvoSE-AuNPs on the two widely used *in vitro* cell lines; Human liver hepatocellular carcinoma (HepG2) and Human epithelial colorectal adenocarcinoma (Caco-2).

Normal growth and development of a cell is dependent on cell-cycle control (Mahmoudi *et al*., 2011). The cell cycle comprises of four distinct phases (G1 phase, S phase, G2 phase and M-phase) and two check points (G0/G1 and G2/M) which ensure normal development of a cell (Crosby, 2007). Cell exposure to AuNPs could have various effects including triggering loss of cell cycle control (Mahmoudi *et al*., 2011). Therefore assessing cell cycle arrest in the presence of NPs can enable an understanding of the NPs' antitumour mechanisms (Ashokkumar *et al.*, 2014; Lee *et al*., 2019). The cell cycle assay allows for the determination of a cell's cycle stage by measuring DNA amount present (Gomes *et al*., 2018). The DNA content is determined by means of a fluorescent molecule, propidium iodide, that binds to DNA in a stoichiometric manner (Martin, Leonhardt, & Cardoso, 2005). In this study the cell cycle assay was used to elucidate the antitumour mechanisms of AvoSE-AuNPs on HepG2 and Caco-2 cells.

5.3.1 Results and discussion: Cytotoxic effects of biogenic AvoSE-AuNPs

5.3.1.1 Cell viability by MTT assay

The ability of the synthesized AvoSE-AuNPs to inhibit growth of HepG2 and Caco-2 cells was determined as described in Chapter 3 (section 3.2.5). The cells were treated at various concentrations ranging over 31.25 - 500 µg/ml and incubated over 24 hrs to determine the half maximal inhibitory concentration value (IC_{50}). Non-linear regression analysis: log (inhibitor) vs. normalized response was performed to calculate log IC_{50} values (GraphPad Prism version 5.03 software). Figure 5.5 represents viability of HepG2 cell lines. Cell viability decreased with increasing extract concentration. A significant decrease in viability was exhibited at the highest concentration tested of AvoSE (500 µg/ml). AvoSE at 500 µg/ml reduced the viability of HepG2 cells by 30% (Fig. 5.5. A). Plant extracts and their active compounds have been reported to have potential anticancer agents (Rao *et al*., 2016). Polyphenols, such as phenolic acids, flavonoids, terpenes and alkaloids present in plants are reported to have anticancer activities (Rao *et al*., 2016). AvoSE is also rich in these active components and there have been reported studies of its anticancer activities (Abubakar, Achmadi, & Suparto, 2017; Camberos

et al., 2013; Widiyastuti *et al*., 2018). Abubakar, Achmadi, & Suparto (2017), reported the effects of AvoSE on HepG2 cells with a significant IC_{50} value under 100 µg/ml. Hence, the aqueous avocado seed extract in this study was expected to exhibit a level of cytotoxicity based on available literature. In Figure 5.5.B similar results were exhibited by the AvoSE synthesized AuNPs, which displayed a significant decrease in cell viability at 500 µg/ml. The AvoSE-AuNPs reduced cell viability by 40 %, with an IC_{50} value of 382.2 µg/ml. Compared to the extract alone, the AvoSE-AuNPs cell viability decreased by over 10%. A study by Mmola *et al*. (2016) also showed that plant extracts synthesized AuNPs exhibited enhanced activity compared to its extract. Green synthesized AuNPs using *Corchorus olitorius* extract also showed superior activity compared to the plant extract (Ismail *et al.*, 2018) and the study concluded that the biogenic NPs enhanced extract activity.

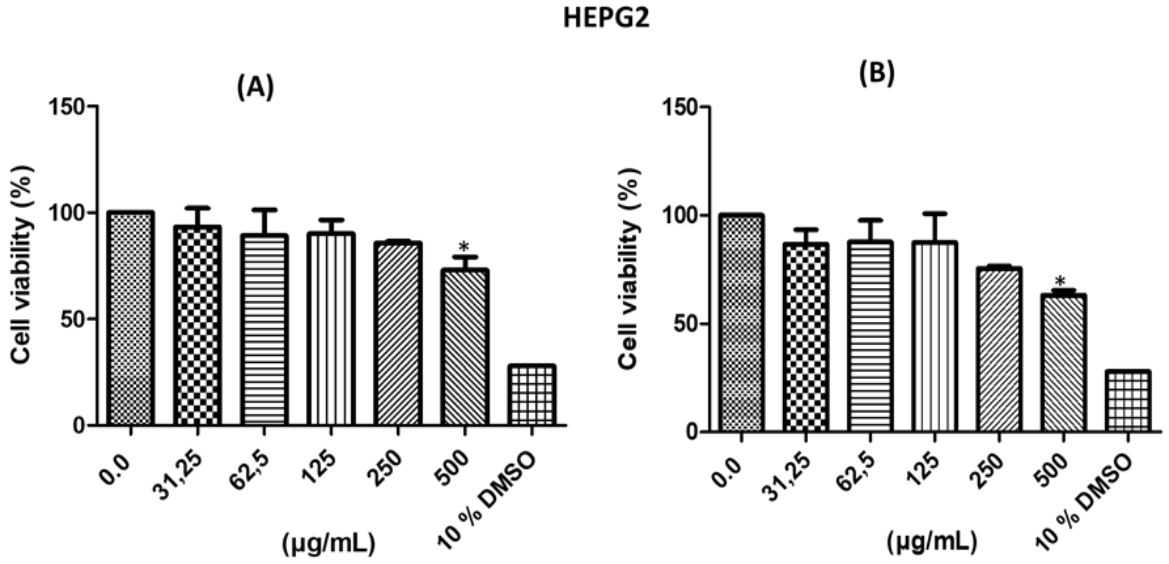

Figure 5.5: Cell viability (%) measured by MTT assay of HEPG2 cells treated with (A) AvoSE at concentrations ranging from 15.625-500 µg/ml and (B) AvoSE-AuNPs at concentrations ranging from 15.625-500 µg/ml. Data are presented as mean ± SD of n = 2 (* $p \leq 0.05$).

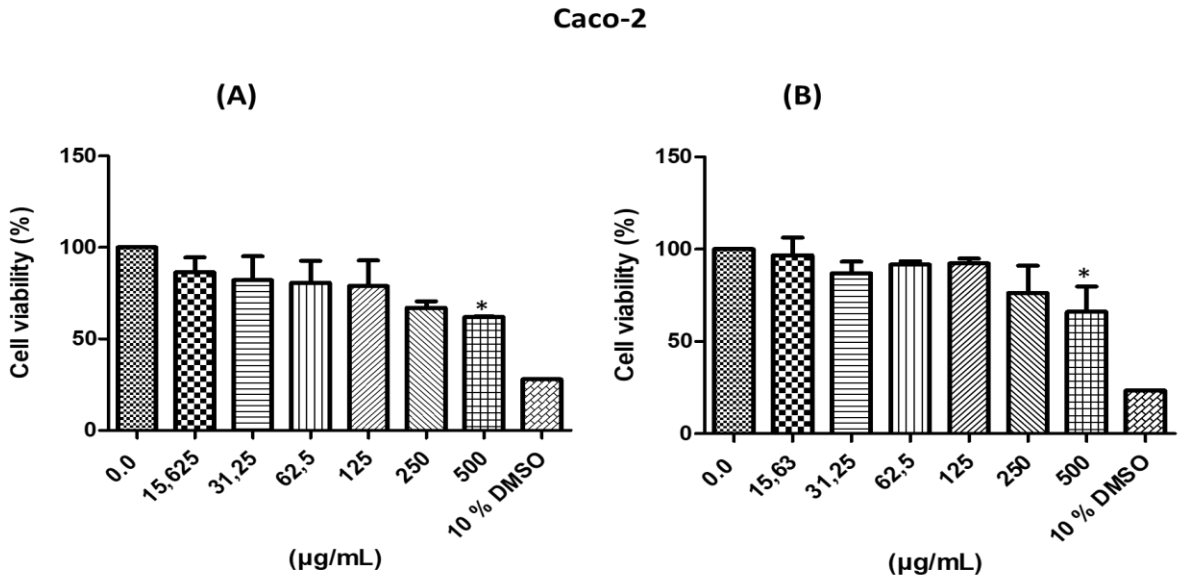

Figure 5.6: Cell viability (%) measured by MTT assay of Caco-2 cells treated with (A) AvoSE at concentrations ranging from 15.625-500 µg/ml and (B) AvoSE-AuNPs at concentrations ranging from 15.625-500 µg/ml. Data are presented as mean ± SD of n = 2 (* $p \leq 0.05$)

Figure 5.6 indicates viability of Caco-2 cells after treatment with extract and AvoSE-AuNPs. The cell viability decreased with increasing extract and AvoSE-AuNPs concentration. A significant decrease in viability was exhibited at the highest concentration tested (500 µg/ml) for both extract and AuNPs. Cell viability for extract and AvoSE-AuNPs was above 70% at treatment concentration 500 µg/ml. Graph Pad prism (version 5.03) predicted IC_{50} values at 546.5 µg/ml for AvoSE-AuNPs and 910.1 µg/ml for extract based on the exhibited viability trend. The cytotoxicity of the extract and AvoSE-AuNPs results in this study was low. Despite this result, it is important to note that decreased cell viability may be an indication that the cells underwent early apoptosis due to treatment exposure (Husøy, Syversen, & Jenssen, 1993; Tian *et al*., 2015).

The cytotoxicity of AuNPs has been studied *in vivo* and *in vitro* and it has been suggested that AuNPs can exhibit anticancer properties through inducing oxidative stress on the cell (Pan *et al*., 2009). Oxidative stress can be induced by an increase in the generation of reactive oxygen species, which leads to the oxidation of several molecules such as lipids and proteins and this ultimately leads to cell death (Martínez-Torres *et al*., 2018). Shape, size and surface properties of NPs are said to influence circulation time, cellular uptake, biodistribution, drug delivery and anticancer activity (Arvizo, Bhattacharya, & Mukherjee, 2010). The synthesized AvoSE-AuNPs are larger because the hydrodynamic size is more than 100 nm (133.3 ± 0.9 nm). Hence, the moderate cytotoxicity can be partially attributed to the size of AvoSE-AuNPs. In general, it has been shown that the anticancer activity of NPs is size-dependent, where the smaller (less

than 100 nm) the NPs the greater the inhibition of proliferation of cancer cells (Rao *et al*., 2016; Skalska & Strużyńska, 2015). This is due to the fact that small-sized NPs can penetrate deeply into the tumorous cells and thus are more effective than larger-sized NPs.

5.3.1.2 Cell cycle distribution

The cell cycle of HepG2 cells was analysed after treatment with the synthesized AvoSE-AuNPs and AvoSE for 24 hours (Figure 5.7). Upon treatment, the AvoSE-AuNPs treated cells showed a slight decrease in percentage of G0/G1 phase (from 60.1 ± 11.5 % to 53.9 ± 13.1 %) compared to the untreated control sample. The S phase increased in percentage (from 19.9 ± 5.8 % to 25.5 ± 3.7 %) and G2/M phase increased (from 19.6 ± 10.5 % to 22.6 ± 10.2 %). The extract showed a similar trend, the G0/G1 phase decreased (from 60.1 ± 11.5 % to 54.6 ± 13.6 %), S phase increased (from 19.9 ± 5.8 % to 31.3 ± 16.3 %), G2/M phase slightly increased (from 19.6 ± 10.5 % to 21.0 ± 6.8 %). It is known that anti-tumour drugs often exert their effect by inducing cell cycle arrest.

The cells treated with AvoSE-AuNPs showed accumulation of cells at the S phase, indicating a disruption of the G1-to-S transition in the cell cycle, but the AuNPs did not cause apoptosis, as indicated by the absence of a subG1 cell population. G0/G1 represents the phase in which the cells are preparing for growth and producing enzymes that are necessary for cell division (Cooper, 2000). There are two classes of regulatory molecules which determine a cell's progress through the cell cycle; these molecules are cyclins and cyclin-dependant kinases (CDK's) (Alberts *et al*., 2002). When these molecules are active coordinated entry into the next phase of the cycle is either activated or inactivated. For example, G1 cyclin-CDK complexes become active and prepare cells for the S phase when a pro-mitotic extracellular signal is received (Alberts *et al*., 2002). The G1 cyclin-CDK complexes also promote the degradation of molecules that function as S phase inhibitors by targeting them for ubiquitination (Bertoli, Skotheim, & de Bruin, 2013). Since the cell cycle aims to regulate cell development, the arrest at the S phase (Figure 5.7) may be an indication that treatment promotes the degradation of S phase inhibitors. Hence, it can be suggested in this study that the arrest signifies that the G1 cyclin-CDK complexes are active and target S phase inhibitors for degradation. There was an increase in DNA content at the G2/M phase as well, meaning a temporary or permanent arrest during mitosis. A similar study by Lee *et al*. (2019) conducted cell cycle analysis on MCF-7 cells treated with resveratrol conjugated AuNPs (RES-AuNPs). The RES-AuNPs exhibited similar results to this study, the treatment also caused cell cycle arrest at the S phase and a decrease in percentage was observed at the G0/G1 phase. The study suggested that the S phase

arrest was caused by defected cell signalling possibly involving Akt signalling pathway, Cdk2, Cyclin A and Cyclin E which are known to be key regulators of the cell cycle (Chen *et al*., 2014; Lee *et al*., 2013). The study further concluded that resveratrol is involved in the regulation of at least one component of the above mentioned signalling pathways. The mitosis (M) phase corresponds to cell division and cytokinesis (Cooper, 2000). Mitosis is complex and highly regulated. Errors can either kill a cell through apoptosis or cause mutations (Cooper, 2000). There was also an increase at the G2/M phase as expected because S phase means the cell is preparing components for mitosis. Hence it would be ready for cytokinesis once the DNA is ready.

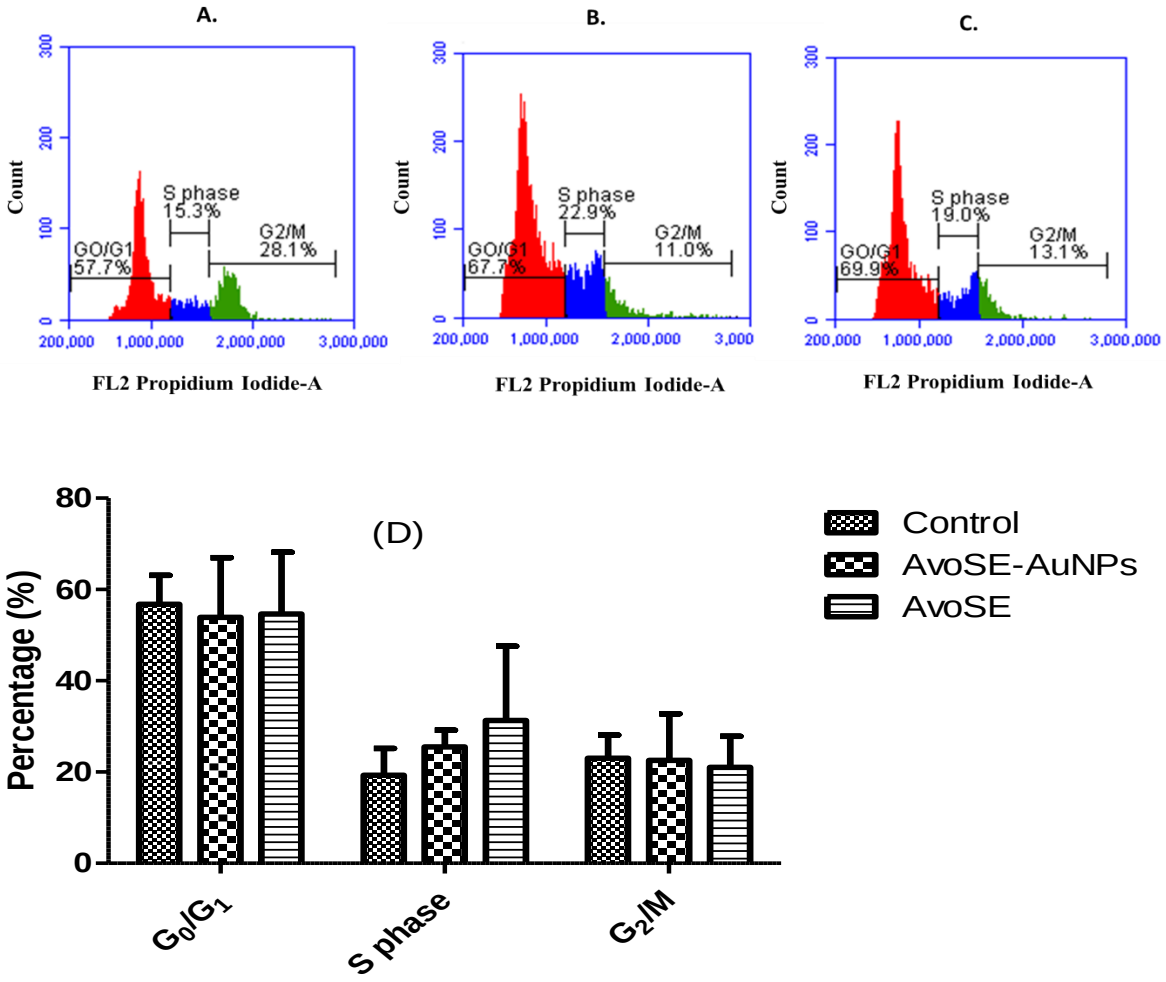

Figure 5.7: Effect of AvoSE-AuNPs on cell cycle progression of HepG2 cells. The cells were harvested after 24 hrs, fixated with ethanol, and analysed via flow cytometry. The percentage of cell populations in phase of G0/G1, S, and G2/M were estimated and presented in (A) control (B) AvoSE-AuNPs and (C) AvoSE treated groups. The bar graph represents the combined data from graph A, B and C for comparisons (D) The bar graph represents the combined data from graph A, B and C for comparisons. Data expressed as the mean ± SD of 3 independent experiments.

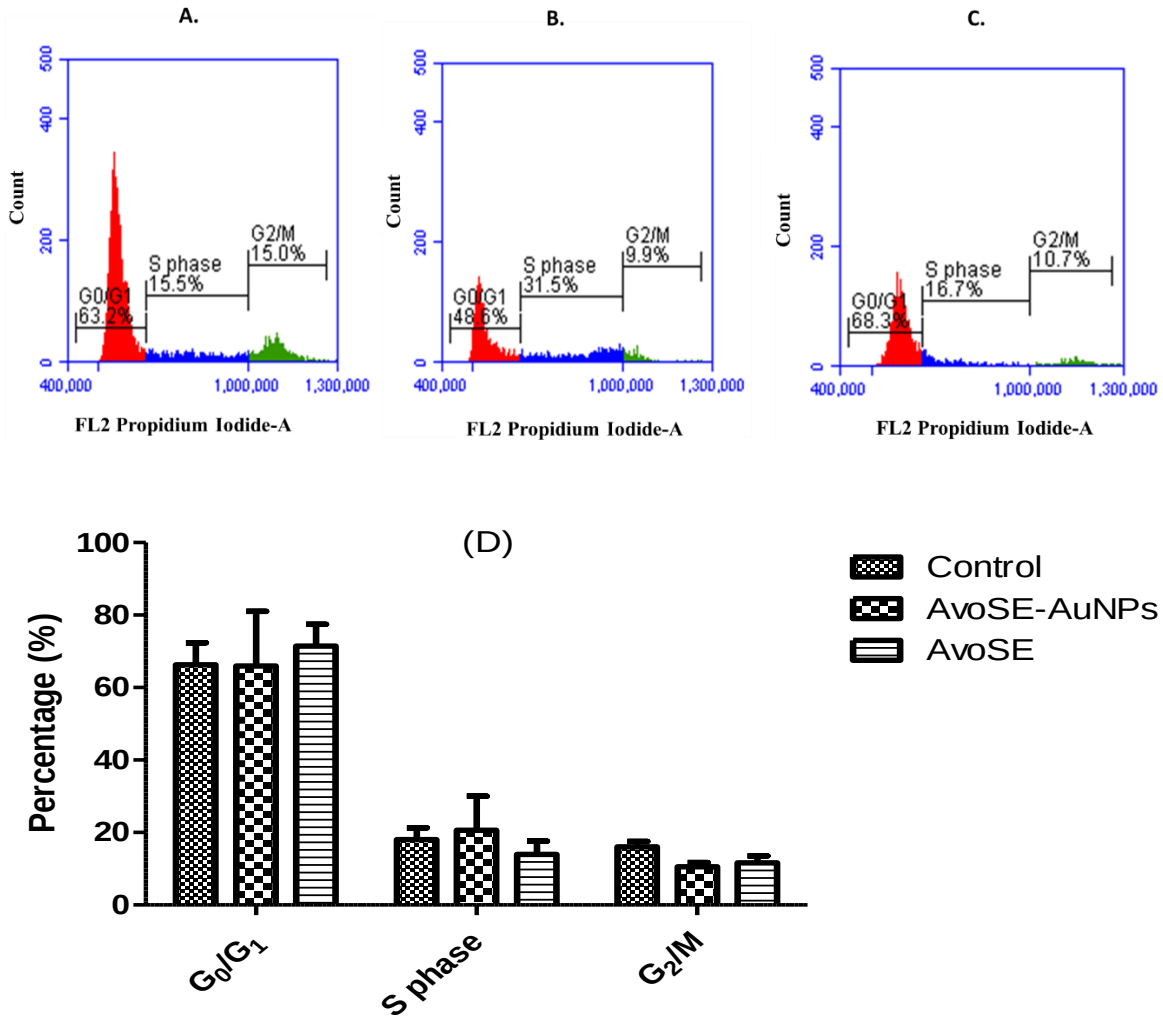

Figure 5.8: Effect of AvoSE-AuNPs on cell cycle progression of Caco-2 cells. The percentage of cell populations in phase of G0/G1, S, and G2/M were estimated and presented in (A) control (B) AvoSE-AuNPs and (C) AvoSE treated groups. The bar graph represents the combined data from graph A, B and C for comparisons (D) The bar graph represents the combined data from graph A, B and C for comparisons. Data expressed as the mean ± SD of 3 independent experiments.

Figure 5.8 represents cell cycle analysis of Caco-2 cells after treatment with the synthesized AvoSE-AuNPs and AvoSE for 24 hours. The AvoSE-AuNPs treated group showed that G0/G1 phase slightly decreased in DNA content (from 66.3 ± 6.1 % to 66.0 ± 15.0 %) compared to the untreated control sample. The S phase slightly increased in DNA content percentage (from 18.1 ± 3.2 % to 20.6 ± 9.4 %) and G2/M phase decreased (from 16.1 ± 1.4 % to 10.6 ± 1.2 %). The extract showed accumulation at G0/G1 phase (from 66.3 ± 6.1 % to 71.4 ± 6.0 %), S phase decreased (from 18.1 ± 3.2 % to 13.9 ± 3.7 %), G2/M phase decreased (from 16.1 ± 1.4 % to 11.6 ± 1.9 %). The AvoSE treated group showed accumulation of DNA content at the G0/G1 phase when compared to the untreated group. Based on the AvoSE-AuNPs treated group the DNA content exhibited slight changes when compared to the control group. Cyclin-dependent

protein kinases (Cdk1)/nuclear cyclin B (B) complex is essential for entry into and progression through mitosis (Wolf, Sigl, & Geley, 2007). Thus, the activation of the Cdk1/B1 complex plays a key regulatory role in cell proliferation. Therefore the decrease in DNA content at the G2/M phase of the AvoSE-AuNPs treated group may be attributed to the up-regulation of this complex.

The findings of this study showed no appearance of a sub G0 phase which acts as an indication of apoptosis. Suggesting that the AvoSe-AuNPs may not induce apoptosis when exposed to cancer cells. Monitoring the cell cycle changes is an important index of both the cytotoxicity of the nanoparticle, and its effectiveness when the study aims at studying dysregulated cells. Cell cycle analysis helped improve understanding of the low cytotoxicity observed by the MTT assay results.

CHAPTER 6

GENERAL CONCLUSION AND RECOMMENDATIONS FOR FUTURE RESEARCH

6.1 General summary and conclusion

Developing new methods for sustainable synthesis of nanomaterials is a stepping stone for new developments in nanotechnology. In search for greener alternatives to producing NPs, this study investigated the use of an agricultural waste product for AuNP synthesis. Avocado seed extract was used as a potential reducing agent of $HAuCl_4$ for the production of biogenic AuNPs. The formation of AvoSE-AuNPs was confirmed by the presence of SPR absorption peaks in the visible light region of the spectrum. The biosynthesis was optimized by changing the reaction conditions and the study proved that size and shape of the synthesized AvoSE-AuNPs can be tuned by adjusting reaction conditions. HRTEM analysis confirmed the anisotropy of the AvoSE-AuNPs produced. FTIR provided a clue to these mechanisms by enabling the confirmation of biomolecules present on the surface of the AvoSE-AuNPs. This helped support the notion that the phytochemicals from AvoSE were responsible for the reduction of Au ions in AvoSE-AuNP synthesis.

The study also investigated bactericidal effects of the AvoSE and AvoSE-AuNPs against biomedically important bacterial strains which are known to exhibit resistance to a number of antibiotics. From the results, AvoSE was bactericidal against the tested strains and *S. aureus* was the most susceptible. In contrast, AvoSE-AuNPs did not exhibit any antibacterial effects.

AvoSE-AuNPs demonstrated excellent catalytic activity in the reduction of 4-NP by NaBH4. Furthermore, the rate constants calculated demonstrated that the reaction occurs faster in the presence of more concentrated AvoSE-AuNPs.

The cytotoxicity of the AvoSE-AuNPs was assessed and only showed significant cytotoxicity against the highest concentration tested (500 µg/ml). Cell cycle analysis showed that in both cell lines treatment with AvoSE-AuNPs and AvoSE indeed caused a disruption in the regulation of cell cycle. In both cell lines the findings showed no appearance of a sub G0 phase, suggesting that the AvoSE-AuNPs may not induce apoptosis when exposed to cancer cells. Cell cycle analysis helped improve understanding of the low cytotoxicity observed by the MTT assay results.

The results presented in this study clearly demonstrate the feasibility of using AvoSE for the synthesis of AuNPs. This study demonstrated that AvoSE mediated AuNPs synthesis is a greener alternative as it abides by the green chemistry principles. The aims of the study were achieved as the results presented demonstrate that agricultural waste like avocado seeds can be utilised for green synthesis of AuNPs and essentially contribute to the development of greener alternatives of nanoparticle synthesis in nanotechnology. Furthermore, the study outcomes will contribute to minimizing environmental pollution by finding use for agricultural waste.

6.2 Recommendations

The study demonstrated that reaction parameters have an effect on AuNPs formation. This was confirmed by DLS and UV-Vis analysis, to further expand these results HRTEM analysis can be included to demonstrate if optimization of the reaction parameters results in changes on the core size. Nuclear magnetic resonance (NMR) studies can also be included to supplement the FTIR results and confirm the possible functional groups involved in the biosynthesis of AvoSE-AuNPs. NMR provides chemical content information which can be used to confirm functional groups present by comparing NMR spectra of AvoSE, AvoSE-AuNPs and the reaction medium of the AvoSE-AuNPs.

Due to the burden of multidrug resistant microorganisms and fast growing antimicrobial resistance, there is a need for new antimicrobial agents. Since AvoSE-AuNPs exhibited no bactericidal effects.,an experiment which explores the effects of conjugation of an existing antibacterial drug like penicillin on AvoSE-AuNPs can be conducted, which could possibly demonstrate the use of AvoSE-AuNPs in improving antibacterial drug efficacy. Finally, the cytotoxicity of AvoSE-AuNPs showed insufficient significant results. Further work should be done to supplement the MTT assay and cell cycle results. These include apoptosis and ROS assays in order to prove whether AvoSE-AuNPs induces apoptosis in cancer cells.

BIBLIOGRAPHY

Abubakar, A., Achmadi, S., & Suparto, I. (2017). Triterpenoid of avocado (Persea americana) seed and its cytotoxic activity toward breast MCF-7 and liver HepG2 cancer cells. *Asian Pacific Journal of Tropical Biomedicine*, *7*. https://doi.org/10.1016/j.apjtb.2017.01.010

Adams, F. C., & Barbante, C. (2013). Nanoscience, nanotechnology and spectrometry. *Spectrochimica Acta - Part B Atomic Spectroscopy*, *86*, 3–13. https://doi.org/10.1016/j.sab.2013.04.008

Ahmad, A., Senapati, S., Khan, M. I., Kumar, R., & Sastry, M. (2003). Extracellular Biosynthesis of Monodisperse Gold Nanoparticles by a Novel Extremophilic Actinomycete, Thermomonospora sp. *Langmuir*, *19*(8), 3550–3553. https://doi.org/10.1021/la026772l

Ahmad, N., Bhatnagar, S., Saxena, R., Iqbal, D., Ghosh, A. K., & Dutta, R. (2017). Biosynthesis and characterization of gold nanoparticles: Kinetics, in vitro and in vivo study. *Materials Science and Engineering: C*, *78*, 553–564. https://doi.org/10.1016/J.MSEC.2017.03.282

Ahmad, T., Irfan, M., Bustam, M. A., & Bhattacharjee, S. (2016). Effect of Reaction Time on Green Synthesis of Gold Nanoparticles by Using Aqueous Extract of Elaise Guineensis (Oil Palm Leaves). In *Procedia Engineering*. https://doi.org/10.1016/j.proeng.2016.06.465

Ajitha, B., Reddy, A. K., & Reddy, P. S. (2015). Green synthesis and characterization of silver nanoparticles using Lantana camara leaf extract. *Materials Science and Engineering*, *49*, 373–381. https://doi.org/10.1016/J.MSEC.2015.01.035

Akhtar, M. S., Panwar, J., & Yun, Y.S. (2013). Biogenic Synthesis of Metallic Nanoparticles by Plant Extracts. *ACS Sustainable Chemistry & Engineering*, *1*(6), 591–602. https://doi.org/10.1021/sc300118u

Alberts, B., Johnson, A., & Lewis, J. (2002). Components of the Cell-Cycle Control System. In *Molecular Biology of the Cell.* (4th ed.). New York: Garland Science. Retrieved from https://www.ncbi.nlm.nih.gov/books/NBK26824/

Ali, Z., Jabir, M., & Al-Shammari, A. (2019). Gold Nanoparticles Inhibiting Proliferation of

Human Breast Cancer Cell line. *Research Journal of Biotechnology*, *14*, 79–82.

Alizadeh, S., & Nazari, Z. (2019). A Review on Gold Nanoparticles Aggregation and Its Applications. *Journal of Chemistry*.

Aljabali, A. A. A., Akkam, Y., Al Zoubi, M. S., Al-Batayneh, K. M., Al-Trad, B., Alrob, O. A., … Evans, D. J. (2018). Synthesis of gold nanoparticles using leaf extract of ziziphus zizyphus and their antimicrobial activity. *Nanomaterials*, *8*(3), 1–15. https://doi.org/10.3390/nano8030174

Alkhalf, M. I., Alansari, W. S., Ibrahim, E. A., & ELhalwagy, M. E. A. (2018). Anti-oxidant, anti-inflammatory and anti-cancer activities of avocado (Persea americana) fruit and seed extract. *Journal of King Saud University - Science*. https://doi.org/10.1016/J.JKSUS.2018.10.010

Allahverdiyev, A. M., Kon, K. V., Abamor, E. S., Bagirova, M., & Rafailovich, M. (2011). Coping with antibiotic resistance: combining nanoparticles with antibiotics and other antimicrobial agents. *Expert Review of Anti-Infective Therapy*, *9*(11), 1035–1052. https://doi.org/10.1586/eri.11.121

Amendola, V., & Meneghetti, M. (2009). Size Evaluation of Gold Nanoparticles by UV−vis Spectroscopy. *The Journal of Physical Chemistry C*, *113*(11), 4277–4285. https://doi.org/10.1021/jp8082425

Amendola, V., Polizzi, S., & Meneghetti, M. (2006). Laser Ablation Synthesis of Gold Nanoparticles in Organic Solvents. *The Journal of Physical Chemistry B*, *110*(14), 7232–7237. https://doi.org/10.1021/jp0605092

Anastas, P., & Eghbali, N. (2010). Green Chemistry: Principles and Practice. *Chem. Soc. Rev.*, *39*(1), 301–312. https://doi.org/10.1039/B918763B

Arun, G., Eyini, M., & Gunasekaran, P. (2014). Green synthesis of silver nanoparticles using the mushroom fungus Schizophyllum commune and its biomedical applications. *Biotechnology and Bioprocess Engineering*, *19*(6), 1083–1090. https://doi.org/10.1007/s12257-014-0071-z

Arvizo, R., Bhattacharya, R., & Mukherjee, P. (2010). Gold nanoparticles: opportunities and challenges in nanomedicine. *Expert Opinion on Drug Delivery*, *7*(6), 753–763. https://doi.org/10.1517/17425241003777010

Ashokkumar, T., Prabhu, D., Geetha, R., Govindaraju, K., Manikandan, R., Arulvasu, C., & Singaravelu, G. (2014). Apoptosis in liver cancer (HepG2) cells induced by functionalized gold nanoparticles. *Colloids and Surfaces B: Biointerfaces*, *123*, 549–556. https://doi.org/10.1016/J.COLSURFB.2014.09.051

Aslam, B., Wang, W., Arshad, M. I., Khurshid, M., Muzammil, S., Rasool, M. H., … Baloch, Z. (2018). Antibiotic resistance: a rundown of a global crisis. *Infection and Drug Resistance*, *11*, 1645–1658. https://doi.org/10.2147/IDR.S173867

Astefanei, A., Núñez, O., & Galceran, M. T. (2015). Characterisation and determination of fullerenes: A critical review. *Analytica Chimica Acta*, *882*, 1–21. https://doi.org/10.1016/J.ACA.2015.03.025

Augustyn, A., Bauer, P., Duignan, B., Eldridge, A., Gregersen, E., Luebering, J. E., … Zelazko, A. (2019). Avocado. Retrieved April 19, 2019, from https://www.britannica.com/plant/avocado

Baker, S., Rakshith, D., Kavitha, K. S., Santosh, P., Kavitha, H. U., Rao, Y., & Satish, S. (2013). Plants: Emerging as Nanofactories towards Facile Route in Synthesis of Nanoparticles. *BioImpacts : BI*, *3*(3), 111–117. https://doi.org/10.5681/bi.2013.012

Balashanmugam, P., Durai, P., Balakumaran, M. D., & Kalaichelvan, P. T. (2016). Phytosynthesized gold nanoparticles from C. roxburghii DC. leaf and their toxic effects on normal and cancer cell lines. *Journal of Photochemistry and Photobiology B: Biology*, *165*, 163–173. https://doi.org/10.1016/J.JPHOTOBIOL.2016.10.013

Bali, R., & Harris, A. T. (2010). Biogenic Synthesis of Au Nanoparticles Using Vascular Plants. *Industrial & Engineering Chemistry Research*, *49*(24), 12762–12772. https://doi.org/10.1021/ie101600m

Barazzouk, S., Kamat, P. V, & Hotchandani, S. (2005). Photoinduced Electron Transfer between Chlorophyll a and Gold Nanoparticles. *The Journal of Physical Chemistry B*, *109*(2), 716–723. https://doi.org/10.1021/jp046474s

Begum, N. A., Mondal, S., Basu, S., Laskar, R. A., & Mandal, D. (2009). Biogenic synthesis of Au and Ag nanoparticles using aqueous solutions of Black Tea leaf extracts. *Colloids and Surfaces B: Biointerfaces*, *71*(1), 113–118. https://doi.org/10.1016/J.COLSURFB.2009.01.012

Benelmekki, M., & Benelmekki, M. (2015). An introduction to nanoparticles and nanotechnology. *Designing Hybrid Nanoparticles*. https://doi.org/10.1088/978-1-6270-5469-0ch1

Bertling, I., Tesfay, S., & Bower, J. (2007). Antioxidants in "Hass" avocado. *South African Avocado Growers' Asociation*, *30*, 17–19. Retrieved from http://www.avocadosource.com/journals/saaga/saaga_2007/SAAGA_2007_V30_PGS_17-19_Bertling.pdf

Bertoli, C., Skotheim, J. M., & de Bruin, R. A. M. (2013). Control of cell cycle transcription during G1 and S phases. *Nature Reviews. Molecular Cell Biology*, *14*(8), 518–528. https://doi.org/10.1038/nrm3629

Beveridge, T. J., Hughes, M. N., Lee, H., Leung, K. T., Savvaidis, I., Silver, S., & Trevors, J. T. (1996). Metal-Microbe Interactions: Contemporary Approaches. *Advances in Microbial Physiology*, *38*, 177–243. https://doi.org/10.1016/S0065-2911(08)60158-7

Bogireddy, N. K. R., Pal, U., Gomez, L. M., & Agarwal, V. (2018). Size controlled green synthesis of gold nanoparticles using Coffea arabica seed extract and their catalytic performance in 4-nitrophenol reduction. *RSC Advances*, *8*(44), 24819–24826. https://doi.org/10.1039/C8RA04332A

Boisselier, E., & Astruc, D. (2009). Gold nanoparticles in nanomedicine: preparations, imaging, diagnostics , therapies and toxicity. *Chem. Soc. Rev.*, *38*(6), 1759–1782. https://doi.org/10.1039/B806051G

Brust, M., Walker, M., Bethell, D., Schiffrin, D. J., & Whyman, R. (1994). Synthesis of thiol-derivatised gold nanoparticles in a two-phase Liquid–Liquid system. Journal of Chemical Society, Chemical Communications, (7), 801-802sen. https://doi.org/10.103, M., Walker, M., Bethell, D., Schiffrin, D. J., & Whyman, R. (1994). Synthesis of thiol-derivatised gold nanoparticles in a two-phase Liquid–Liquid system. *Journal of Chemical Society, Chemical Communications*, (7), 801-802sen. https://doi.org/10.1039/C39940000801

Caballero, B., Finglas, P., & Toldra, F. (2015). Avocados. In *Encyclopedia of Food and Health* (2nd ed.). Elsevier Science.

Cai, Y., Luo, Q., Sun, M., & Corke, H. (2004). Antioxidant activity and phenolic compounds

of 112 traditional Chinese medicinal plants associated with anticancer. *Life Sciences*, *74*(17), 2157–2184. https://doi.org/10.1016/J.LFS.2003.09.047

Callegari, A. (2003). Nano Lett. https://doi.org/10.1021/jp0441588

Camberos, E. P., Velázquez, M. M., Fernández, J. M. F., & Rodríguez, S. V. (2013). Acute toxicity and genotoxic activity of avocado seed extract (Persea americana Mill., c.v. Hass). *The Scientific World Journal*, *2013*. https://doi.org/10.1155/2013/245828

Caneiras, C., Lito, L., Melo-Cristino, J., & Duarte, A. (2019). Community- and Hospital-Acquired Klebsiella pneumoniae Urinary Tract Infections in Portugal: Virulence and Antibiotic Resistance. *Microorganisms*, *7*(5), 138. https://doi.org/10.3390/microorganisms7050138

Cañizares, P., Sáez, C., Lobato, J., & Rodrigo, M. A. (2004). Electrochemical Treatment of 4-Nitrophenol-Containing Aqueous Wastes Using Boron-Doped Diamond Anodes. *Industrial & Engineering Chemistry Research*, *43*(9), 1944–1951. https://doi.org/10.1021/ie034025t

Carvalho, C. P., Jorge, B. E., Velásquez, M. A., & Cartagena, J. R. (2015). Fatty acid content of avocados (Persea americana Mill. cv. Hass) in relation to orchard altitude and fruit maturity stage. *Agronomía Colombiana 33(2), 220-227*, *2015*, *33*(2), 220–227.

Chambers, H. F., & Deleo, F. R. (2009). Waves of resistance: Staphylococcus aureus in the antibiotic era. *Nature Reviews. Microbiology*, *7*(9), 629–641. https://doi.org/10.1038/nrmicro2200

Chandrappa, C. P., Vinay, S. P., & Chandrashekar, N. (2017). Silver nanoparticles: Synthesized by leaves extract of Avocado and their antibacterial activity. *International Journal of Engineering Development and Research (IJEDR)*, *5*(2), 1608–1613.

Chang, J.-S., Kuo, H. P., Chang, K. L. B., & Kong, Z. L. (2015). Apoptosis of Hepatocellular Carcinoma Cells Induced by Nanoencapsulated Polysaccharides Extracted from Antrodia Camphorata. *PloS One*, *10*(9), e0136782–e0136782. https://doi.org/10.1371/journal.pone.0136782

Chen, K.C., Yang, T.Y., Wu, C.C., Cheng, C.C., Hsu, S.L., Hung, H.W., Chang, G.C. (2014). Pemetrexed Induces S-Phase Arrest and Apoptosis via a Deregulated Activation of Akt Signaling Pathway. *PLOS ONE*, *9*(5), e97888. Retrieved from

https://doi.org/10.1371/journal.pone.0097888

Chiou, J.R., Lai, B.H., Hsu, K.C., & Chen, D.H. (2013). One-pot green synthesis of silver/iron oxide composite nanoparticles for 4-nitrophenol reduction. *Journal of Hazardous Materials*, *248–249*, 394–400. https://doi.org/10.1016/J.JHAZMAT.2013.01.030

Cooper, G. (2000). The Origin and Evolution of Cells. In *The Cell: A Molecular Approach* (2nd ed.). Sunderland (MA): Sinauer Associates. Retrieved from https://www.ncbi.nlm.nih.gov/books/NBK9841/

Corma, A., & Garcia, H. (2008). Supported gold nanoparticles as catalysts for organic reactions. *Chem. Soc. Rev.*, *37*(9), 2096–2126. https://doi.org/10.1039/B707314N

Cowan, M. M. (1999). Plant Products as Antimicrobial Agents. *Clinical Microbiology Reviews*, *12*(4), 564 LP – 582. https://doi.org/10.1128/CMR.12.4.564

Crosby, M. E. (2007). Cell Cycle: Principles of Control. *The Yale Journal of Biology and Medicine*, *80*(3), 141–142. Retrieved from https://www.ncbi.nlm.nih.gov/pmc/articles/PMC2248297/

Dabas, D., Elias, R. J., Lambert, J. D., & Ziegler, G. R. (2011). A Colored Avocado Seed Extract as a Potential Natural Colorant. *Journal of Food Science*, *76*(9), 1335–1341. https://doi.org/10.1111/j.1750-3841.2011.02415.x

Dadwal, A., Baldi, A., & Narang, R. K. (2018). Nanoparticles as carriers for drug delivery in cancer. *Artificial Cells, Nanomedicine and Biotechnology*, *46*(2).

Dahl, J. A., Maddux, B. L. S., & Hutchison, J. E. (2007). Toward Greener Nanosynthesis. *Chemical Reviews*, *107*(6), 2228–2269. https://doi.org/10.1021/cr050943k

Dai, Q., Lei, L., & Zhang, X. (2008). Enhanced degradation of organic wastewater containing p-nitrophenol by a novel wet electrocatalytic oxidation process: Parameter optimization and degradation mechanism. *Separation and Purification Technology*, *61*(2), 123–129. https://doi.org/10.1016/J.SEPPUR.2007.10.006

Danaei, M., Dehghankhold, M., Ataei, S., Hasanzadeh Davarani, F., Javanmard, R., Dokhani, A., … Mozafari, M. R. (2018). Impact of Particle Size and Polydispersity Index on the Clinical Applications of Lipidic Nanocarrier Systems. *Pharmaceutics*, *10*(2), 57. https://doi.org/10.3390/pharmaceutics10020057

Daniel, M.C., & Astruc, D. (2004). Gold Nanoparticles: Assembly, Supramolecular Chemistry, Quantum-Size-Related Properties, and Applications toward Biology, Catalysis, and Nanotechnology. *Chemical Reviews*, *104*(1), 293–346. https://doi.org/10.1021/cr030698+

Das, S., Das, J., Samadder, A., Bhattacharyya, S. S., Das, D., & Khuda-Bukhsh, A. R. (2013). Biosynthesized silver nanoparticles by ethanolic extracts of Phytolacca decandra, Gelsemium sempervirens, Hydrastis canadensis and Thuja occidentalis induce differential cytotoxicity through G2/M arrest in A375 cells. *Colloids and Surfaces B: Biointerfaces*, *101*, 325–336. https://doi.org/10.1016/J.COLSURFB.2012.07.008

Davies, J., & Davies, D. (2010). Origins and evolution of antibiotic resistance. *Microbiology and Molecular Biology Reviews : MMBR*, *74*(3), 417–433. https://doi.org/10.1128/MMBR.00016-10

de Freitas, L., Varca, G. H. C., Dos Santos Batista, J. G., & Benévolo Lugão, A. (2018). An Overview of the Synthesis of Gold Nanoparticles Using Radiation Technologies. *Nanomaterials*, *8*(11), 939. https://doi.org/10.3390/nano8110939

Deepak, P., Amutha, V., Kamaraj, C., Balasubramani, G., Aiswarya, D., & Perumal, P. (2019). Chemical and green synthesis of nanoparticles and their efficacy on cancer cells. *Green Synthesis, Characterization and Applications of Nanoparticles*, 369–387. https://doi.org/10.1016/B978-0-08-102579-6.00016-2

Dhamecha, D., Jalalpure, S., Jadhav, K., & Sajjan, D. (2015). Green Synthesis of Gold Nanoparticles Using Pterocarpus marsupium : Characterization and Biocompatibility Studies. *Particulate Science and Technology*, *34*, 151005094221000. https://doi.org/10.1080/02726351.2015.1054972

Dhand, V., Soumya, L., Bharadwaj, S., Chakra, S., Bhatt, D., & Sreedhar, B. (2016). Green synthesis of silver nanoparticles using Coffea arabica seed extract and its antibacterial activity. *Materials Science and Engineering: C*, *58*, 36–43. https://doi.org/https://doi.org/10.1016/j.msec.2015.08.018

Dieckmann, M. S., & Gray, K. A. (1996). A comparison of the degradation of 4-nitrophenol via direct and sensitized photocatalysis in TiO2 slurries. *Water Research*, *30*(5), 1169–1183. https://doi.org/10.1016/0043-1354(95)00240-5

Domínguez, M., Araus, K., Bonert, P., Sánchez, F., San Miguel, G., & Toledo Torres, M. (2014). The Avocado and Its Waste: An Approach of Fuel Potential/Application. In *Environment, Energy and Climate Change II* (Vol. 34). https://doi.org/10.1007/698_2014_291

Donetti, M., & Terry, L. A. (2014). Biochemical markers defining growing area and ripening stage of imported avocado fruit cv. Hass. *Journal of Food Composition and Analysis*, *34*(1), 90–98.

Dorosti, N., & Jamshidi, F. (2016a). Plant-mediated gold nanoparticles by Dracocephalum kotschyi as anticholinesterase agent: Synthesis, characterization, and evaluation of anticancer and antibacterial activity. *Journal of Applied Biomedicine*, *14*(3), 235–245. https://doi.org/10.1016/J.JAB.2016.03.001

Dorosti, N., & Jamshidi, F. (2016b). Plant-mediated gold nanoparticles by Dracocephalum kotschyi as anticholinesterase agent: Synthesis, characterization, and evaluation of anticancer and antibacterial activity. *Journal of Applied Biomedicine*, *14*(3), 235–245. https://doi.org/10.1016/j.jab.2016.03.001

Dreaden, E. C., Alkilany, A. M., Huang, X., Murphy, C. J., & El-Sayed, M. A. (2012). The golden age: gold nanoparticles for biomedicine. *Chemical Society Reviews*, *41*(7), 2740–2779. https://doi.org/10.1039/C1CS15237H

Dubey, S. P., Lahtinen, M., & Sillanpää, M. (2010). Tansy fruit mediated greener synthesis of silver and gold nanoparticles. *Process Biochemistry*, *45*(7), 1065–1071. https://doi.org/10.1016/J.PROCBIO.2010.03.024

Dwivedi, A. D., & Gopal, K. (2010). Biosynthesis of silver and gold nanoparticles using Chenopodium album leaf extract. *Colloids and Surfaces A: Physicochemical and Engineering Aspects*, *369*(1–3), 27–33. https://doi.org/10.1016/J.COLSURFA.2010.07.020

Dykman, L. A., & Khlebtsov, N. G. (2011). Gold nanoparticles in biology and medicine: recent advances and prospects. *Acta Naturae*, *3*(2), 34–55. Retrieved from https://www.ncbi.nlm.nih.gov/pubmed/22649683

Ealias, A. M., & Saravanakumar, M. P. (2017). A review on the classification, characterisation, synthesis of nanoparticles and their application. *IOP Conference*

Series: Materials Science and Engineering, *263*(3). https://doi.org/10.1088/1757-899X/263/3/032019

El-Bahy, Z. M. (2013). Preparation and characterization of Pt-promoted NiY and CoY catalysts employed for 4-nitrophenol reduction. *Applied Catalysis A: General*, *468*, 175–183. https://doi.org/10.1016/J.APCATA.2013.08.047

Elbagory, M. A., Cupido, N. C., Meyer, M., & Hussein, A. A. (2016). Large Scale Screening of Southern African Plant Extracts for the Green Synthesis of Gold Nanoparticles Using Microtitre-Plate Method. *Molecules* . https://doi.org/10.3390/molecules21111498

Elia, P., Zach, R., Hazan, S., Kolusheva, S., Porat, Z., & Zeiri, Y. (2014). Green synthesis of gold nanoparticles using plant extracts as reducing agents. *International Journal of Nanomedicine*, *9*, 4007–4021. https://doi.org/10.2147/IJN.S57343

Eltarahony, M., Zaki, S., Kheiralla, Z., & Abd-El-Haleem, D. (2016). Biogenic synthesis of Iron oxide nanoparticles via optimization of nitrate reductase Enzyme using statistical experimental design. *Journal of Advances in Biotechnology*, *5*(2), 667–684.

Esposito, A., Pagnanelli, F., & Vegliò, F. (2002). pH-related equilibria models for biosorption in single metal systems. *Chemical Engineering Science*, *57*(3), 307–313. https://doi.org/10.1016/S0009-2509(01)00399-2

Eustis, S., Hsu, H.-Y., & El-Sayed, M. A. (2005). Gold Nanoparticle Formation from Photochemical Reduction of Au3+ by Continuous Excitation in Colloidal Solutions. A Proposed Molecular Mechanism. *The Journal of Physical Chemistry B*, *109*(11), 4811–4815. https://doi.org/10.1021/jp0441588

Faraday, M. (1997). X. The Bakerian Lecture. —Experimental relations of gold (and other metals) to light. *The Royal Society*, *147*.

Feng, Y., Yu, Y., Wang, Y., & Lin, X. (2007). Biosorption and Bioreduction of Trivalent Aurum by Photosynthetic Bacteria Rhodobacter capsulatus. *Current Microbiology*, *55*(5), 402–408. https://doi.org/10.1007/s00284-007-9007-6

Fernandez-Castaneda, L. A., Arias-Candamil, H., Zapata-Torres, B., & Ardila-Castaneda, M. P. (2018). Evaluation of the antimicrobial capacity of Hass avocado seed extract (Persea americana) for potential application in the meat industry. *DYNA*, *85*, 346–350. Retrieved from http://www.scielo.org.co/scielo.php?script=sci_arttext&pid=S0012-

73532018000400346&nrm=iso

Feynman, P. R. (1960). There's plenty of room at the bottom. *Engineering and Science*, *23*, 22–36.

Figueira, M. M., Volesky, B., & Mathieu, H. J. (1999). Instrumental Analysis Study of Iron Species Biosorption by Sargassum Biomass. *Environmental Science & Technology*, *33*(11), 1840–1846. https://doi.org/10.1021/es981111p

Gangula, A., Podila, R., M, R., Karanam, L., Janardhana, C., & Rao, A. M. (2011). Catalytic Reduction of 4-Nitrophenol using Biogenic Gold and Silver Nanoparticles Derived from Breynia rhamnoides. *Langmuir*, *27*(24), 15268–15274. https://doi.org/10.1021/la2034559

Gardea-Torresdey, J. L., Parsons, J. G., Gomez, E., Peralta-Videa, J., Troiani, H. E., Santiago, P., & Yacaman, M. J. (2002). Formation and Growth of Au Nanoparticles inside Live Alfalfa Plants. *Nano Letters*, *2*(4), 397–401. https://doi.org/10.1021/nl015673+

Gemini, V. L., Gallego, A., de Oliveira, V. M., Gomez, C. E., Manfio, G. P., & Korol, S. E. (2005). Biodegradation and detoxification of p-nitrophenol by Rhodococcus wratislaviensis. *International Biodeterioration & Biodegradation*, *55*(2), 103–108. https://doi.org/10.1016/J.IBIOD.2004.08.003

Geraldes, A., Alves da Silva, A., Leal, J., Mayeli Estrada-Villegas, G., Lincopan, N., Katti, K., & Benévolo Lug&atildeo, A. (2016). Green Nanotechnology from Plant Extracts: Synthesis and Characterization of Gold Nanoparticles. *Advances in Nanoparticles*, *05*, 176–185. https://doi.org/10.4236/anp.2016.53019

Gericke, M., & Pinches, A. (2006). Biological synthesis of metal nanoparticles. *Hydrometallurgy*, *83*(1–4), 132–140. https://doi.org/10.1016/J.HYDROMET.2006.03.019

Golkar, Z., Bagasra, O., & Pace, D. G. (2014). Bacteriophage therapy: a potential solution for the antibiotic resistance crisis. *The Journal of Infection in Developing Countries*, *8*(02), 129–136. https://doi.org/10.3855/jidc.3573

Gomes, C. J., Harman, M. W., Centuori, S. M., Wolgemuth, C. W., & Martinez, J. D. (2018). Measuring DNA content in live cells by fluorescence microscopy. *Cell Division*, *13*, 6.

https://doi.org/10.1186/s13008-018-0039-z

Gould, I. M., & Bal, A. M. (2013). New antibiotic agents in the pipeline and how they can help overcome microbial resistance. *Virulence*, *4*(2), 185–191. https://doi.org/10.4161/viru.22507

Grundmann, H., Aires-de-Sousa, M., Boyce, J., & Tiemersma, E. (2006). Emergence and resurgence of meticillin-resistant Staphylococcus aureus as a public-health threat. *The Lancet*, *368*(9538), 874–885. https://doi.org/10.1016/S0140-6736(06)68853-3

Gu, H., Ho, P. L., Tong, E., Wang, L., & Xu, B. (2003). Presenting Vancomycin on Nanoparticles to Enhance Antimicrobial Activities. *Nano Letters*, *3*(9), 1261–1263. https://doi.org/10.1021/nl034396z

Guidos, R. J. (2011). Combating antimicrobial resistance: policy recommendations to save lives. *Clinical Infectious Diseases*, *52*(Suppl 5), S397–S428. https://doi.org/10.1093/cid/cir153

Haiss, W., Thanh, N. T. K., Aveyard, J., & Fernig, D. G. (2007). Determination of Size and Concentration of Gold Nanoparticles from UV−Vis Spectra. *Analytical Chemistry*, *79*(11), 4215–4221. https://doi.org/10.1021/ac0702084

Hallett-Tapley, G. L., D'Alfonso, C., Pacioni, N. L., McTiernan, C. D., González-Béjar, M., Lanzalunga, O., … Scaiano, J. C. (2013). Gold nanoparticle catalysis of the cis–trans isomerization of azobenzene. *Chem. Commun.*, *49*(86), 10073–10075. https://doi.org/10.1039/C3CC41669K

Hanan, N. A., Chiu, H. I., Ramachandran, M. R., Tung, W. H., Mohamad Zain, N. N., Yahaya, N., & Lim, V. (2018). Cytotoxicity of plant-mediated synthesis of metallic nanoparticles: A systematic review. *International Journal of Molecular Sciences*, *19*(6). https://doi.org/10.3390/ijms19061725

Harish, K., Venkatesh, N., Bhowmik, H., & Kuila, A. (2018). Metallic Nanoparticle : A Review. *Biomedical Journal of Scientific and Technical Research*, *4*(2), 3765–3775. https://doi.org/10.26717/BJSTR.2018.04.001011

Hashimi, A. S., Nohan, M. A. N. M., Chin, S. X., Zakaria, S., & Chia, H. C. (2019). Rapid Catalytic Reduction of 4-Nitrophenol and Clock Reaction of Methylene Blue using Copper Nanowires. *Nanomaterials*, *9*, 936–949.

Hassoun, A., Linden, P. K., & Friedman, B. (2017). Incidence, prevalence, and management of MRSA bacteremia across patient populations—a review of recent developments in MRSA management and treatment. *Critical Care*, *21*(1), 211. https://doi.org/10.1186/s13054-017-1801-3

He, S., Guo, Z., Zhang, Y., Zhang, S., Wang, J., & Ning, G. (2007). Biosynthesis of gold nanoparticles using the bacteria Rhodopseudomonas capsulata. *Materials Letters - MATER LETT*, *61*, 3984–3987. https://doi.org/10.1016/j.matlet.2007.01.018

Hemeg, H. A. (2017). Nanomaterials for alternative antibacterial therapy. *International Journal of Nanomedicine*, *12*, 8211–8225. https://doi.org/10.2147/IJN.S132163

Herizchi, R., Abbasi, E., Milani, M., & Akbarzadeh, A. (2016). Current methods for synthesis of gold nanoparticles. *Artificial Cells, Nanomedicine and Biotechnology*, *44*(2), 596–602. https://doi.org/10.3109/21691401.2014.971807

Hernández-Sierra, J. F., Ruiz, F., Cruz Pena, D. C., Martínez-Gutiérrez, F., Martínez, A. E., de Jesús Pozos Guillén, A., Martínez Castañón, G. (2008). The antimicrobial sensitivity of Streptococcus mutans to nanoparticles of silver, zinc oxide, and gold. *Nanomedicine: Nanotechnology, Biology and Medicine*, *4*(3), 237–240. https://doi.org/10.1016/J.NANO.2008.04.005

Hozawa, A., Jacobs, D. R., Steffes, M. W., Gross, M. D., Steffen, L. M., & Lee, D.-H. (2007). Relationships of Circulating Carotenoid Concentrations with Several Markers of Inflammation, Oxidative Stress, and Endothelial Dysfunction: The Coronary Artery Risk Development in Young Adults (CARDIA)/Young Adult Longitudinal Trends in Antioxidants (YALT. *Clinical Chemistry*, *53*(3), 447–455.

Huh, A. J., & Kwon, Y. J. (2011). "Nanoantibiotics": A new paradigm for treating infectious diseases using nanomaterials in the antibiotics resistant era. *Journal of Controlled Release*, *156*(2), 128–145. https://doi.org/10.1016/J.JCONREL.2011.07.002

Hulkoti, N. I., & Taranath, T. C. (2014). Biosynthesis of nanoparticles using microbes-A review. *Colloids and Surfaces B: Biointerfaces*, *121*, 474–483. https://doi.org/10.1016/j.colsurfb.2014.05.027

Hurtado-Fernández, E., & Carrasco-Pancorbo, A Fernández-Gutiérrez, A. (2011). Profiling LC-DAD-ESI-TOF MS method for the determination of phenolic metabolites from

avocado (Persea americana). *Journal of Agricultural and Food Chemistry*, *59*(6), 2255–2267.

Husøy, T., Syversen, T., & Jenssen, J. (1993). Comparisons of four in vitro cytotoxicity tests: The MTT assay, NR assay, uridine incorporation and protein measurements. *Toxicology in Vitro*, *7*(2), 149–154. https://doi.org/10.1016/0887-2333(93)90125-O

Hutchings, G. J., & Edwards, J. K. (2012). *Application of gold nanoparticles in catalysis*. *Frontiers of Nanoscience* (1st ed., Vol. 3). Elsevier Ltd. https://doi.org/10.1016/B978-0-08-096357-0.00001-7

Idris, S., Ndukwe, G. I., & Gimba, C. (2010). Preliminary phytochemical screening and antimicrobial activity of seed extracts of Persea americana (avocado pear). *Bayero Journal of Pure and Applied Sciences*, *2*. https://doi.org/10.4314/bajopas.v2i1.58538

Iravani, S. (2011). Green synthesis of metal nanoparticles using plants. *Green Chemistry*, *13*(10), 2638–2650. https://doi.org/10.1039/c1gc15386b

Ismail, E. H., Saqer, A. M. A., Assirey, E., Naqvi, A., & Okasha, R. M. (2018). Successful Green Synthesis of Gold Nanoparticles using a Corchorus olitorius Extract and Their Antiproliferative Effect in Cancer Cells. *International Journal of Molecular Sciences*, *19*(9), 2612. https://doi.org/10.3390/ijms19092612

ISO. (2015). Nanotechnologies – Vocabulary part 1: Core terms. Retrieved November 7, 2019, from https://www.iso.org/obp/ui/#iso:std:iso:ts:80004:-1:ed-2:v1:en

Jain, N., Bhargava, A., Majumdar, S., Tarafdar, J. C., & Panwar, J. Extracellular biosynthesis and characterization of silver nanoparticles using Aspergillus flavusNJP08: A mechanism perspective, 3 Nanoscale 635–641 (2011). The Royal Society of Chemistry. https://doi.org/10.1039/C0NR00656D

Jain, P., Lee, K. S., El-Sayed, I., & El-Sayed, M. (2006). Calculated Absorption and Scattering Properties of Gold Nanoparticles of Different Size, Shape, and Composition: Applications in Biological Imaging and Biomedicine. *The Journal of Physical Chemistry B*, *110*(14), 7238–7248. https://doi.org/10.1021/jp057170o

Jendrzej, S., Gökce, B., Epple, M., & Barcikowski, S. (2017). How Size Determines the Value of Gold: Economic Aspects of Wet Chemical and Laser-Based Metal Colloid Synthesis. *ChemPhysChem*, *18*(9), 1012–1019. https://doi.org/10.1002/cphc.201601139

Jiménez, E., Abderrafi, K., Abargues, R., Valdés, J. L., & Martínez-Pastor, J. P. (2010). Laser-Ablation-Induced Synthesis of SiO2-Capped Noble Metal Nanoparticles in a Single Step. *American Chemical Society*, *26*(10), 7458–7463. https://doi.org/10.1021/la904179x

Jones, S. A., Bowler, P. G., Walker, M., & Parsons, D. (2004). Controlling wound bioburden with a novel silver-containing Hydrofiber® dressing. *Wound Repair and Regeneration*, *12*(3), 288–294. https://doi.org/10.1111/j.1067-1927.2004.012304.x

Kanaras, A. G., Wang, Z., Bates, A. D., Cosstick, R., & Brust, M. (2003). Towards Multistep Nanostructure Synthesis: Programmed Enzymatic Self-Assembly of DNA/Gold Systems. *Angewandte Chemie*, *115*(2), 201–204. https://doi.org/10.1002/ange.200390043

Kashyap, P. L., Kumar, S., Srivastava, A. K., & Sharma, A. K. (2013). Myconanotechnology in agriculture: a perspective. *World Journal of Microbiology and Biotechnology*, *29*(2), 191–207. https://doi.org/10.1007/s11274-012-1171-6

Khan, I., Saeed, K., & Khan, I. (2019). Nanoparticles: Properties, applications and toxicities. *Arabian Journal of Chemistry*, *12*(7), 908–931. https://doi.org/10.1016/J.ARABJC.2017.05.011

Khan, J., Kudgus, R., Szabolcs, A., Dutta, S., Wang, E., Cao, S., … Mukhopadhyay, D Robertson, JD Bhattacharya, R Mukherjee, P. (2011). Designing nanoconjugates to effectively target pancreatic cancer cells in vitro and in vivo. *PLOS One*, *6*(6), e20347.

Khandel, P., & Kumar, S. S. (2016). Microbes mediated synthesis of metal nanoparticles: current status and future prospects. *International Journal of Nanomaterials and Biostructures*, *6*(1), 1–24.

Khandel, P., Yadaw, R. K., Soni, D. K., Kanwar, L., & Shahi, S. K. (2018). *Biogenesis of metal nanoparticles and their pharmacological applications: present status and application prospects*. *Journal of Nanostructure in Chemistry* (Vol. 8). Springer Berlin Heidelberg. https://doi.org/10.1007/s40097-018-0267-4

Khlebtsov, N., & Dykman, L. (2011). Biodistribution and toxicity of engineered gold nanoparticles: a review of in vitro and in vivo studies. *Chemical Society Reviews*, *40*(3), 1647–1671. https://doi.org/10.1039/C0CS00018C

Kim, J. S., Kuk, E., Yu, K. N., Kim, J.H., Park, S. J., Lee, H. J., Cho, M.H. (2007). Antimicrobial effects of silver nanoparticles. *Nanomedicine: Nanotechnology, Biology and Medicine*, *3*(1), 95–101. https://doi.org/10.1016/J.NANO.2006.12.001

Kim, M., Osone, S., Kim, T., Higashi, H., & Seto, T. (2017). Synthesis of nanoparticles by laser ablation: A review. *KONA Powder and Particle Journal*, *34*, 80–90. https://doi.org/10.14356/kona.2017009

Kimling, J., Maier, M., Okenve, B., Kotaidis, V., Ballot, H., & Plech, A. (2006). Turkevich Method for Gold Nanoparticle Synthesis Revisited. *The Journal of Physical Chemistry B*, *110*(32), 15700–15707. https://doi.org/10.1021/jp061667w

Kochuveedu, S. T., & Kim, D. H. (2014). Surface plasmon resonance mediated photoluminescence properties of nanostructured multicomponent fluorophore systems. *Nanoscale*, *6*(10), 4966–4984. https://doi.org/10.1039/C4NR00241E

Kolhe, S., & Parikh, K. (2012). Application of nanotechnology in cancer: a review. *International Journal Bioinformatics Research and Applications*, *8*(1).

Kong, X., Zhu, H., Chen, C.-L., Huang, G., & Chen, Q. (2017a). Insights into the Reduction of 4-Nitrophenol to 4-Aminophenol on Catalysts. *Chemical Physics Letters*, *684*, 148–152.

Kong, X., Zhu, H., Chen, C. Le, Huang, G., & Chen, Q. (2017b). Insights into the reduction of 4-nitrophenol to 4-aminophenol on catalysts. *Chemical Physics Letters*, *684*, 148–152. https://doi.org/10.1016/j.cplett.2017.06.049

Kulkarni, N., & Muddapur, U. M. (2014). Biosynthesis of Metal Nanoparticles: A Review. *Journal of Nanotechnology*, *2014*, 1–8.

Kuppusamy, P., Yusoff, M. M., Maniam, G. P., & Govindan, N. (2016). Biosynthesis of metallic nanoparticles using plant derivatives and their new avenues in pharmacological applications – An updated report. *Saudi Pharmaceutical Journal*, *24*(4), 473–484. https://doi.org/10.1016/J.JSPS.2014.11.013

Lal, S. S., & Nayak, P. (2012). Green Synthesis of Gold Nanoparticles Using Various Extract of Plants and spices. *International Journal of Science Innovations and Discoveries*, *2*(3), 325–350.

Lee, D. G., Go, E. B., Lee, M., Pak, P. J., Kim, J.-S., & Chung, N. (2019). Gold nanoparticles

conjugated with resveratrol induce cell cycle arrest in MCF-7 cell lines. *Applied Biological Chemistry*, *62*(1), 33. https://doi.org/10.1186/s13765-019-0440-6

Lee, Y.S., Choi, K.M., Kim, W., Jeon, Y.S., Lee, Y.M., Hong, J.T., Yoo, H.S. (2013). Hinokitiol Inhibits Cell Growth through Induction of S-Phase Arrest and Apoptosis in Human Colon Cancer Cells and Suppresses Tumor Growth in a Mouse Xenograft Experiment. *Journal of Natural Products*, *76*(12), 2195–2202. https://doi.org/10.1021/np4005135

Li, M., & Chen, G. (2013). Revisiting catalytic model reaction p-nitrophenol/NaBH4 using metallic nanoparticles coated on polymeric spheres. *Nanoscale*, *5*(23), 11919–11927. https://doi.org/10.1039/C3NR03521B

Li, W.R., Xie, X.B., Shi, Q.S., Zeng, H.Y., OU-Yang, Y.S., & Chen, Y.B. (2010). Antibacterial activity and mechanism of silver nanoparticles on Escherichia coli. *Applied Microbiology and Biotechnology*, *85*(4), 1115–1122. https://doi.org/10.1007/s00253-009-2159-5

Liang, M., Su, R., Huang, R., Qi, W., Yu, Y., Wang, L., & He, Z. (2014). Facile in Situ Synthesis of Silver Nanoparticles on Procyanidin-Grafted Eggshell Membrane and Their Catalytic Properties. *ACS Applied Materials & Interfaces*, *6*(7), 4638–4649. https://doi.org/10.1021/am500665p

Link, S., & El-Sayed, M. A. (1999). Size and Temperature Dependence of the Plasmon Absorption of Colloidal Gold Nanoparticles. *The Journal of Physical Chemistry B*, *103*(21), 4212–4217. https://doi.org/10.1021/jp984796o

Liou, R.-M. (2012). The denitration pathway of p-nitrophenol in the hydrogen peroxide catalytic oxidation with an FeIII-resin catalyst. *Water Science and Technology*, *65*(5), 845–858. https://doi.org/10.2166/wst.2012.627

Liu, G., Li, Q., Ni, W., Zhang, N., Zheng, X., Wang, Y., Tai, G. (2015). Cytotoxicity of various types of gold-mesoporous silica nanoparticles in human breast cancer cells. *International Journal of Nanomedicine*, *10*, 6075–6087. https://doi.org/10.2147/IJN.S90887

Loud, J., & Murphy, J. (2017). Cancer screening and early detection in the 21st century. *Seminars in Oncology Nursing*, *33*(2), 121–128.

Lu, Q., Zhang, Y., Wang, Y., Wang, D., Lee, R., Gao, K., Heber, D. (2009). California Hass avocado: profiling of carotenoids, tocopherol, fatty acid, and fat content during maturation and from different growing areas. *Journal of Agricultural and Food Chemistry*, *57*(21), 10408–10413.

Lu, Y., & Foo, L. Y. (2002). Polyphenolics of Salvia—a review. *Phytochemistry*, *59*(2), 117–140. https://doi.org/10.1016/S0031-9422(01)00415-0

Fumitaka, M., Kohno, J., Takeda, Y., Kondow, T., & Sawabe, H. (2001). Formation of Gold Nanoparticles by Laser Ablation in Aqueous Solution of Surfactant. *The Journal of Physical Chemistry B*, *105*(22), 5114–5120. https://doi.org/10.1021/jp0037091

Magiorakos, A. P., Srinivasan, A., Carey, R. B., Carmeli, Y., Falagas, M. E., Giske, C., … Monnet, D. L. (2012). Multidrug-resistant, extensively drug-resistant and pandrug-resistant bacteria: an international expert proposal for interim standard definitions for acquired resistance. *Clinical Microbiology and Infection*, *18*(3), 268–281. https://doi.org/10.1111/J.1469-0691.2011.03570.X

Mahmoudi, M., Azadmanesh, K., Shokrgozar, M., Journeay, W., & Laurent, S. (2011). Effect of Nanoparticles on the Cell Life Cycle. *Chemical Reviews*, *111*, 3407–3432. https://doi.org/10.1021/cr1003166

Majdalawieh, A., Kanan, M. C., El-Kadri, O., & Kanan, S. M. (2014). Recent Advances in Gold and Silver Nanoparticles: Synthesis and Applications. *Journal of Nanoscience and Nanotechnology*, *14*, 4757–4780. https://doi.org/10.1016/J.ONANO.2017.07.001

Marais, E., & Nyokong, T. (2008). Adsorption of 4-nitrophenol onto Amberlite® IRA-900 modified with metallophthalocyanines. *Journal of Hazardous Materials*, *152*(1), 293–301. https://doi.org/10.1016/J.JHAZMAT.2007.06.096

Martin, R. M., Leonhardt, H., & Cardoso, M. C. (2005). DNA labeling in living cells. *Cytometry Part A*, *67A*(1), 45–52. https://doi.org/10.1002/cyto.a.20172

Martínez-Torres, A. C., Zarate-Triviño, D. G., Lorenzo-Anota, H. Y., Ávila-Ávila, A., Rodríguez-Abrego, C., & Rodríguez-Padilla, C. (2018). Chitosan gold nanoparticles induce cell death in HeLa and MCF-7 cells through reactive oxygen species production. *International Journal of Nanomedicine*, *13*, 3235–3250. https://doi.org/10.2147/IJN.S165289

Melgar, B., Dias, M. I., Ciric, A., Sokovic, M., Garcia-Castello, E. M., Rodriguez-Lopez, A. D., Ferreira, I. C. R. F. (2018). Bioactive characterization of Persea americana Mill. by-products: A rich source of inherent antioxidants. *Industrial Crops and Products*, *111*, 212–218. https://doi.org/10.1016/J.INDCROP.2017.10.024

Menon, S., Shanmugam, R., & Kumar, V. (2017). A review on biogenic synthesis of gold nanoparticles, characterization, and its applications. *Resource-Efficient Technologies*, *3*. https://doi.org/10.1016/j.reffit.2017.08.002

Mishra, A., Tripathy, S. K., & Yun, S.I. (2012). Fungus mediated synthesis of gold nanoparticles and their conjugation with genomic DNA isolated from Escherichia coli and Staphylococcus aureus. *Process Biochemistry*, *47*(5), 701–711. https://doi.org/10.1016/J.PROCBIO.2012.01.017

Mmola, M., Roes-Hill, M. Le, Durrell, K., Bolton, J. J., Sibuyi, N., Meyer, M. E., … Antunes, E. (2016). Enhanced Antimicrobial and Anticancer Activity of Silver and Gold Nanoparticles Synthesised Using Sargassum incisifolium Aqueous Extracts. *Molecules*, *21*(12), 1633. https://doi.org/10.3390/molecules21121633

Modirshahla, N., Behnajady, M. A., & Mohammadi-Aghdam, S. (2008). Investigation of the effect of different electrodes and their connections on the removal efficiency of 4-nitrophenol from aqueous solution by electrocoagulation. *Journal of Hazardous Materials*, *154*(1–3), 778–786. https://doi.org/10.1016/J.JHAZMAT.2007.10.120

Montazer, M., & Harifi, T. (2018). Nanofinishing: Fundamental principles. In *Nanofinishing of Textile Materials* (pp. 19–34). Woodhead Publishing. https://doi.org/10.1016/B978-0-08-101214-7.00002-9

Mountrichas, G., Pispas, S., & Kamitsos, E. I. (2014). Effect of Temperature on the Direct Synthesis of Gold Nanoparticles Mediated by Poly(dimethylaminoethyl methacrylate) Homopolymer. *The Journal of Physical Chemistry C*, *118*(39), 22754–22759. https://doi.org/10.1021/jp505725v

Mukherjee, P., Ahmad, A., Mandal, D., Senapati, S., Sainkar, S. R., Khan, M. I., Kumar, R. (2001). Bioreduction of AuCl4− Ions by the Fungus, Verticillium sp. and Surface Trapping of the Gold Nanoparticles Formed. *Angewandte Chemie International Edition*, *40*(19), 3585–3588. https://doi.org/10.1002/1521-3773(20011001)40:19<3585::AID-ANIE3585>3.0.CO;2-K

Mulvaney, P. (1996). Surface Plasmon Spectroscopy of Nanosized Metal Particles. *Langmuir*, *12*(3), 788–800. https://doi.org/10.1021/la9502711

Munita, J. M., & Arias, C. A. (2016). Mechanisms of Antibiotic Resistance. *Microbiology Spectrum*, *4*(2), 10.1128/microbiolspec.VMBF-0016–2015. https://doi.org/10.1128/microbiolspec.VMBF-0016-2015

Myers, R. L. (2003). *The Basics of Chemistry*. Wesport, London: Greenwood Publishing Group.

Nadagouda, M. N., Hoag, G., Collins, J., & Varma, R. S. (2009). Green synthesis of Au nanostructures at room temperature using biodegradable plant surfactants. *Crystal Growth and Design*, *9*(11), 4979–4983. https://doi.org/10.1021/cg9007685

Nagy, A., Harrison, A., Sabbani, S., Munson, Robert S Jr Dutta, P. K., & Waldman, W. J. (2011). Silver nanoparticles embedded in zeolite membranes: release of silver ions and mechanism of antibacterial action. *International Journal of Nanomedicine*, *2011*(6), 1833—1852.

Narayanan, K., & Sakthivel, N. (2008). Coriander leaf mediated biosynthesis of gold nanoparticles. *Materials Letters*, *62*, 4588–4590. https://doi.org/10.1016/j.matlet.2008.08.044

Nath, D., & Banerjee, P. (2013). Green nanotechnology – A new hope for medical biology. *Environmental Toxicology and Pharmacology*, *36*(3), 997–1014. https://doi.org/10.1016/J.ETAP.2013.09.002

Niño-Martínez, N., Salas Orozco, F. M., Martínez-Castañón, G.-A., Torres Méndez, F., & Ruiz, F. (2019). Molecular Mechanisms of Bacterial Resistance to Metal and Metal Oxide Nanoparticles. *International Journal of Molecular Sciences* . https://doi.org/10.3390/ijms20112808

Noruzi, M., Zare, D., Khoshnevisan, K., & Davoodi, D. (2011). Rapid green synthesis of gold nanoparticles using Rosa hybrida petal extract at room temperature. *Spectrochimica Acta Part A: Molecular and Biomolecular Spectroscopy*, *79*(5), 1461–1465. https://doi.org/10.1016/J.SAA.2011.05.001

Nunes, D., Pimentel, A., Santos, L., Barquinha, P., Pereira, L., Fortunato, E., … Martins, R. (2019). Introduction. *Metal Oxide Nanostructures*, 1–19. https://doi.org/10.1016/B978-

0-12-811512-1.00001-1

Nurliza, D. C., & Savitri, W. (2017). Antibacterial effect of ethanol extract of the avocado seed (Persea Americana Mill.) as an alternative root canal Irrigants against Porphyromonas Gingivalis (In Vitro). *International Journal of Applied Dental Sciences*, *3*(1), 89–93.

O'Connor, O. A., & Young, L. Y. (1989). Toxicity and anaerobic biodegradability of substituted phenols under methanogenic conditions. *Environmental Toxicology and Chemistry*, *8*(10), 853–862. https://doi.org/10.1002/etc.5620081003

Oboh, G., Odubanjo, V. O., Bello, F., Ademosun, A. O., Oyeleye, S. I., Nwanna, E. E., & Ademiluyi, A. O. (2016). Aqueous extracts of avocado pear (Persea americana Mill.) leaves and seeds exhibit anti-cholinesterases and antioxidant activities in vitro. *Journal of Basic and Clinical Physiology and Pharmacology*, *27*(2), 131–140. https://doi.org/10.1515/jbcpp-2015-0049

Oturan, M. A., Peiroten, J., Chartrin, P., & Acher, A. J. (2000). Complete Destruction of p-Nitrophenol in Aqueous Medium by Electro-Fenton Method. *Environmental Science & Technology*, *34*(16), 3474–3479. https://doi.org/10.1021/es990901b

Paczosa, M. K., & Mecsas, J. (2016). Klebsiella pneumoniae: Going on the Offense with a Strong Defense. *Microbiology and Molecular Biology Reviews : MMBR*, *80*(3), 629–661. https://doi.org/10.1128/MMBR.00078-15

Pal, R., Panigrahi, S., Bhattacharyya, D., & Chakraborti, A. S. (2013). Characterization of citrate capped gold nanoparticle-quercetin complex: Experimental and quantum chemical approach. *Journal of Molecular Structure*, *1046*, 153–163. https://doi.org/https://doi.org/10.1016/j.molstruc.2013.04.043

Pan, Y., Bartneck, M., & Jahnen-Dechent, W. (2012). Cytotoxicity of Gold Nanoparticles. *Methods in Enzymology*, *509*, 225–242. https://doi.org/10.1016/B978-0-12-391858-1.00012-5

Pan, Y., Leifert, A., Ruau, D., Neuss, S., Bornemann, J., Schmid, G., … Jahnen-Dechent, W. (2009). Gold Nanoparticles of Diameter 1.4 nm Trigger Necrosis by Oxidative Stress and Mitochondrial Damage. *Small*, *5*(18), 2067–2076. https://doi.org/10.1002/smll.200900466

Pareek, V., Bhargava, A., Gupta, R., Jain, N., & Panwar, J. (2017). Synthesis and Applications of Noble Metal Nanoparticles: A Review. *Advanced Science, Engineering and Medicine*, *9*(7), 527–544. https://doi.org/10.1166/asem.2017.2027

Parveen, K., Banse, V., & Ledwani, L. (2016). Green synthesis of nanoparticles: Their advantages and disadvantages. *AIP Conference Proceedings*, *1724*. https://doi.org/10.1063/1.4945168

Philip, D. (2010). Green synthesis of gold and silver nanoparticles using Hibiscus rosa sinensis. *Physica E: Low-Dimensional Systems and Nanostructures*, *42*(5), 1417–1424. https://doi.org/10.1016/J.PHYSE.2009.11.081

Pichichero, M. E., & Casey, J. R. (2007). Systematic review of factors contributing to penicillin treatment failure in Streptococcus pyogenes pharyngitis. *Otolaryngology–Head and Neck Surgery*, *137*(6), 851–857. https://doi.org/10.1016/j.otohns.2007.07.033

Polte, J., Ahner, T. T., Delissen, F., Sokolov, S., Emmerling, F., Thünemann, A. F., & Kraehnert, R. (2010). Mechanism of Gold Nanoparticle Formation in the Classical Citrate Synthesis Method Derived from Coupled In Situ XANES and SAXS Evaluation. *Journal of the American Chemical Society*, *132*(4), 1296–1301. https://doi.org/10.1021/ja906506j

Pradhan, N., Pal, A., & Pal, T. (2002). Silver nanoparticle catalyzed reduction of aromatic nitro compounds. *Colloids and Surfaces A: Physicochemical and Engineering Aspects*, *196*(2–3), 247–257. https://doi.org/10.1016/S0927-7757(01)01040-8

Prasanna, S. S., Balaji, K., Pandey, S., & Rana, S. (2019). Metal Oxide Based Nanomaterials and Their Polymer Nanocomposites. In *Nanomaterials and Polymer Nanocomposites* (pp. 123–144). Elsevier. https://doi.org/10.1016/B978-0-12-814615-6.00004-7

Qidwai, A., Pandey, A., Kumar, R., Shukla, S. K., & Dikshit, A. (2018). Advances in Biogenic Nanoparticles and the Mechanisms of antimicrobial Effects. *Indian Journal of Pharmaceutical Sciences*, *80*(4), 592–603. https://doi.org/10.4172/pharmaceutical-sciences.1000398

Raghunandan, D., Ravishankar, B., Sharanbasava, G., Mahesh, D. B., Harsoor, V., Yalagatti, M. S., … Venkataraman, A. (2011). Anti-cancer studies of noble metal nanoparticles synthesized using different plant extracts. *Cancer Nanotechnology*, *2*(1), 57–65.

https://doi.org/10.1007/s12645-011-0014-8

Rai, A., Prabhune, A., & Perry, C. C. (2010). Antibiotic mediated synthesis of gold nanoparticles with potent antimicrobial activity and their application in antimicrobial coatings. *Journal of Materials Chemistry*, *20*(32), 6789–6798. https://doi.org/10.1039/C0JM00817F

Rao, P. V., Nallappan, D., Madhavi, K., Rahman, S., Jun Wei, L., & Gan, S. H. (2016). Phytochemicals and Biogenic Metallic Nanoparticles as Anticancer Agents. *Oxidative Medicine and Cellular Longevity*, *2016*, 3685671. https://doi.org/10.1155/2016/3685671

Robertson, T., Sanchez, W., & Roberts, M. (2010). Are Commercially Available Nanoparticles Safe When Applied to the Skin? *Journal of Biomedical Nanotechnology*, *6*, 452–468. https://doi.org/10.1166/jbn.2010.1145

Rosi, N. L., Giljohann, D. A., Thaxton, C. S., Lytton-Jean, A. K. R., Han, M. S., & Mirkin, C. A. (2006). Oligonucleotide-Modified Gold Nanoparticles for Intracellular Gene Regulation. *Science*, *312*(5776), 1027 LP – 1030. https://doi.org/10.1126/science.1125559

Saeed, K., & Khan, I. (2016). Preparation and characterization of single-walled carbon nanotube/nylon 6, 6 nanocomposites. *Instrumentation Science & Technology*, *44*(4), 435–444. https://doi.org/10.1080/10739149.2015.1127256

Saeidnia, S., Manayi, A., Gohari, A. R., & Abdollahi, M. (2014). The Story of Beta-sitosterol- A Review. *European Journal of Medicinal Plants*, *4*(5), 590–609.

Saga, T., & Yamaguchi, K. (2009). History of Antimicrobial Agents and Resistant. *Japan Medical Association Journal*, *52*, 103–108.

Saidi, T., & Douglas, T. S. (2017). Nanotechnology in South Africa - Challenges in evaluating the impact on development. *South African Journal of Science*, *113*, 1–2. Retrieved from http://www.scielo.org.za/scielo.php?script=sci_arttext&pid=S0038-23532017000400011&nrm=iso

Salgado, J. ., Bin, C., Mansi, D. ., & Souza, A. (2008). Effect of the hass avocado (American Persea Mill) on hipercolesterolemic rats. *Ciência e Tecnologia de Alimentos*, *28*(4), 922–928.

Sau, T. K., Pal, A., Jana, N. R., Wang, Z. L., & Pal, T. (2001). Size Controlled Synthesis of

Gold Nanoparticles using Photochemically Prepared Seed Particles. *Journal of Nanoparticle Research*, *3*(4), 257–261. https://doi.org/10.1023/A:1017567225071

Sau, T., Rogach, A., Jäckel, F., Klar, T., & Feldmann, J. (2010). Properties and Applications of Colloidal Nonspherical Noble Metal Nanoparticles. *Advanced Materials*, *22*(16), 1805–1825. https://doi.org/10.1002/adma.200902557

Schaar, V., Uddbäck, I., Nordström, T., & Riesbeck, K. (2013). Group A streptococci are protected from amoxicillin-mediated killing by vesicles containing β-lactamase derived from Haemophilus influenzae. *Journal of Antimicrobial Chemotherapy*, *69*(1), 117–120. https://doi.org/10.1093/jac/dkt307

Schaming, D., & Remita, H. (2015). Nanotechnology: from the ancient time to nowadays. *Foundations of Chemistry*, *17*(3), 187–205. https://doi.org/10.1007/s10698-015-9235-y

Schoenfelder, S. M. K., Lange, C., Eckart, M., Hennig, S., Kozytska, S., & Ziebuhr, W. (2010). Success through diversity – How Staphylococcus epidermidis establishes as a nosocomial pathogen. *International Journal of Medical Microbiology*, *300*(6), 380–386. https://doi.org/10.1016/J.IJMM.2010.04.011

Segovia, F. J., Hidalgo, G. I., Villasante, J., Ramis, X., & Almajano, M. P. (2018). Avocado Seed: A Comparative Study of Antioxidant Content and Capacity in Protecting Oil Models from Oxidation. *Molecules (Basel, Switzerland)*, *23*(10), 2421. https://doi.org/10.3390/molecules23102421

Senapati, S., Ahmad, A., Khan, M. I., Sastry, M., & Kumar, R. (2005). Extracellular Biosynthesis of Bimetallic Au–Ag Alloy Nanoparticles. *Small*, *1*(5), 517–520. https://doi.org/10.1002/smll.200400053

Seo, Y. S., Ahn, E.-Y., Park, J., Kim, T. Y., Hong, J. E., Kim, K., … Park, Y. (2017). Catalytic reduction of 4-nitrophenol with gold nanoparticles synthesized by caffeic acid. *Nanoscale Research Letters*, *12*(1), 7. https://doi.org/10.1186/s11671-016-1776-z

Shahbandeh, M. (2019). Global fruit production in 2017, by variety. Retrieved from https://www.statista.com/statistics/264001/worldwide-production-of-fruit-by-variety/

Shamaila, S., Zafar, N., Riaz, S., Sharif, R., Nazir, J., & Naseem, S. (2016). Gold Nanoparticles: An Efficient Antimicrobial Agent against Enteric Bacterial Human Pathogen. *Nanomaterials (Basel, Switzerland)*, *6*(4), 71.

https://doi.org/10.3390/nano6040071

Shanmugam, R., Kumar, V., Chelladurai, M., Vanaja, M., Paulkumar, K., & Gurusamy, A. (2017). Optimized Synthesis of Gold Nanoparticles using Green Chemical Process and its Invitro Anticancer Activity Against HepG2 and A549 Cell Lines. *Mechanics, Materials Science & Engineering*, *9*.

Sharma, V. K., Yngard, R. A., & Lin, Y. (2009). Silver nanoparticles: Green synthesis and their antimicrobial activities. *Advances in Colloid and Interface Science*, *145*(1–2), 83–96. https://doi.org/10.1016/J.CIS.2008.09.002

Shea, C. M., Grinde, R., & Elmslie, B. (2011). Nanotechnology as general-purpose technology: empirical evidence and implications. *Technology Analysis & Strategic Management*, *23*(2), 175–192. https://doi.org/10.1080/09537325.2011.543336

Shinde, N. C., Keskar, N. J., & Argade, P. D. (2012). Nanoparticles: Advances in Drug Delivery Systems. *INTERNATIONAL JOURNAL OF ADVANCES IN PHARMACY, BIOLOGY AND CHEMISTRY*, *1*(1).

Siddiqi, K. S., & Husen, A. (2017). Recent advances in plant-mediated engineered gold nanoparticles and their application in biological system. *Journal of Trace Elements in Medicine and Biology*, *40*, 10–23. https://doi.org/10.1016/J.JTEMB.2016.11.012

Siddiqi, K. S., Husen, A., & Rao, R. A. K. (2018). A review on biosynthesis of silver nanoparticles and their biocidal properties. *Journal of Nanobiotechnology*, *16*(1), 14. https://doi.org/10.1186/s12951-018-0334-5

Silver, S., & Phung, L. T. (1996). BACTERIAL HEAVY METAL RESISTANCE: New Surprises. *Annual Review of Microbiology*, *50*(1), 753–789. https://doi.org/10.1146/annurev.micro.50.1.753

Singh, P., Garg, A., Pandit, S., Mokkapati, V. R. S. S., & Mijakovic, I. (2018). Antimicrobial Effects of Biogenic Nanoparticles. *Nanomaterials (Basel, Switzerland)*, *8*(12), 1009. https://doi.org/10.3390/nano8121009

Singh, P., Kim, Y.J., Zhang, D., & Yang, D.C. (2016). Biological Synthesis of Nanoparticles from Plants and Microorganisms. *Trends in Biotechnology*, *34*(7), 588–599. https://doi.org/10.1016/J.TIBTECH.2016.02.006

Singh, P., Pandit, S., Mokkapati, V., Garg, A., Ravikumar, V., & Mijakovic, I. (2018). Gold

Nanoparticles in diagnostics and therapeutics for Human Cancer. *International Journal of Molecular Sciences*, *19*(7), 1979.

Singh, Rajesh, & Lillard, J. (2009). Nanoparticle-based targeted drug delivery. *Experimental and Molecular Pathology*, *86*(3), 215–223.

Singh, Richa, Shedbalkar, U. U., Wadhwani, S. A., & Chopade, B. A. (2015). Bacteriagenic silver nanoparticles: synthesis, mechanism, and applications. *Applied Microbiology and Biotechnology*, *99*(11), 4579–4593. https://doi.org/10.1007/s00253-015-6622-1

Skalska, J., & Strużyńska, L. (2015). Toxic effects of silver nanoparticles in mammals – does a risk of neurotoxicity exist? *Folia Neuropathologica*, *53*(4), 281–300. https://doi.org/10.5114/fn.2015.56543

Slavin, Y. N., Asnis, J., Häfeli, U. O., & Bach, H. (2017). Metal nanoparticles: understanding the mechanisms behind antibacterial activity. *Journal of Nanobiotechnology*, *15*(1), 65. https://doi.org/10.1186/s12951-017-0308-z

Sloan, M., & Farnsworth, S. (2006). *Testing and Evaluation of Nanoparticle Efficacy on E. Coli, and Bacillus Anthracis Spores*. Bangalore. Retrieved from https://pdfs.semanticscholar.org/ed51/4b6f851bdcd23f9cf6b10b33f7f20f3df213.pdf

Sneharani, H., Prabhudev, S. H., & Sachin, H. (2019). Effect of phytochemicals on optical absorption spectra during biogenic synthesis of selfassembled silver nanoparticles and studies relevant to food applications. *SPECTROSCOPY LETTERS*, *52*(7), 413–422.

Sosa, I. O., Noguez, C., & Barrera, R. G. (2003). Optical Properties of Metal Nanoparticles with Arbitrary Shapes. *The Journal of Physical Chemistry B*, *107*(26), 6269–6275. https://doi.org/10.1021/jp0274076

Sportelli, M., Izzi, M., Volpe, A., Clemente, M., Picca, R., Ancona, A., … Cioffi, N. (2018). The Pros and Cons of the Use of Laser Ablation Synthesis for the Production of Silver Nano-Antimicrobials. *Antibiotics*, *7*, 67. https://doi.org/10.3390/antibiotics7030067

Sweet, M. J., Chessher, A., & Singleton, I. (2012). Review: Metal-Based Nanoparticles; Size, Function, and Areas for Advancement in Applied Microbiology. *Advances in Applied Microbiology*, *80*, 113–142. https://doi.org/10.1016/B978-0-12-394381-1.00005-2

Swierczewska, M., Lee, S., & Chen, X. (2011). The design and application of fluorophore-gold nanoparticle activatable probes. *Physical Chemistry Chemical Physics*, *13*(21),

9929–9941. https://doi.org/10.1039/c0cp02967j

Thakkar, K., Mhatre, S., & Parikh, R. (2009). Biological synthesis of metallic nanoparticles. Nanomed Nanotechnol Biol Med 6:257-262. *Nanomedicine : Nanotechnology, Biology, and Medicine*, *6*, 257–262. https://doi.org/10.1016/j.nano.2009.07.002

Tian, F., Clift, M. J. D., Casey, A., del Pino, P., Pelaz, B., Conde, J., … Stoeger, T. (2015). Investigating the role of shape on the biological impact of gold nanoparticles in vitro. *Nanomedicine*, *10*(17), 2643–2657. https://doi.org/10.2217/nnm.15.103

Tiegam, T., Rufis Fregue, T., Ionel, I., Gabche, S., & Mihaiuti, A.-C. (2019). Optimization of the Activated Carbon Preparation from Avocado Seeds, using the Response Surface Methodology. *Revista de Chimie -Bucharest- Original Edition-*, *70*, 410–416.

Tiwari, D. K., Behari, J., & Sen, P. (2008). Application of Nanoparticles in Waste Water Treatment. *World Applied Sciences Journal*, *3*(3), 417–433.

Tiwari, J. N., Tiwari, R. N., & Kim, K. S. (2012). Zero-dimensional, one-dimensional, two-dimensional and three-dimensional nanostructured materials for advanced electrochemical energy devices. *Progress in Materials Science*, *57*(4), 724–803. https://doi.org/10.1016/J.PMATSCI.2011.08.003

Toderas, F., Baia, M., Maniu, D., & Astilean, S. (2008). Tuning the plasmon resonances of gold nanoparticles by controlling their size and shape. *Journal of Optoelectronics and Advanced Materials*, *10*(9), 2282–2284.

Toma, A., & Deyno, S. (2015). Overview on Mechanisms of Antibacterial Resistance. *International Journal of Research in Pharmacy and Biosciences*, *2*(1), 27–36.

Trivedi, M., Patlolla, K. C., Misra, N., & Pandey, M. (2019). Cucurbit[6]uril Glued Magnetic Clay Hybrid as a Catalyst for Nitrophenol Reduction. *Catalysis Letters*, *149*, 2355–2367. https://doi.org/10.1007/s10562-019-02853-0

Tshikantwa, T. S., Ullah, M. W., He, F., & Yang, G. (2018). Current Trends and Potential Applications of Microbial Interactions for Human Welfare. *Frontiers in Microbiology*, *9*, 1156. https://doi.org/10.3389/fmicb.2018.01156

Vijayaraghavan, K., & Ashokkumar, T. (2017). Plant-mediated biosynthesis of metallic nanoparticles: A review of literature, factors affecting synthesis, characterization techniques and applications. *Journal of Environmental Chemical Engineering*, *5*(5),

4866–4883. https://doi.org/10.1016/J.JECE.2017.09.026

Villarreal-Lara, R., Rodríguez-Sánchez, D. G., Díaz De La Garza, R. I., García-Cruz, M. I., Castillo, A., Pacheco, A., & Hernández-Brenes, C. (2019). Purified avocado seed acetogenins: Antimicrobial spectrum and complete inhibition of Listeria monocytogenes in a refrigerated food matrix. *CyTA - Journal of Food*, *17*(1), 228–239. https://doi.org/10.1080/19476337.2019.1575908

Vimalraj, S., Ashokkumar, T., & Saravanan, S. (2018). Biogenic gold nanoparticles synthesis mediated by Mangifera indica seed aqueous extracts exhibits antibacterial, anticancer and anti-angiogenic properties. *Biomedicine & Pharmacotherapy*, *105*, 440–448. https://doi.org/10.1016/J.BIOPHA.2018.05.151

Viswanathan, V. K. (2014). Off-label abuse of antibiotics by bacteria. *Gut Microbes*, *5*(1), 3–4. https://doi.org/10.4161/gmic.28027

Wadhwani, S. A., Shedbalkar, U. U., Singh, R., Karve, M. S., & Chopade, B. (2014). Novel polyhedral gold nanoparticles: green synthesis, optimization and characterization by environmental isolate of Acinetobacter sp. SW30. *World Journal of Microbiology and Biotechnology*, *30*(10), 2723–2731.

Wang, L., Hu, C., & Shao, L. (2017). The antimicrobial activity of nanoparticles: present situation and prospects for the future. *International Journal of Nanomedicine*, *12*, 1227–1249. https://doi.org/10.2147/IJN.S121956

Wang, W., Bostic, T. R., & Gu, L. (2010). Antioxidant capacities, procyanidins and pigments in avocados of different strains and cultivars. *Food Chemistry*, *122*(4), 1193–1198. https://doi.org/10.1016/j.foodchem.2010.03.114

Widiyastuti, Y., Pratiwi, R., Riyanto, S., & Wahyuono, S. (2018). Cytotoxic activity and apoptosis induction of Avocado (Persea americana) seed extract on MCF-7 cancer cell line. *Indonesian Journal of Biotechnology*, *23*, 61. https://doi.org/10.22146/ijbiotech.32141

Wolf, F., Sigl, R., & Geley, S. (2007). '… The End of the Beginning': Cdk1 Thresholds and Exit from Mitosis. *Cell Cycle (Georgetown, Tex.)*, *6*, 1408–1411. https://doi.org/10.4161/cc.6.12.4361

Wright, G. D. (2010). Antibiotic resistance in the environment: a link to the clinic? *Current*

Opinion in Microbiology, *13*(5), 589–594. https://doi.org/10.1016/J.MIB.2010.08.005

Yasmin, A., Ramesh, K., & Rajeshkumar, S. (2014). Optimization and stabilization of gold nanoparticles by using herbal plant extract with microwave heating. *Nano Convergence*, *1*(1), 12. https://doi.org/10.1186/s40580-014-0012-8

Yeh, C.C., & Chen, D.H. (2014). Ni/reduced graphene oxide nanocomposite as a magnetically recoverable catalyst with near infrared photothermally enhanced activity. *Applied Catalysis B: Environmental*, *150–151*, 298–304. https://doi.org/10.1016/J.APCATB.2013.12.040

Yeh, Y.-C., Crerana, B., & Rotelloa, V. M. (2012). Gold nanoparticles: preparation, properties, and applications in bionanotechnology. *Nanoscale*, *4*(6), 1871–1880.

Yin, X., Chen, S., & Wu, A. (2010). Green chemistry synthesis of gold nanoparticles using lactic acid as a reducing agent. *Micro & Nano Letters*, *5*(5), 270–273. https://doi.org/10.1049/mnl.2010.0117

Zhang, X., Qu, Y., Shen, W., Wang, J., Li, H., Zhang, Z., … Zhou, J. (2016). Biogenic synthesis of gold nanoparticles by yeast Magnusiomyces ingens LH-F1 for catalytic reduction of nitrophenols. *Colloids and Surfaces A: Physicochemical and Engineering Aspects*, *497*, 280–285. https://doi.org/10.1016/J.COLSURFA.2016.02.033

Zhang, Y., Shareena, D., Deng, H., & Yu, H. (2015). Antimicrobial Activity of Gold Nanoparticles and Ionic Gold. *Journal of Environmental Science and Health Part C Environmental Carcinogenesis & Ecotoxicology Reviews*, *33*(3), 286–327.

Zhou, Y., Wang, C. Y., Zhu, Y. R., & Chen, Z. Y. (1999). A Novel Ultraviolet Irradiation Technique for Shape-Controlled Synthesis of Gold Nanoparticles at Room Temperature. *Chemistry of Materials*, *11*(9), 2310–2312. https://doi.org/10.1021/cm990315h

Zhu, X., Pathakoti, K., & Hwang, H.-M. (2019). Green synthesis of titanium dioxide and zinc oxide nanoparticles and their usage for antimicrobial applications and environmental remediation. In *Green Synthesis, Characterization and Applications of Nanoparticles* (pp. 223–263). Elsevier. https://doi.org/10.1016/B978-0-08-102579-6.00010-1